The Dissertation Committee for Leor Nadav Katz
certifies that this is the approved version of the following dissertation:

Decision-making in the primate brain: formation, location, and causal manipulation

Committee:

Alexander Huk, Supervisor

Richard Aldrich

Lawrence Cormack

Mary Hayhoe

Nicholas Priebe

Eyal Seidmann

Decision-making in the primate brain: formation, location, and causal manipulation

by

Leor Nadav Katz, B.S.

DISSERTATION

Presented to the Faculty of the Graduate School of

The University of Texas at Austin

in Partial Fulfillment

of the Requirements

for the Degree of

DOCTOR OF PHILOSOPHY

THE UNIVERSITY OF TEXAS AT AUSTIN

May 2016

Dedicated to Patrick and Nancy

Acknowledgments

This thesis could not have come to life without the guidance and support of many people. Alex Huk in particular, has been a tremendous source of wisdom and motivation throughout it all. When I began my graduate studies I knew very little about the brain, but I was confident I wanted to study it under Alex's mentorship. He has inspired me as a scientist and serves as a role model, both inside and out of the lab. I will be forever grateful for his unmatched mentorship and for his enduring friendship (and for multiple dinners, drinks, and Tool concert tickets). As if one extraordinary advisor is not enough, I have been fortunate to enjoy Larry Cormack as a second, unofficial advisor. Larry has been an inexhaustible fountain of council and clarity, a mentor, and partner in crime (disc golf is more enjoyable when it's during work hours). Thank you Alex, and thank you Larry.

A big thank you to my dissertation committee who have guided and challenged me throughout the years: Eyal Seidemann, Nicholas Priebe, Rick Aldrich, and Mary Hayhoe (with whom I published my first graduate school paper). Many thanks to Brian Corneil for a fruitful scientific collaboration, and thanks to Jonathan Pillow for council, collaboration, and for "allowing" me crowd-surf him at a Danzig show. I am also grateful to the University of Texas at Austin, INS and CPS, for providing me with a thriving community

within which to grow.

I am immensely appreciative of my lab mates, old and new, for innumerable scientific discussions, ideas, and inspiration. Most notably, Jacob Yates, a close friend and collaborator, without whom my journey would simply not be possible— Jake, thank you, for everything. Together with dear friends, Benjamin Scholl, Kenneth Latimer and Stephen Sebastian, graduate school has been an adventure packed full of scientific debates (usually over beer) and ridiculousness (usually during karaoke). I could not have asked for better companions in my journey. These friends, together with Alex and Larry, are what made science so incredibly rewarding, and a career I wholeheartedly choose to pursue.

I am also grateful to many friends in and outside of grad school who have made life in Austin so special. And to my closest friends from Israel: Juv, Michael, Assaf, Yonatan, Omch and Mimi, I am hugely indebted to you. Thank you for your ongoing friendship, love and support. Finally, to Dana, the driving force behind my choice to pursue a PhD abroad, thank you.

Most importantly, I would like to thank my parents, brother and sister, who have always encouraged me to follow my dreams. My family has provided me with the most nourishing environment a "youngster" could dream for. Thank you for your continuous support and unconditional love.

Decision-making in the primate brain: formation, location, and causal manipulation

Publication No. _____

Leor Nadav Katz, Ph.D.
The University of Texas at Austin, 2016

Supervisor: Alexander Huk

Interaction within the environment relies on the ability to accumulate sensory evidence in favor of a decision. Despite the paramount importance of decision-making to survival, the neural instantiations and computational principles governing the process have remained elusive. In this thesis I consider how sensory evidence is accumulated to guide decisions, and where in the primate brain this process takes place. I report the results of three main experiments. In the first, I test whether sensory evidence is accumulated differentially for motion in the frontoparallel plane (i.e. 2D motion; left/right) compared to motion through depth (i.e. 3D motion; towards/away). I show that integration of 3D motion is different than 2D and likely relies on a mechanism that is distinct. In the second experiment, I test an influential theory in cognitive neuroscience: that neurons in the monkey lateral intraparietal (LIP)

cortex accumulate sensory information in favor of a decision communicated by an eye-movement. I found that despite strong correlations between LIP responses and decisions, reversible inactivation of neurons in LIP had no measurable impact on decision-making performance. More generally, I show that decision-related activity does not necessarily play a causal role in choices. In the final experiment, I test whether the process of making a decision stands to influence functions that are decision irrelevant. I found that causally manipulating the amount of sensory evidence available to human observers influenced decision-irrelevant oculomotor commands, suggesting that even during non-oculomotor decisions, oculomotor regions of the brain are recruited. Taken together, the experimental findings reported motivate new ideas about evidence accumulation and advance our understanding of the decision-making process in the primate brain.

Table of Contents

List of Tables

List of Figures

Chapter 1

Introduction

"Life is a sum of all your choices"

– Albert Camus

1.1 Overview

Living creatures must make decisions to navigate the environment. The choices made determine whether they succeed or fail, survive or perish. Not surprisingly, a central goal of cognitive and systems neuroscience is to understand the principles that guide such decision-making. Some of the greatest strides in elucidating the neurobiology subserving this process come from the study of simple perceptual decisions. These include the detection of an ambiguous signal, or the discrimination of the direction of motion. As an ecological example, consider identifying whether a predator is hiding behind the bush or not (detection), or determining whether the predator is lunging to the right or to the left (discrimination). Such decisions, in nature or in the laboratory, are thought to take place by a deliberative process in which evidence is accumulated over time to favor one alternative over another. However, the neural instantiations subserving this process are unclear. Elucidating how evidence

is accumulated to form decisions, and where in the brain this process occurs, is one of the central challenges in cognitive and systems neuroscience today.

Advances in solving this puzzle come from a synthesis of theory and experimentation. Approaches from statistical decision theory such as signal detection theory and sequential analysis have shaped the field of decision-making by putting forth a basic set of computational principles that explain behavior and neural responses (Gold & Shadlen 2007). One of the most successful applications of this synthesis took place in the context of a motion direction discrimination task, in which monkeys were required to discriminate the direction of a moving stimulus (Parker & Newsome 1998). Neural recordings from the middle temporal (MT) area established MT's critical role in representing the sensory evidence that guides decisions about motion. The next natural step was to identify how sensory evidence in MT is "read out", or accumulated, to form decisions. But this step is extremely challenging because a large number of neural structures exhibit activity consistent with the accumulation of sensory evidence, and the locus of integration is unknown (Gold & Shadlen 2001). One of these areas, the lateral intraparietal (LIP) cortex, has garnered the largest amount of attention and is proposed to play a key role in evidence accumulation (Shadlen & Newsome 1996, Shadlen & Newsome 2001).

In this thesis I focus on three main topics. First, I address how sensory evidence is accumulated to form decisions (Chapter 2). Second, whether this process takes place in LIP (Chapters 3 and 4). Third, whether other behaviors

are influenced by the decision-making process (Chapter 5).

This introduction consists two main sections: *Approaches for studying decision formation* and *Decision formation in Neurons*. The first section lays the general framework within which perceptual decision-making is studied. I introduce the primary theories that guide the field, describe an influential model for decision formation, and report results from key psychophysical experiments. In the second introductory section I review neural structures that are involved in decision formation with a primary emphasis on area LIP, one of the best-studied areas of the primate brain. Neurons in area LIP exhibit decision-related activity during decision-making tasks and thus been proposed as a key locus for evidence accumulation in the primate brain. However, this theory not been tested, despite having influenced the field substantially. This introduction will specify the multiple flaws in the logic that links LIP responses to decision formation and motivate the need for causal manipulations to test the role of LIP in decision formation directly.

In Chapter 2 I report a psychophysical experiment that compared the accumulation of evidence in favor of a decision between two stimulus conditions. In one condition, subjects were required to discriminate the direction of standard left/right ("2D") motion. In the other, subjects were required to discriminate the direction of towards/away ("3D") motion. A descriptive model that accounts for multiple phases of evidence accumulation identified that the accumulation of 3D motion evidence is inferior to that of 2D, suggesting that the neural integration mechanism for 3D motion is distinct.

In Chapter 3 I focus on area LIP of the macaque and report results of a causal manipulation, testing whether the correlations between LIP neurons and decisions correctly imply causation. Briefly, I found that pharmacologically inactivating LIP had no causal impact on decision-making behavior, despite strong decision-related activity in LIP neurons. This finding indicates that LIP does not play a critical role in decision-making. More generally, the result calls for a reconsideration of the nature of decision-related signals in the brain, and how they are read out by downstream brain regions. Extended analyses of this experiment are presented in Chapter 4.

In Chapter 5 I address the interactive nature of decision-making. I report results from an experiment that tested whether non-oculomotor decision-making stands to affect oculomotor commands that are decision-*irrelevant*. Even though the decision was communicated with a button press, the decision-making process influenced the decision-irrelevant oculomotor command. This finding indicates that oculomotor regions in the brain are recruited even during non-oculomotor decisions.

The immediate implications of each experiment are discussed within each chapter individually, and a broader synthesis is presented in the general Discussion (Chapter 6).

1.2 Approaches for studying Decision Formation

1.2.1 Theory

The study of decision formation begins with psychophysics, where inferences about the brain are made by relating a physical stimulus to the perceptual reports of a subject (Fechner 1860, von Helmholtz 1867). For example, a motion stimulus of variable strength may be presented to the subject who is required to respond: "left" vs. "right". Naturally, the stronger the motion stimulus, the easier it is for the subject to discriminate the direction of motion. The mathematical relationship between stimulus strength and subject response can be used to make inferences about how the stimulus is represented in the subject brain. Two branches of statistical decision theory have advanced our understanding of the stimulus-response relationship substantially: signal detection theory and sequential analysis.

1.2.1.1 Signal detection Theory

The relationship between stimulus and response was rigorously formalized by Green and Swets (Green & Swets 1966) in their seminal work on signal detection theory (SDT), an application of radar detection methods to psychophysics. In SDT, the sensory stimulus is represented by the nervous sensory system, corrupted by both external noise (i.e. physical perceptibility of the stimulus) and internal noise (the inherently irregular responses of neurons to identical stimulation) (Eccles 1957, Shadlen & Newsome 1994). SDT takes noise into account, providing the probabilistic means by which to

evaluate the likelihood that a given sample of the signal, *evidence*, is drawn from one category or another (e.g. "left motion" or "right motion"). Thus, two likelihoods are computed and compared: $p(evidence|leftmotion)$ and $p(evidence|rightmotion)$. The comparison leads to a simple decision rule: the decision-maker should choose the category that is more likely, computed from the ratio of the two likelihoods (the "likelihood ratio"). The likelihood ratio, then, is a mathematical quantity that reflects whether the observer should make one decision or another. It has been termed the "decision variable", i.e. the variable that determines the decision category (Gold & Shadlen 2007). Thus, SDT provides the means by which to make statistical inferences about internal representations of noisy sensory evidence, and relate them to decisions. It has been extremely successful both in the field of psychophysics and in drawing quantitative relationships between subject responses and the activity of single sensory neurons (Britten, Shadlen, Newsome & Movshon 1992, Parker & Newsome 1998). However, while SDT formalizes the representation of sensory evidence for a given stimulus, it does not account for how the representation evolves over time. To accumulate multiple likelihood ratios over time, the logarithm of likelihood ratios may be taken and then summed, a method prescribed by sequential analysis models.

1.2.1.2 Sequential analysis and the drift diffusion model

Sequential analysis compliments SDT by using similar methods, but over multiple samples (or intervals) (Wald 1947, Stone 1960, Link 1992). It

refers to a family of sequential sampling models that treat the sensory input as a sequential stream of incoming evidence. The evidence is weighed on every sample such that the likelihood ratio can be derived for each. Thus, sequential analysis provides the same likelihood ratio as SDT, but for every sample in time. If the multiple samples are independent then their logarithm can be summed and give rise to the log likelihood ratio ("logLR"), resulting in a better estimate of signal given the evidence similar to how multiple samples of noisy signal are combined to improve the signal-to-noise ratio (SNR). How much evidence is enough evidence? The sequential probability ratio test (Wald & Wolfowitz 1948) prescribes an optimal mathematical procedure by which to update the decision variable (the logLR) until a stopping point. The stopping rule depends on the level of error the subject is willing to tolerate. To achieve high accuracy, many samples are needed. For low accuracy, less. This results in the well-known tradeoff between speed and accuracy in decision-making (Laming 1968, Luce 1986, Smith & Ratcliff 2004, Palmer, Huk & Shadlen 2005). A related model, the drift diffusion model, relies on similar principles and has become one of the most influential models in decision theory.

1.2.2 Drift diffusion model for decision formation

The drift diffusion model is based on sequential sampling but formalized in continuous time (Ratcliff 1978, Ratcliff, Smith, Brown & McKoon 2016). The model treats the accumulated evidence (the decision variable) as a particle diffusing randomly (in Brownian motion) between two absorbing bounds.

The bounds represent the two choices such that when enough accumulated evidence has pushed the particle into a bound, the decision-making process is complete and a choice is made. Figure 1.1 illustrates the model along with three example decision trials, one for each stimulus strength (Fig. 1.1A). Each stimulus is represented by sensory neurons as noisy sensory evidence (Gaussian distributions). For the discrimination of motion direction, these Gaussians represent the noisy representation of motion evidence in pools of MT neurons (Britten et al. 1992, Britten et al. 1992). For a given stimulus strength, evidence at every moment is drawn from the appropriate distribution and pushes the randomly diffusing particle to drift in proportion to the mean of the sensory evidence Gaussian (Fig. 1.1B). For example, strong sensory evidence (orange Gaussian) will drive the noisy particle in a trajectory with a slope proportion to the distribution mean (dashed orange arrow), resulting in rapid accumulation (orange curve). Accumulation of a weaker signal (green) will result in slower accumulation. The noisy accumulation persists until either reaching the stopping rule (either bound) and making the appropriate choice, or until the stimulus is terminated (dashed gray line example) and the choice follows the sign of the decision variable at that time.

A simple diffusion model can be devised with three parameters that govern the accumulation of evidence: a drift rate, bound height, and accumulator noise. Drift rate relates stimulus strength to the rate of particle diffusion towards a bound (dashed arrows in Figure 1.1B). Bound height serves as the stopping rule, i.e., the amount of evidence required to end the decision

process and commit to a choice. Requiring less evidence (lower bounds) will facilitate faster decisions but also increase the probability that noise will drive the particle to the wrong bound, resulting in decreased accuracy. Accumulator noise reflects the noise in the accumulation process and is invariant across stimulus conditions. These three parameters do a fair job in fitting data obtained from response time tasks and in fact, can be reduced to just two, but these parameterizations fail to account for certain phenomena (e.g. prolonged response times for incorrect choices) and do not account for non-decision factors such as sensorimotor delays. Incorporation of additional parameters (e.g. bias, non-decision time, trial-to-trial variability in parameters) can improve model performance substantially (Ratcliff 1978, Ratcliff & Smith 2004, Ratcliff & McKoon 2008). For example, Palmer et al. (Palmer et al. 2005) fit the diffusion model to subject response times in a motion discrimination task, which accounted for subject accuracy over a wide range of stimulus strengths and subject strategies. The diffusion model's simplicity and closed form mathematical convenience make it amenable to fit many forms of decision behavior in both response time and fixed duration tasks (Link 1992, Ratcliff & Smith 2004, Palmer et al. 2005, Ratcliff & McKoon 2008, Kiani, Hanks & Shadlen 2008, Selen, Shadlen & Wolpert 2012, Huk, Katz & Yates 2015, Ratcliff et al. 2016), and an appealing model for evidence accumulation in the brain (Gold & Shadlen 2007).

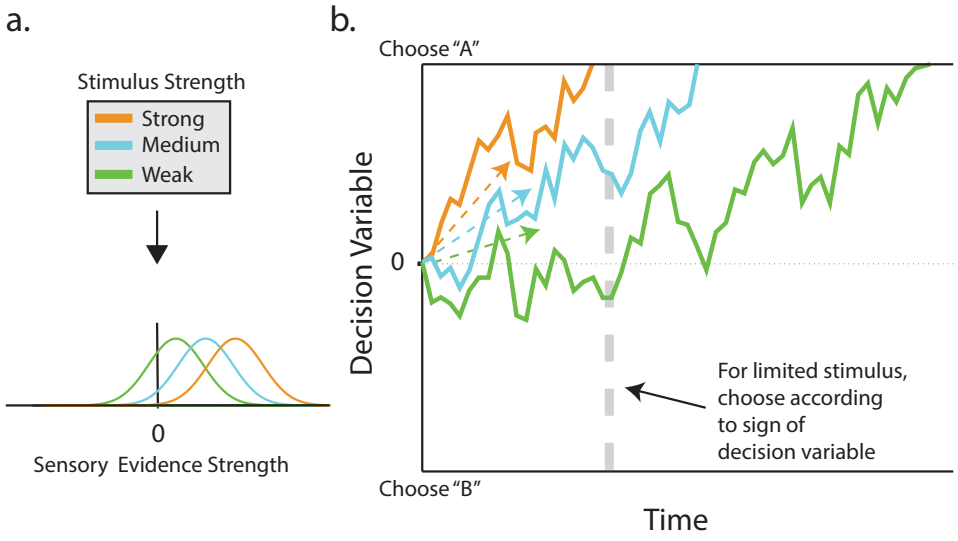

Figure 1.1: Illustration of a simple sequential sampling model with equal bounds. Three trials, for three signals strengths are shows. **(A)** Each stimulus strength is represented by sensory neurons as noisy sensory evidence in the form of Gaussian distributions. **(B)** For a given trial, the evidence on every sample is drawn from a Gaussian distribution such that the evidence mean across samples is the distribution mean (dashed arrows). Every sampled evidence is accumulated by a noisy integrator, leading to a noisy trajectory through time (solid curves). In a response time task, the accumulation continues until the upper or lower bound is reached, whereupon a choice is made. For a stimulus of a given duration, the accumulation continues until the stimulus is terminated. In the case that the stimulus is terminated before the accumulator hit a bound, the choice is made according to the sign of the decision variable at that point. For example, if a weak stimulus (green) is terminated at the gray dashed line, subject choice would be the incorrect "B", even though a longer stimulus duration would result in the correct choice, "A".

1.2.3 Experimental measurements

The primary paradigms used to study evidence accumulation are the response time (RT) and fixed duration (FD) task. In the RT task, the observer is presented with a stimulus and is free to accumulate as much evidence as necessary to inform her decision(Laming 1968). In terms of the diffusion model parameters, the necessary amount of evidence is set by bound height (Fig. 1.1). In the FD task, the duration of evidence available to the subject is dictated by the experimenter, presented for a limited amount of time regardless to whether the subject had reached a decision or not. An example is illustrated in Figure 1.1 by the gray dashed line. The advantage of the RT task is that on every trial a decision is made in favor of one alternative or another, reflecting the internal process of accumulation in the observer. However, the total response time consists of components other than evidence accumulation, such as sensory and motor delays and other potentially unknown components related to response preparation. This is particularly problematic when studying neurons in a RT task because distinguishing between neural activity related to accumulation may be obfuscated by activity related to motor response preparation. In the FD task, in contrast, the motor response is prompted at a given time after the stimulus has been extinguished such that neural activity related to accumulation can be teased apart from response preparation. Although the FD task does not allow for the accumulation process to terminate on its own as in the RT case, the FD task can include stimuli with variable durations (VD) between trials, enabling the researcher to probe the evolving decision at

different times.

Within the SDT framework, a straightforward estimation of subject sensitivity can be made for every stimulus duration used to probe decision formation, resulting in a link between stimulus duration and subject sensitivity. If evidence is integrated perfectly, the improvement in sensitivity will grow by the square root of time in the same manner that integrating noisy signal improves SNR. On logarithmic coordinates, perfect integration of noisy signal results in a linear duration-sensitivity relationship with a slope of 0.5 (Barlow 1958, Watson 1986, Burr 1981). For the simple detection of a visual stimulus (i.e. "present" or "absent"), temporal integration takes place on very brief time scales, on the order of few hundreds of milliseconds (Graham & Margaria 1935, Watson 1979, Burr 1981, Chen, Geisler & Seidemann 2008). The integration of such stimuli can be described by a basic principle in sensory processing, Bloch's law (Bloch 1885, Graham & Margaria 1935, Huk et al. 2015). In Bloch's law, signal multiplied by time is a constant, such that time simply equals signal. This is not unlike how a camera sensor would absorb light in proportion to exposure time. However, Bloch's law is only applicable for very short stimulus durations (under $\sim$100ms) and does not model noise, a critical tool for manipulating stimulus strength in many decision-making paradigms. Thus, the law is more of a theoretical handhold than a model for decision-making, especially given that most decision-making study relies on decisions that evolve over durations far longer than 100ms.

For the discrimination of a broadband random dot motion stimulus

(Newsome & Pare 1988), temporal integration of evidence takes place over far longer durations than for simple detection. Studies have found integration time of over 1 second in either humans (Watamaniuk & Sekuler 1992, Festa & Welch 1997, Barlow & Tripathy 1997, Burr & Santoro 2001, Selen et al. 2012, Melcher, Crespi, Bruno & Morrone 2004, Palmer et al. 2005) or monkeys (Britten et al. 1992, Gold & Shadlen 2003, Kiani et al. 2008), likely because this type of stimulus relies on higher motion sensing areas in the brain such as area MT (Newsome & Pare 1988, Britten et al. 1992, Burr & Santoro 2001). Long integration times are also observed for the discrimination of circular and radial motion (Morrone, Burr & Vaina 1995, Burr & Santoro 2001), and biological motion (Neri, Morrone & Burr 1998). The prolonged evidence integration time is advantageous for the study of decision-making, because it provides a longer period over which to analyze behavior and neural activity (Britten et al. 1992).

Within the context of task that include longer integration times, temporal integration likely consists of two accumulation phases. First, motion signal is integrated by the direction selective "sensor" consistent with Bloch's law. This likely takes place in direction selective neurons in MT where motion integration takes under 100ms (Bair & Movshon 2004, Born & Bradley 2005). The remainder, from 100ms onwards, is the phase where noisy sensory signals are integrated downstream to form decisions. The duration-sensitivity relationship for this stage often approximates 0.5 on logarithmic coordinates, implying that sensor signals are being integrated perfectly. This has been shown in previous studies (Watamaniuk & Sekuler 1992, Burr & Santoro 2001, Melcher

et al. 2004, Gold & Shadlen 2003, Kiani et al. 2008), and replicated in Chapter 2 for frontoparallel motion that is moving two dimensions. However, motion in three dimensions (towards/away), was found to be integrated less perfectly (Chapter 2). Regardless to whether or not sensory evidence is integrated perfectly, integration does not persist indefinitely. Subject sensitivity tends to increase with stimulus viewing duration until roughly 1 second (for motion discrimination), whereupon performance saturates and ceases to improve despite additional viewing time (Barlow & Tripathy 1997, Burr & Santoro 2001). In the following section I consider how the accumulation of signals represented by sensory neurons is implemented in the brain.

1.3 Decision formation in neurons

Sensory neurons in area MT represent motion stimuli with great fidelity (Parker & Newsome 1998). But how are MT signals integrated downstream? Let us first consider how MT represents the sensory evidence, and then consider its integration. Newsome and colleagues studied the response of MT neurons in monkeys trained to discriminate the direction of random dot motion (Newsome & Pare 1988). They quantitatively related responses of direction selective MT cells to psychophysical behavior within the SDT framework (Newsome, Britten & Movshon 1989) and found that the sensitivity of MT neurons often matched the overall sensitivity of the monkey (Britten et al. 1992, Britten, Shadlen, Newsome & Movshon 1993). The group proposed that the information used by the monkey to guide decisions must be based on

MT signals, and specifically, on the difference between pools of MT neurons with opposite directional selectivity (Britten et al. 1992, Zohary, Shadlen & Newsome 1994, Shadlen, Britten, Newsome & Movshon 1996). Causal perturbations of area MT support this claim: inactivation of area MT impairs discrimination performance (Newsome & Pare 1988), and microstimulation of MT shifts monkey choices to reflect an added motion signal that is directionally specific (Salzman, Murasugi, Britten & Newsome 1992). In addition to characterizing mean MT responses, the group studied the variability in MT neurons to identical stimuli (i.e. the noise). Newsome and colleagues found that the variability in monkeys' choices was slightly (but significantly) correlated with the variability in MT responses, for a given stimulus (Celebrini & Newsome 1994, Britten, Newsome, Shadlen, Celebrini & Movshon 1996). The relationship was coined *Choice Probability* (CP), and taken as further evidence that the monkey is basing its decisions on pools of MT neurons (Parker & Newsome 1998)(although different interpretations of CP exist, see Chapter 3 and Nienborg & Cumming 2009, Cumming & Nienborg 2016).

If MT signals are being accumulated by downstream neurons, these integrator neurons should exhibit responses in proportion to the signal integrated. A simple neural integration hypothesis is shown in Figure 1.2. The following section describes key brain regions that have been identified as potential loci for evidence accumulation during decision-making.

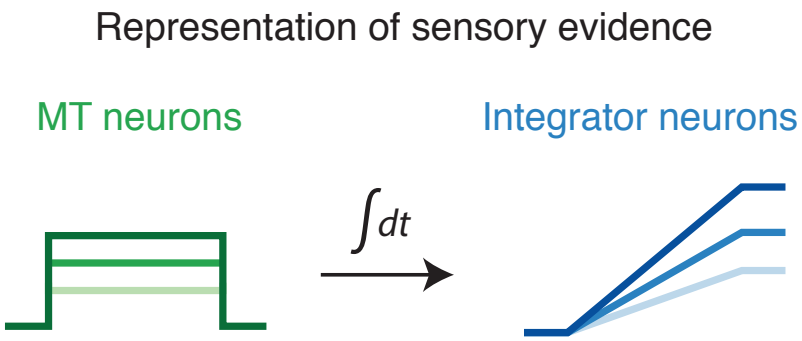

Figure 1.2: Hypothesis for neural integration. The schematic shows a boxcar function of variable magnitude (shades) and the result of its mathematical integral. The principle put forth by this toy model is that the integration of signals should be dependent on signal strength. This dependence has been observed in certain neural structures to implicate their activity in decision formation.

1.3.1 Multiple correlates of decision formation

The hypothesis illustrated in Figure 1.2 indicates that if a neuron is integrating a signal, the slope of its ramping response should depends on the signal strength. I refer to this form of dependence as "decision-related activity". Decision-related activity has been observed in multiple regions in the brain during decision-making tasks (Fig 1.3). In the direction discrimination task where the decision is communicated by an eye movement, decision-related signals have been identified in multiple oculomotor cortical areas: area LIP (Shadlen & Newsome 1996, Shadlen & Newsome 2001), and the frontal eye fields (FEF) (Kim & Shadlen 1999, Ding & Gold 2012*a*, Gold & Shadlen 2000), (Fig. 1.3A and B, respectively, showing either mean firing rate (A) and predictive index[1] (B)). It is unknown whether these areas process decision information in unison or in sequence, though recent simultaneous recordings in LIP and FEF found that decision-related activity in LIP precedes FEF (Siegel, Buschman & Miller 2015).

To complicate matters further, decision-related activity has also been observed in subcortical structures such as the superior colliculus (SC) (Horwitz & Newsome 1999, Horwitz & Newsome 2001, Horwitz, Batista & Newsome 2004) and the caudate nucleus (Ding & Gold 2010, Ding & Gold 2012*b*), (Fig. 1.3C and D, respectively). Decision-related activity has been observed

[1]The predictive index is a measure of decision-related activity that is derived from the cell's firing rate. The index approximates the accuracy with which an ideal observer can predict the monkey's choice based on the neural activity (Shadlen & Newsome 1996). A value of 0.5 indicates chance performance, a value of 1 indicates perfect accuracy.

for other forms of decisions too. The parietal reach region (PRR) exhibits decision-related responses for decisions communicated with a reach (Fig. 1.3E). The PRR also exhibits decision-related activity for decisions communicated with saccades, but the degree of ramping dependence on stimulus strength is not as pronounced (de Lafuente, Jazayeri & Shadlen 2015). Even outside the central nervous system, decision-related activity has been identified. In humans responding to motion discrimination task with reaches, the gain in electromyographic activity of the bicep stretch reflex reflected the amount of motion evidence accrued at every stimulus duration probed (Selen et al. 2012)(Fig. 1.3F). In fact, even the overt arm movements can reflect some degree of decision-related activity by exhibiting a trajectory that depends on stimulus strength (Spivey, Grosjean & Knoblich 2005, Song & Nakayama 2009).

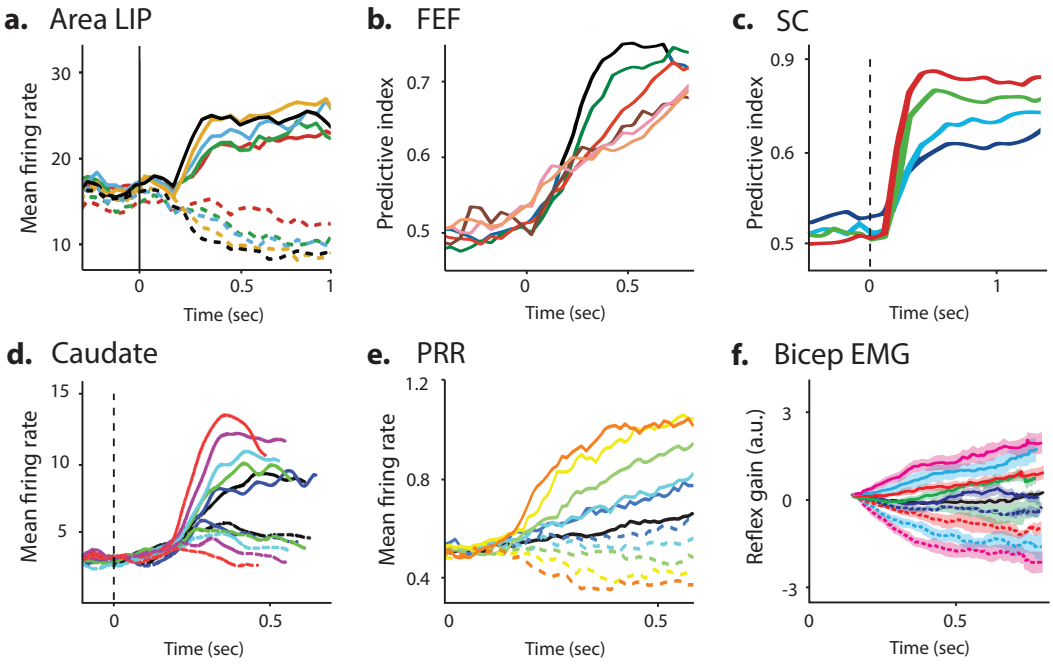

Figure 1.3: Decision-related activity during a direction discrimination task, in multiple sites in the brain. **(A)** LIP physiology, adapted from (Shadlen & Newsome 2001). The average population response of 104 LIP neurons aligned to motion onset. Solid and dashed lines represent trials where the monkey made an eye-movement in and out of the neuron response field, respectively. 200ms after motion onset, LIP neurons ramp in activity in proportion to the degree of motion strength (different colors). The stimulus strength-dependent ramping is the key feature that gave rise to the hypothesis that LIP neurons represent the accumulation of evidence. **(B-F)** Panels show decision-related activity in neural structures in similar format to panel A, where different colors represent different stimulus strengths. Decisions were communicated either by a an eye-movement (A-D) or reach (E, F). If a figure of mean firing rate (y-axis) was unavailable, predictive index[1] is presented instead (panels B and C). **(B)** Frontal eye fields (FEF) adapted from (Kim & Shadlen 1999). **(C)** Superior colliculus (SC) adapted from (Horwitz & Newsome 1999). **(D)** Caudate nucleus, adapted from (Ding & Gold 2010). **(E)** Posterior reach region (PRR), adapted from (de Lafuente et al. 2015). **(F)** Electromyographic (EMG) response of bicep stretch reflex gain, adapted from (Selen et al. 2012).

It is unclear whether each node in the decision-making network operates independently or not, or whether the pervasive nature of decision-related activity is indicative of parallel processing in service of flexibility (Zandbelt, Purcell, Palmeri, Logan & Schall 2014, Cisek & Kalaska 2010, de Lafuente et al. 2015, Siegel et al. 2015). Attempts to elucidate the differential role of decision-related activity in these and related areas have recently emerged in the rat model system, with a particular focus on posterior parietal cortex (Harvey, Coen & Tank 2012, Raposo, Kaufman & Churchland 2014, Erlich, Brunton, Duan, Hanks & Brody 2015, Hanks, Kopec, Brunton, Duan, Erlich & Brody 2015). Intriguing advances have been made in this animal model (detailed in the Discussion, Chapter 6) but homology between rodent and primate is tenuous. Rodent work — while extremely valuable — is still far from translating to primate (including human) cognition. In primates, it is unknown how or whether removal of a node would impact the decision-making process. This is tested in Chapters 3 and 4. It is also unknown whether the general form by which brain regions are recruited during decision-making stands to influence other behaviors and functions that may rely on these brain regions. A psychophysical experiment that tests interaction between decision formation and decision-irrelevant functions is reported in Chapter 5.

Despite the large number of brain regions exhibiting decision-related activity, area LIP has garnered the most attention, by far. It has been proposed to play an important role in evidence accumulation during decision-making, to the extent that LIP neurons have been proposed to perform the integration

computation per se (Mazurek, Roitman, Ditterich & Shadlen 2003, Gold & Shadlen 2007). In the following sections I examine the physiological properties linking LIP to decision-making and question whether LIP plays a role in evidence accumulation.

1.3.2 Does LIP play a role in evidence accumulation?

1.3.2.1 A historical perspective

The first functional identification of what we now refer to as LIP was likely performed by Ferrier in the 19th century (Ferrier 1876), in which coarse electrical stimulation of the posterior parietal cortex elicited eye movements in the awake monkey. The area was simplistically but appropriately termed "the parietal eye field". Later work would show that the posterior parietal cortex is involved in a staggering number of processes beyond merely moving the eyes. The first clue came a century after Ferrier's observation when Mountcastle performed recordings in Brodmann area 7 of awake and behaving monkeys (Mountcastle, Lynch, Georgopoulos, Sakata & Acuna 1975). In today's literature we draw a distinction between area LIP and area 7 but in Mountcastle's studies, "area 7" included both area 7 and modern "LIP". Mountcastle's work was the first to show that neurons in LIP respond persistently to both visual sensation and motor action, and that these visuomotor responses were selective to particular areas of visual space. This visuomotor role was well aligned with the idea that LIP (and the posterior parietal cortex more generally) associates visual input with motor output.

The experiments that followed advanced the understanding of LIP anatomy and function. Anatomically, LIP was identified by Andersen (Andersen, Asanuma & Cowan 1985), and found to be highly connected with both occipital and frontal regions (Desimone & Ungerleider 1986, Andersen, Asanuma, Essick & Siegel 1990, Felleman & Van Essen 1991), bolstering the proposed visuomotor role. However, it is important to note that anatomical connections do not guarantee functional interaction (a point that I return to later). Functionally, the finding that brought LIP to the attention of cognitive neuroscientists was made by Gnadt and Andersen (Gnadt & Andersen 1988), who had identified a response property not previously reported: persistent activity in LIP neurons during the delay period of a memory guided delayed saccade task (Hikosaka & Wurtz 1983), consistent with working-memory responses observed previously in the prefrontal cortex (Goldman-Rakic 1987). The Andersen lab held that this motor plan maintenance was in favor of shifting the location of gaze, and indicates oculomotor intention (Andersen, Snyder, Bradley & Xing 1997). The Goldberg lab, in contrast, reported correlations between LIP activity and events within attentional tasks, and held that LIP responses are more consistent with the allocation of attention (Colby & Goldberg 1999). However, dissociating attention from intention is challenging because primates look to where they attend, and attend to where they look (Rizzolatti, Riggio, Dascola & Umiltá 1987). The "attention vs. intention" debate has yet to be resolved (though an integrative framework has been put forth, Bisley & Goldberg 2010), but the focus on LIP function began to shift when a number

of reports were made linking LIP function to the formation of a perceptual decision.

1.3.2.2 Measurements of LIP during decision formation

The first characterization of LIP neurons during decision-making was done in the Newsome lab, following the rigorous characterization of area MT. To put it in the words of Shadlen and Newsome, they ventured from "sensor" (MT), to "decider" (LIP) (Shadlen & Newsome 1996). The group listed a number of reasons why area LIP may integrate noisy sensory signals from MT. First, LIP receives strong anatomical input from extrastriate cortex including area MT (Maunsell & Van Essen 1983, Desimone & Ungerleider 1986, Lewis & Van Essen 2000*a*, Lewis & Van Essen 2000*b*). Second, LIP projects to oculomotor centers such as FEF and SC (Andersen et al. 1985, Andersen et al. 1990, Pare & Wurtz 1997, Wurtz, Sommer, Pare & Ferraina 2001, Ferraina, Paré & Wurtz 2002). Together with the persistent activity during delay periods (Gnadt & Andersen 1988) and ideas of cortical hierarchy (Felleman & Van Essen 1991, Lennie 1998), area LIP appeared well poised to integrate momentary motion evidence from MT in favor of an oculomotor decision that is sent downstream. It struck the researchers as the sensorimotor continuation of the primate dorsal stream.

Shadlen and Newsome used the same motion direction discrimination task used for the MT studies but instead of placing the motion stimulus in the MT RF, they placed one of the two choice targets in the RF of the LIP

neuron under study (Shadlen & Newsome 1996, Shadlen & Newsome 2001). Shadlen and Newsome found that when the monkey communicated its choice by a saccade into the RF of the neuron, neural activity increased in activity long before the saccade (Fig. 1.3A). This ramping in activity was reminiscent of other "buildup" activity like that observed in FEF or SC during saccade preparation (Wurtz et al. 2001), but with one crucial difference. The ramping in mean LIP responses was proportional to the amount of motion evidence available to the monkey, consistent with decision-related activity (Fig. 1.2). Importantly, the activity began to ramp already during the motion presentation epoch, leading the authors to suggest that LIP neurons are accumulating the motion evidence provided by area MT. Similar observations were made in a RT version of the task with either two choice targets (Roitman & Shadlen 2002) or four (Churchland, Kiani & Shadlen 2008).

Two experiments primarily lent support to the hypothesis that LIP is integrating motion evidence. In the first, Huk and Shadlen (Huk & Shadlen 2005) used a RT version of the task but introduced a small amount of motion in addition to the primary motion stimulus, in the form of a weak background motion pulse. The prediction was simple: if LIP reflects integrated motion evidence, then the additional evidence should be reflected in LIP firing a sustained (as opposed to transient) manner, as well as in the behavior. Indeed, the effect of the motion pulses was sustained in LIP activity, and manifest in both psychometric and chronometric functions of the monkey, consistent with an integration role for LIP. In the second experiment, Hanks et al. (Hanks,

Ditterich & Shadlen 2006) used microstimulation to excite LIP neurons during the motion presentation epoch of the direction discrimination task. They found that microstimulation shortened response times in both monkeys, and shifted the proportions of choices in favor of the target in the microstimulated LIP RF (in one of the two monkeys). Reduction in RT and increased choices to the target in the RF of microstimulated LIP neuron is consistent with a facilitation of the integration process, where the slope of the ramping response is increased. However, the results from this experiment should be interpreted with caution. First, microstimulation may recruit areas other than LIP via antidromic stimulation. Second, the reduction in RT and increase in choices can be explained in multiple forms outside the evidence accumulation framework (detailed in Chapter 4). Nevertheless, results from these two experiments, in conjunction with many others (Yang & Shadlen 2007, Kiani et al. 2008, Kira, Yang & Shadlen 2015), were interpreted as explicit evidence for LIP's causal role in decision making.

1.3.2.3 Problems in linking LIP to decision formation

First and foremost, no study to date has evaluated the effect of LIP inactivation on decision-making, despite 20 years of LIP investigation. If LIP is causally related to the accumulation of evidence, removal of LIP during a motion direction discrimination task is expected to negatively impact subject sensitivity. In experimental contexts other than direction discrimination, inactivation of LIP produces small but reliable effects. In visual search tasks, inac-

tivation in LIP impairs search times for targets placed in the the contralesional hemifield (Wardak, Olivier & Duhamel 2002, Balan & Gottlieb 2009, Liu, Yttri & Snyder 2010). This effect is observed regardless to whether the response is made with an eye movement or lever release (Wardak, Olivier & Duhamel 2004). In "free-choice" tasks, where the subject is free to select between two or more targets, inactivation in LIP decreases the number of choices made to the contralesional hemifield (Wardak et al. 2002, Wardak et al. 2004, Balan & Gottlieb 2009, Wilke, Kagan & Andersen 2012, Kubanek, Li & Snyder 2015, Zirnsak, Chen, Lomber & Moore 2015), consistent with parietal lesions in humans (cortical neglect) (Kerkhoff 2001). Inactivation in LIP can also impair oculomotor processing in a memory guided saccade task, leading to reduced saccade accuracy (Li, Mazzoni & Andersen 1999) or increased saccade reaction time (Liu et al. 2010) to targets presented in the contralesional hemifield. (A comprehensive review of causal manipulations performed in LIP — inactivation and microstimulation — are presented in table 4.3, Chapter 4). With no direct evidence that LIP is necessary for the accumulation of sensory evidence, experiments that treat it as such run the risk of being misguided. The decision-related activity in LIP could instead be an echo of computations taking place elsewhere or a feedback signal from higher brain regions (Crowe, Goodwin, Blackman, Sakellaridi, Sponheim, MacDonald & Chafee 2013, Balan & Gottlieb 2009, Sarma, Masse, Wang & Freedman 2015).

A second problem in tying LIP function to evidence accumulation relates to the aforementioned diffusion model. The model was well-aligned with

the hypothesis that LIP integrates noisy sensory evidence from MT (Mazurek et al. 2003, Ditterich, Mazurek & Shadlen 2003, Ditterich 2006*b*, Ditterich 2006*a*, Huk & Shadlen 2005, Gold & Shadlen 2007) and was often referenced in experimental studies as a good match for LIP firing (Gold & Shadlen 2001, Gold & Shadlen 2002, Shadlen & Gold 2004, Gold & Shadlen 2007, Shadlen & Kiani 2013). Indeed, I invite the reader to compare the average firing rates of LIP neurons during the ramping phase in Figure 1.3A to the example drift rates (dashed arrows) in Figure 1.1. However, despite the diffusion model's qualitative match to LIP response, there are multiple arguments against its use to model LIP.

First, the average firing in LIP was taken to represent the log likelihood ratio (logLR) between the two decision alternatives, captured by the diffusion model (Gold & Shadlen 2001, Gold & Shadlen 2002, Yang & Shadlen 2007, Kira et al. 2015, Gold & Shadlen 2007, Shadlen & Kiani 2013). However, a careful manipulation of decision-*irrelevant* factors (removing the two saccadic choice targets) reduces LIP firing rate substantially (Meister, Hennig & Huk 2013), indicating that the spike rate in LIP cannot only be a correlate of the logLR as it also carries signals that are unrelated to accumulation. Second, many models that do not call for temporal integration of information per se, can still fit average LIP firing very well. Ditterich et al. (Ditterich 2006*b*) compared a large number of models— with and without temporal integration— and found that regardless of model choice, the problem is simply ill posed because the psychophysical data do not sufficiently constrain the model choice.

Thus, while the diffusion model is a fair choice, it is as fair a choice as any. Additionally, even though average LIP responses are explained fairly well by the diffusion model (or variants of the model), it has not been directly applied to *single* trial dynamics until very recently (Latimer, Yates, Meister, Huk & Pillow 2015) (but see Churchland, Kiani, Chaudhuri, Wang, Pouget & Shadlen 2011, Bollimunta, Totten & Ditterich 2012). Latimer et al. used latent state modeling to test whether LIP neurons are better explained by a diffusion model (consistent with gradual accumulation of decision evidence) or by a stepping model. The group found that a large proportion of LIP cells were better modeled as stepping than diffusing, at odds with the evidence accumulation hypothesis (at least within the level of the single cell). Thus, LIP responses cannot be straightforwardly reconciled with either a diffusion process or the integration of sensory signals over time.

The third problem in linking LIP function to integration concerns the lack of functional connections between MT and LIP. Recall that LIP was originally proposed as a potential integrator because of its anatomical location: a nexus between motion sensors (MT) and oculomotor executers (FEF and SC). However, despite the frequent treatment of LIP as an MT integrator (Shadlen & Newsome 2001, Mazurek et al. 2003, Wong 2007, Gold & Shadlen 2007, Beck, Ma, Kiani, Hanks, Churchland, Roitman, Shadlen, Latham & Pouget 2008), LIP responses in the direction discrimination task occur with a 100ms latency compared to those in MT (Roitman & Shadlen 2002, Osborne, Bialek & Lisberger 2004, Huk & Shadlen 2005, Gold & Shadlen 2007). In addition, LIP

exhibits decision-related responses in tasks that do not rely on MT at all (Yang & Shadlen 2007, Kira et al. 2015). To date, there is no published account of any functional MT-to-LIP connection. If anything, there is stronger evidence for the reverse: feedback connections from LIP to MT have been demonstrated in attention tasks. Simultaneous recordings in areas MT and LIP revealed that LIP exhibits a ∼6ms phase lead in the spike train coherence compared to MT (gamma frequency range) (Saalmann, Pigarev & Vidyasagar 2007). A second study found that the attentional modulation of LIP spikes preceded that in MT by 60ms (Herrington & Assad 2010). In a recent study where six cortical areas were recorded simultaneously during a flexible decision-making task, LIP responses also precede MT's (Siegel et al. 2015). Thus, there is little direct evidence to support a role for LIP in integration of motion evidence from MT.

Fourth, LIP cells in many seminal papers were selected if and only if they exhibited persistent activity during the delay period of a memory guided delayed saccade task (Shadlen & Newsome 1996, Shadlen & Newsome 2001, Roitman & Shadlen 2002, Huk & Shadlen 2005, Janssen & Shadlen 2005, Hanks et al. 2006, Yang & Shadlen 2007, Churchland et al. 2008, Kiani et al. 2008, Kiani & Shadlen 2009, Law & Gold 2008, Bennur & Gold 2011, Hanks, Mazurek, Kiani, Hopp & Shadlen 2011). However, not only was this criterion subjective and unformalized, but only one quarter of LIP cells exhibit this persistent activity (approximated from: Gnadt & Andersen 1988, Hamed, Duhamel, Bremmer & Graf 2001, Barash, Bracewell, Fogassi, Gnadt & Andersen 1991*a*, Premereur, Vanduffel & Janssen 2011, Meister et al. 2013).

In addition, the criterion was not applied on the basis of a mechanistic understanding (e.g. cell type or cortical layer) but rather, on the basis of the temporal integration hypothesis. There was no evidence that the presence of persistent activity is correlated with decision-related activity. Indeed, Meister et al. found very little correlation between the degree of persistent activity and the degree of decision related activity (Meister et al. 2013). Inclusion of such an unconstrained subset of cells makes it difficult gain an understanding of LIP function as a whole, let alone relate these studies to experimental methods that target more than the select few cells, e.g. multi-unit recordings, imaging, local field potentials, microstimulation or inactivation.

Finally, decision-related activity is far from being the signature property of LIP neurons. In fact, LIP neurons have been implicated in a staggering number of functions other than those described thus far. These include (but are not limited to) the intention to execute an eye movement (Andersen et al. 1997), attentional allocation (Colby & Goldberg 1999), shape selectivity (Sereno & Maunsell 1998), reward (Platt & Glimcher 1999), stimulus color (Toth & Assad 2002), subjective value (Sugrue, Corrado & Newsome 2005), perceptual categorization (Freedman & Assad 2006), handedness (Oristaglio, Schneider, Balan & Gottlieb 2006), numerosity (Roitman, Brannon & Platt 2007), motion direction (Fanini & Assad 2009), decision confidence (Kiani & Shadlen 2009), decision bias (Hanks et al. 2011, Rao, DeAngelis & Snyder 2012), salience (Wardak, Olivier & Duhamel 2011), reaching movements (de Lafuente et al. 2015), and timing (Leon & Shadlen 2003, Janssen & Shadlen 2005,

Jazayeri & Shadlen 2015). Most likely, LIP neurons are multiplexing a number of signals, often within the same spike train (Huk 2012). Meister et al. used a visual manipulation during a decision-making task to show that LIP neurons multiplex at the very least, visual and decision-related activity (Meister et al. 2013). Some studies have succeeded in teasing apart multiplexed signals in LIP by virtue of clever experimental designs (Bennur & Gold 2011, Rishel, Huang & Freedman 2013), but a more general approach was recently presented by Park et al. who used regression-based methods to capture the contribution of individual signals to the overall neural code (Park, Meister, Huk & Pillow 2014). Without the use of sophisticated methods to tease apart the decision-related activity, studies may be mischaracterizing the observed activity in LIP.

1.4 Next steps

Taken together, despite a large number of studies promoting LIP as a neural integrator for decision formation, the evidence in favor of this hypothesis is tenuous. It is almost surprising that the hypothesis has never been put to the test directly. All the more so, in light of the explicit proposal to do so by the very authors who brought LIP into the decision-making spotlight in the first place:

"Obviously, we have not yet addressed the critical question of whether LIP plays a causal role in performance of this task. Microstimulation and inactivation techniques may allow us to investigate this possibility in future

experiments."

— Shadlen and Newsome, 1996

This sets the stage for the main experimental chapter of this thesis, Chapter 3, where I describe the results of reversibly inactivating LIP during a direction discrimination task.

Chapter 2

A Distinct Mechanism of Temporal Integration for Motion through Depth

This work has been published in the *Journal of Neuroscience* on July 15, 2015. Katz LN, Henning J, Cormack LK, Huk AC: A Distinct Mechanism of Temporal Integration for motion through depth. Journal of Neuroscience, 35(28): 10212-10216.

2.1 Abstract

Temporal integration of visual motion has been studied extensively within the frontoparallel plane (i.e., 2D). However, the majority of motion occurs within a 3D environment, and it is unknown whether the principles from 2D motion processing generalize to more realistic 3D motion. We therefore characterized and compared temporal integration underlying 2D (left/right) and 3D (toward/away) direction discrimination in human observers, varying motion coherence across a range of viewing durations. The resulting discrimination-versus-duration functions followed three stages, as follows: (1) a steep improvement during the first ∼150 ms, likely reflecting early sensory processing; (2) a subsequent, more gradual benefit of increasing duration over

several hundreds of milliseconds, consistent with some form of temporal integration underlying decision formation; and (3) a final stage in which performance ceased to improve with duration over ∼1 s, which is consistent with an upper limit on integration. As previously found, improvements in 2D direction discrimination with time were consistent with near-perfect integration. In contrast, 3D motion sensitivity was lower overall and exhibited a substantial departure from perfect integration. These results confirm that there are overall differences in sensitivity for 2D and 3D motion that are consistent with a sensory difference between binocular and dichoptic sensory mechanisms. They also reveal a difference at the integration stage, in which 3D motion is not accumulated as perfectly as in the 2D motion model system.

2.2 Introduction

Perceptual decision making is often explained in terms of the temporal integration of noisy sensory evidence (Barlow 1958, Laming 1968, Burr & Santoro 2001). In a well-studied random dot direction discrimination task (Newsome & Pare 1988), performance reflects near-perfect integration of noisy sensory signals over hundreds of milliseconds (Gold & Shadlen 2003, Palmer et al. 2005, Kiani et al. 2008). Previous work has focused on discriminations in which the axis of motion is on the fronto-parallel plane. For example, subjects may be asked to discern whether the dots translate left versus right or up versus down. Little, if anything, is known about whether the conclusions of such work in the frontoparallel (i.e., 2D) plane extend to the processing of

motion through depth — motions toward versus away from the observer — hereafter called "3D motion."

By measuring the effects of both the strength and duration of motion, prior work (Burr & Santoro 2001, Gold & Shadlen 2001, Palmer et al. 2005, Kiani et al. 2008) has shown that 2D over some nontrivial time range (between 250 and 2000 ms), during which discrimination sensitivity improves with the square root of viewing duration. Although this decision integration stage has received primary focus, it is likely to be bounded by earlier and later stages where sensitivity follows different dependencies on duration. For very short durations, sensitivity can increase more steeply with duration, reflecting the properties of early sensory-processing stages (Bair & Movshon 2004). For very long durations, sensitivity can stop improving with viewing du- ration and instead saturate (Watamaniuk & Sekuler 1992, Burr & Santoro 2001).

To compare the temporal integration of 2D and 3D motion, we measured accuracy as a function of stimulus duration and motion coherence for stimuli that were identical except for the axis of motion. Consistent with prior work, discrimination accuracy was typically higher for 2D than for corresponding 3D conditions (Tyler 1971, Brooks & Stone 2006). Sensitivity for both 2D and 3D direction improved rapidly over the first ∼150 ms of viewing duration, followed by a more gradual improvement from 150 ms to ∼1 s, until ultimately saturating. Although it is unlikely that motion processing relies on three absolutely separate stages, this pattern suggests distinguishable phases that are interpretable as an early sensory period, a later decision stage involving some

form of temporal integration, and a terminal period in which performance was basically constant.

During the early sensory period, 3D sensitivity was lower than 2D sensitivity but increased with duration in a similar manner, implying a lower signal-to-noise ratio for 3D sensory mechanisms. During the decision phase, 3D sensitivity was still lower than 2D, but increased with a shallower slope, indicating a less-than-perfect mechanism for integrating sensory evidence over time. Finally, 3D sensitivity stopped improving at a slightly later time, but still at a lower level than for 2D motion. Together, these results suggest that both sensory and decision components of discriminating 3D motion direction cannot be parsimoniously explained by what is known about frontoparallel motion processing, motivating further work to explain both the sensory and decision differences.

2.3 Methods

2.3.1 General Procedure

Data were collected from five observers (four males and one female; age range, 24–50 years; including three of the authors), all with good stereopsis and normal or corrected-to-normal vision. Experiments were undertaken with the written consent of each observer, and all procedures were approved by the University of Texas at Austin Institutional Review Board.

We characterized direction discrimination for 2D and 3D motion using a random dot kinetogram inspired by (Newsome & Pare 1988), which was

stereoscopically generalized so that motion could be controlled either on the x-axis (leftward/rightward; 2D) or the z-axis (toward/away; 3D) (Czuba, Rokers, Huk & Cormack 2010). 2D frontoparallel motion was generated by presenting the same motion direction to each eye. At high coherences, this generated a percept of many dots at various depths moving leftward/rightward. For 3D motion, opposite directions of motion were presented in the two eyes. At high coherences, this generated a percept of many dots at different depths flowing toward/away through a cylinder Fig. 2.1. Most monocular properties of the stimuli were there- fore identical, allowing us to compare 2D and 3D sensitivity in common stimulus units of motion coherence. Each subject completed between 10 and 20 sessions (mean, 15 ± 5 sessions). 2D and 3D motion types were presented in separate experimental runs. A total of 73,800 trials were collected across the five observers.

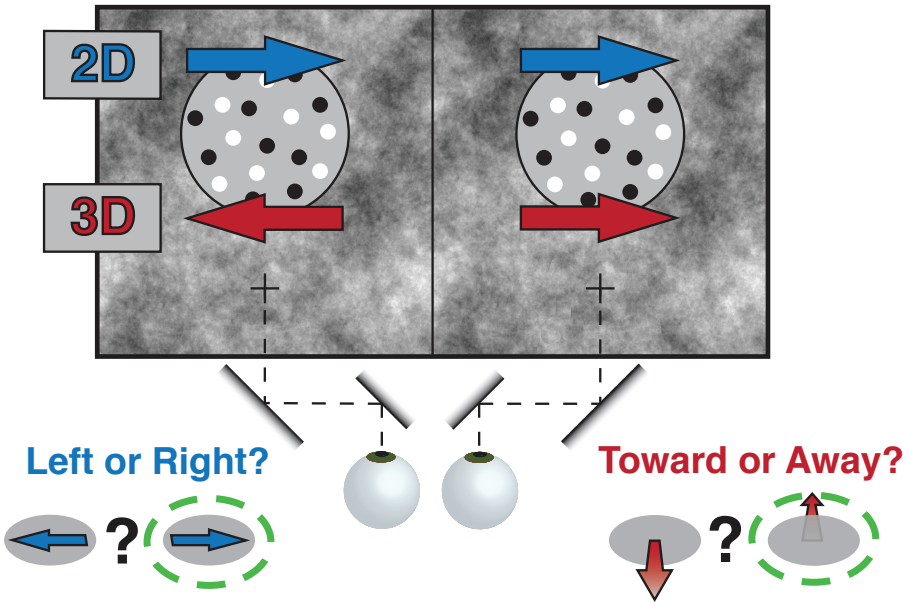

Figure 2.1: Subjects viewed the stimulus through a mirror stereoscope. Motion appeared in a circular aperture above the fixation cross. In the frontoparallel 2D motion condition, the two monocular views of the moving dots were identical except for fixed horizontal disparities. In the 3D motion condition, paired dots in the two monocular images moved in opposite directions from one another, consistent with motion-through-depth. Motion was presented at variable coherence values and for a variable duration. In this example, 2D motion is to the right; 3D motion is away from the observer (the correct answer is circled in green).

Each trial began with a 300 ms presentation of a fixation cross, followed by a motion stimulus of variable viewing duration and motion coherence. Observers reported the perceived direction of motion with a keypress. Auditory feedback was provided 700 ms after the response, and the next trial began 400 ms later. Within each run (360 – 600 pseudo- randomized trials), stimuli were drawn from one of six different motion coherences and two directions (rightward or leftward for 2D motion; toward or away for 3D motion). Motion coherence was defined as the proportion of coherently moving dots. Coherences were 3%, 6%, 12%, 25%, 50%, and 100%; one subject was presented with 1.5% coherence (and none were presented at 100%) due to especially high sensitivity.

Each coherence/direction parameter combination was presented over a range of durations. In the first round of data collection, durations were selected from a truncated exponential distribution to approximate a flat hazard rate (minimum of 33 ms/two monitor frames at 60 Hz; maximum of either 1.2 or 1.5 s). The distribution was divided into deciles from which durations were randomly selected to approximate an exponential shape. A total number of 69,000 trials was collected across all observers in this round. We performed a second round of data collection using longer viewing durations (uniform distribution, 300 – 6000 ms). Both phases were combined after verifying that performance did not differ on overlapping durations (likelihood ratio rest, $p = 0.999$). All subjects completed two runs with these longer durations for both 2D and 3D, netting 4800 trials across the five observers.

2.3.2 Display and stimulus

Stimuli were presented on a single linearized 42 inch LCD monitor (60 Hz, 1920 x 1080 resolution; LC-42D64U, Sharp) viewed through a 70 cm optical path of a mirror stereoscope. The monitor was confirmed to produce reliable refreshes and luminance additivity, and was driven by a Mac Pro computer with an NVIDIA GeForce 8800 GT video card. The stereoscopic stimuli (described in detail previously by Czuba et al. 2010) were generated using the Psychophysics Toolbox (Brainard 1997) and MATLAB (MathWorks) version 2012a. Monocular half-images were presented separately on the left and right halves of the display, with a septum and baffles. Each half-image (sub- tending 30) had a white fixation dot in the center of a small central square (1.0), with horizontal (black) and vertical (red) nonius lines located 2 off-center of each monocular half-image. To further aid fixation and binocular alignment, static 1/f noise texture was presented in the background of the fixation square and stimulus aperture.

The random dot stimulus (6 diameter aperture, centered 5 above fixation) consisted of 40 uniformly distributed and binocularly paired moving dots (average density, 1.4 dots/degree2; Michelson contrast of 0.3 on a middle gray background). Half the dots (9 arcmin diameter) were dark, and half were bright (19.5 and 36.5 cd/m2, respectively). Individual dots subtended a visual angle of 9 arcmin, and each dot moved at a monocular speed of 1.0/s, with a maximum lifetime of 250 ms. Dots reaching the edge of the stimulus volume before their lifetime expired were "wrapped" to the opposite end. Dot

disparities were constrained to uniformly span a cylindrical volume ±0.7 from the plane of fixation. For 2D conditions, each dot was at a fixed disparity and moved along the frontoparallel plane; for 3D conditions, each dot moved along the z-axis within a volume that spanned the same range of disparities as for the 2D conditions. The different wrapping contingencies between 3D and 2D decreased the 3D lifetimes by one to two video frames compared with the 2D dots, but this small lifetime difference had no measurable consequences on direction discrimination performance over time as assessed in other experiments (data not shown), in line with previous studies (Scase, Braddick & Raymond 1996, Festa & Welch 1997).

2.3.3 Data analysis

Data were analyzed in Python, and used the pandas, numpy, scipy, and pypsignifit packages (Fründ, Haenel & Wichmann 2011). Figures were generated in MATLAB (Mathworks) version 2014a. All code is available at https://huklab.github.io/3d-integ.

Each subject contributed at least 3400 trials in a given condition (2D or 3D), although the exact number of trials varied because subjects completed different numbers of runs. To compute the average across all subjects, we sampled 3400 trials (with replacement) from each subject and then combined the data across all five subjects, resulting in 17,000 trials contributing to the averages. In all analyses, we discarded trials with viewing durations or motion coherences that were not shown to every subject, leaving a total of 61,500

trials (57,500 from the initial round of data collection, 4000 from the second round). All reported confidence intervals (CIs) were generated as bootstrapped estimates of ±1 SEM (i.e., the central 68.2%).

To assess the effect of motion coherence (x) on accuracy, we fit psychometric functions of logistic form to trials from each duration bin, with lower bound 50% and upper bound (1- λ), as follows:

$$P(x) = \frac{1}{2} + (\frac{1}{2} - \lambda)(1 + e^{-4\log(3)(x-m)/w})^{-1}$$

This is a three-parameter fit where m and w represent the midpoint and width of the curve, respectively, along with an additional parameter specifying a stimulus-independent lapse rate, λ. These parameters were fit using the Bayesian inference framework in pypsignifit, with priors m $\approx$ normal(0, 5), w $\approx$ normal(1,3), $\lambda \approx \beta$ (1.5, 12).

We extracted the 75% motion coherence threshold as the numerical inverse of the fitted psychometric function where P(x) = 0.75. Error bars were calculated from 10,000 bootstrapped thresholds.

To characterize motion sensitivity as a function of duration, we divided the distribution of motion durations into 20 equal quantiles, computed a threshold for each bin, defined sensitivity as the inverse of threshold, and fit sensitivity values versus duration using a continuous trilimb function on logarithmic coordinates. The slope of the third line was fixed to zero. Given the constraint of continuity, sensitivity as a function of stimulus duration, with

five free parameters, becomes the following:

$$f(x) = \begin{cases} S_0(t/t_{1\longrightarrow 2})^{m_1}(t_{2\longrightarrow 3})^{m_2}, & t \leq t_{1\longrightarrow 2} \\ S_0(t_{2\longrightarrow 3})^{m_2}, & t_{1\longrightarrow 2} < t \leq t_{2\longrightarrow 3} \\ S_0, & t > t_{2\longrightarrow 3} \end{cases}$$

where the elbow points $t_{1\longrightarrow 2}$ and $t_{2\longrightarrow 3}$ specify the transition times between the three line segments; m_1 and m_2 are the slopes of the first and second phases (recall that the third phase is fixed at zero slope); and S_0 is the asymptotic sensitivity (i.e., accuracy in the third phase).

We could not confidently obtain sensitivity estimates in the two shortest duration bins of the 3D condition because accuracies in this range did not reach the threshold value of 75% correct. These data points were excluded from analysis.

2.4 Results

Subjects stereoscopically viewed a random dot motion stimulus and discriminated between two possible directions of motion. In the 2D motion (frontoparallel) condition, the coherent dots moved either leftward or rightward. In the 3D motion (motion-through-depth) condition, coherent dots moved through depth either toward or away from the observer (Fig. 2.1). From trial to trial, we manipulated the proportion of coherently moving dots similarly in both 2D and 3D motion conditions, allowing sensitivity comparisons between the two motion types in common units of motion coherence.

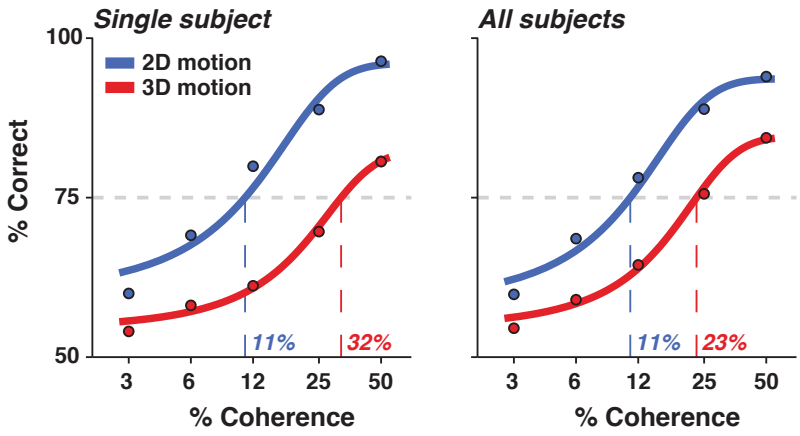

Figure 2.2: Psychometric function for a single subject (left) and for all five subjects (right), for both motion conditions. The proportion of correct responses as a function of motion coherence for 2D (blue) and 3D (red), over all stimulus durations. Thresholds are indicated on the x-axis. Error bars of ±1 SEM are often smaller than the rendered data points

Accuracy for both 2D and 3D direction discrimination improved with motion coherence (Fig. 2.2) shows the overall psychometric functions, combining all stimulus durations). Consistent with previous reports of "stereomotion suppression", 2D direction discrimination was superior to 3D (Tyler 1971, Brooks & Stone 2006). Average discrimination thresholds were 11% coherence for 2D motion and 24% coherence for 3D motion (68% CIs, 10.8–11.0 and 23.4–24.1, respectively).

2.4.1 Discrimination accuracy depends on motion coherence and viewing duration

Viewing duration also affected discrimination accuracy for both 2D and 3D motion. Accuracies for 2D and 3D motion (as a function of both duration and coherence) are shown as surfaces in Figure 2.3, A and B, respectively. Accuracy increased with either motion coherence or duration. The effect of duration on the psychometric function (i.e., slices of the surface parallel to the motion coherence axis) is illustrated for four sample duration ranges (Fig. 2.3, C, D).

For 2D motion, accuracy increased steeply as a function of motion coherence and reached perfect or near-perfect levels, even at viewing durations as short as 67–83 ms (Fig. 1E, green curve). Thresholds were 4%, 8%, 15%, and 24% coherence for the four sample duration ranges shown, confirming the systematic dependence of sensitivity on duration. This pattern also held for 3D motion, with thresholds of 12%, 18%, 40%, and 83% for the same four duration ranges, despite thresholds being overall higher than those for matched 2D conditions.

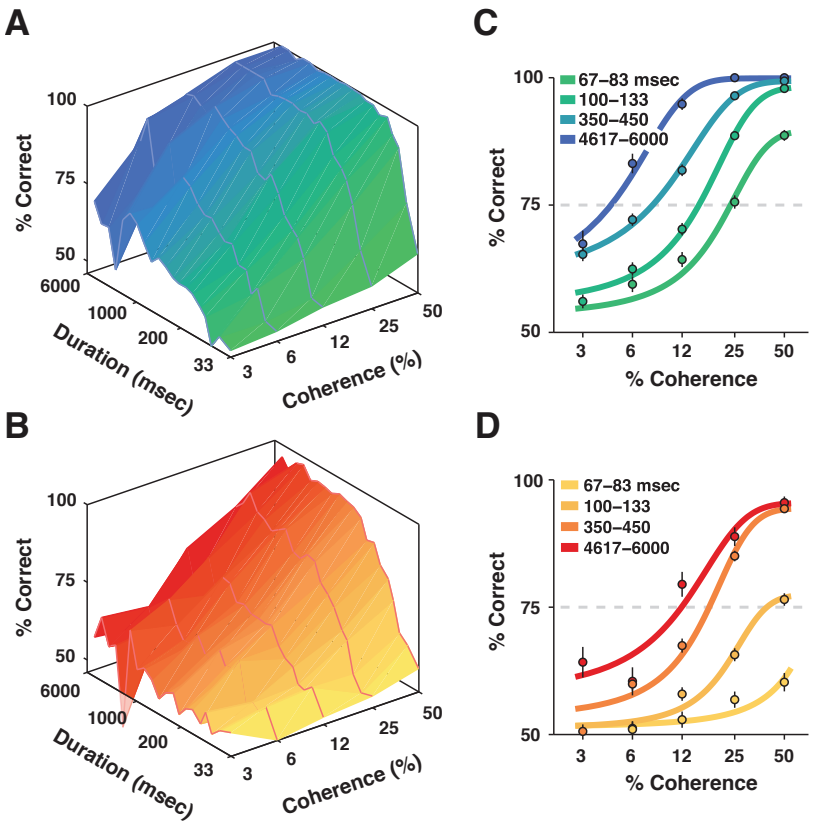

Figure 2.3: **A**, **B**, Surface plot shows the joint influence of motion coherence and motion viewing duration (x and y "floor" axes) for 2D (A) and 3D (B) direction discrimination accuracy (height). **C**, **D**, Slices from the surfaces can be taken to make sample psychometric functions for more conventional visualizations of these dependencies for 2D sensitivity (C) and 3D sensitivity (D). Each psychometric function was computed for a particular duration range, color coded to match the corresponding location on the surface plot. Only 4 functions are illustrated for clarity. Error bars of ±1 SEM are often smaller than the rendered data points.

2.4.2 Temporal integration of 2D and 3D motion

To more completely compare 2D and 3D temporal integration, we analyzed direction discrimination sensitivity (inverse threshold) across the full range of viewing durations (from a minimum of two video frames to a maximum of 6 s). These sensitivity-versus-duration functions are shown in Figure 2.4. For both 2D and 3D motion direction discrimination, sensitivity first increased steeply, followed by a more gradual increase over an intermediate range, capped by an asymptotic sensitivity level. For simplicity, we fitted trilimb piecewise linear functions to these curves. Although not a mechanistic model (nor an endorsement of cleanly discrete stages), the three linear regimes loosely map onto the following three distinguishable phases: first, a brief sensory phase where small increases in duration can have dramatic effects on direction sensitivity; second, a decision stage, where prolonged sampling of the stimulus benefits performance, given some form of temporal integration of noisy sensory evidence; and third, a final regime where prolonged viewing has no additional effect on performance. The trilimb fits describe these stages with five free parameters: slopes for the first (m_1) and second (m_2) limbs, transition times between the first and second ($t_{1\longrightarrow 2}$) and second and third limbs ($t_{2\longrightarrow 3}$), and an asymptotic sensitivity value (S_0).

The most obvious difference between the two functions, the vertical shift, captures the higher overall sensitivity for 2D motion over 3D motion. Despite this large offset in overall sensitivity, the transition times between stages were quite similar between 2D and 3D conditions. The median transi-

tion times from the first phase to the second, $t_{1\longrightarrow 2}$, were 136 ms for 2D and 171 ms for 3D (CIs, 86–149 and 141–194, respectively). Median $t_{2\longrightarrow 3}$ values were 983 ms for 2D and 1267 for 3D (CIs, 983–1040 and 1199–3110, respectively). Thus, it appears that in both types of motion the early sensory stage persists for $\sim$150 ms, which transitions to the decision phase until $\sim$1s, after which sensitivity ceases to benefit from longer viewing duration.

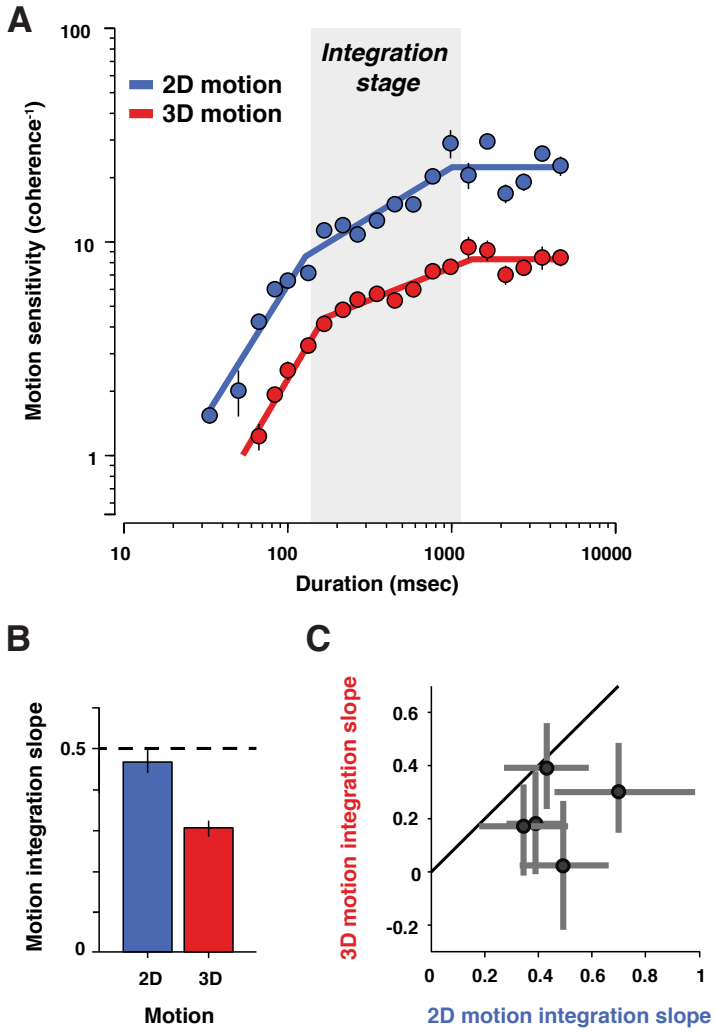

Figure 2.4: 2D and 3D motion sensitivity exhibit different patterns of dependency on duration. **A**, Sensitivity versus stimulus viewing duration for 2D motion (blue) and 3D motion (red), on logarithmic axes. Each data point is a sensitivity value derived from a psychometric function within a given stimulus duration range. The trilimb function fit describes the three stages of integration. The second stage (decision integration) is emphasized in gray. **B**, Best fitting slope values for the integration stage limb for 2D and 3D motion (perfect integration of noisy evidence indicated by the dashed line; slope, 0.5). Error bars indicate ±1 SEM. **C**, Individual subject integration stage slopes, for 2D motion (abscissa) and 3D motion (ordinate).

2.4.3 Integration of 3D motion is different than 2D motion

Despite similarities in the timings of transition points among the three stages, the slopes and intercepts revealed differences between 2D and 3D motion. The putative sensory stage had higher sensitivities for 2D than for 3D motion, but had similar m1 values of 1.23 and 1.30 (CIs, 1.11–1.54 and 1.10–1.60, respectively). The offset points to a lower sensory signal-to-noise ratio for 3D motion, but the similar slopes suggest commonality in temporal summation of the sensory mechanisms.

Of primary interest is the difference between integration slopes during the second (putative decision) stage (Fig 2.4 A). 2D motion had an m_2 value of 0.47, whereas the m_2 value for 3D motion was significantly shallower (0.31; CIs, 0.41–0.53 and 0.20–0.35, respectively). The 2D motion slope was close to 0.5 (Fig 2.4 B, dashed line), which is indicative of near-perfect integration of noisy evidence and is consistent with the results of prior studies of frontoparallel direction discrimination (Palmer et al. 2005, Kiani et al. 2008). The shallower 3D motion slope, in contrast, does not uniquely specify a particular integration mechanism but is clearly distinct from the frequently observed near-perfect integration for 2D motion. This difference was statistically reliable in four of five subjects when fit individually (Fig 2.4 C).

3D sensitivity did not continue to improve with viewing duration to levels comparable to those for 2D motion. Even though, if anything, the second phase of evidence accumulation may have continued for a slightly longer time than that for 3D (hitting an asymptote at 1267 ms, compared with 983 ms

for 2D), the final level of performance (S_0) for 3D (8.3 coherence^{-1}) was still significantly lower than that for 2D (22.4 coherence^{-1}; CIs, 8.0–8.8 and 21.5–23.6, respectively).

2.4.4 Support for the three-stage descriptive model

We have favored trilimb fits with two separate integration stages before saturation (Neri et al. 1998), but it is also conventional to consider a simpler bilimb fit with a single integration phase followed by an asymptotic regime (Watamaniuk & Sekuler 1992, Burr & Santoro 2001). We therefore compared the previously used bilimb and our proposed trilimb functions directly by fitting each to the data and evaluating the fitting errors (Fig. 2.5). For both 2D and 3D motion, the bilimb fit resulted in substantially larger residuals than the trilimb fit. This is not surprising given that the trilimb function has a larger number of parameters, but closer inspection reveals that the residuals for the bilimb fit ex- hibit a systematic pattern, beginning with a large negative lobe followed by a positive one. This is not apparent for the trilimb fits. The structure of these residuals implies that bilimb fits may underestimate the steepness of the temporal integration sensory stage—and, more critically, can overestimate the steepness of the decision phase. The first ∼150 ms of motion processing appear distinct enough from decision-related temporal integration to warrant care that the two phases be modeled separately in quantitative fits. Although we do not propose trilinear fits as a biophysically plausible model, we do favor them as a tractable descriptive form. That said, other functions

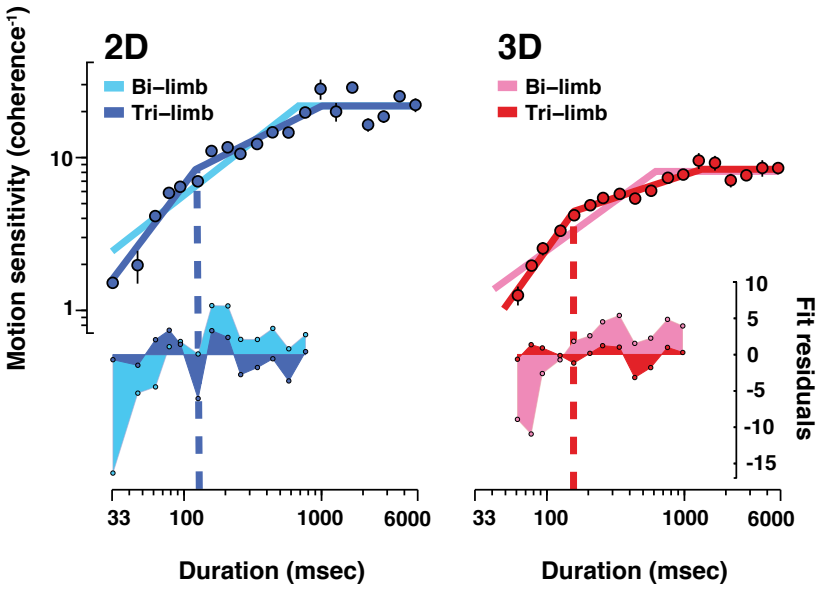

Figure 2.5: Comparison of a trilimb and bilimb fits for 2D motion (left) and 3D motion (right). Top, The two fits applied to data from Fig. 2.4 A. Bottom, Residuals for both fits (up until performance saturation). The dashed line represents the elbow point in the trilimb fit, at which a systematic change in bilimb residuals is evident (from underestimation to overestimation of slopes).

yield similar results. Saturating exponential fits also reveal that 2D integration is closer to perfect than 3D integration (time constants, 291 and 413 ms, respectively; CIs, 260–324 and 377–457 ms, respectively). Furthermore, a model-free comparison that does not enforce distinct phases also supports differential integration: the log-difference between 2D and 3D sensitivities (across all durations for which thresholds could be estimated) is approximately linear with non-zero slope (slope, 0.34; CI, 0.32–0.35).

2.5 Discussion

Our characterization of 3D direction discrimination revealed several important differences from the well-established near-perfect integration of 2D (frontoparallel) motion. First, 3D sensitivity was lower than 2D sensitivity across all viewing durations, consistent with a lower sensory signal-to-noise ratio. Second, decision formation for 3D motion deviated significantly from lossless accumulation of noisy evidence. A similar distinction has been noted for complex motions that were not stereoscopic, but were consistent with motion through depth (Burr & Santoro 2001).

Although our results do not definitively reveal why the discrimination of motion through depth does not rely on the near-perfect temporal integration that is so often found for frontoparallel motion, the differential ecological importance of toward/away versus left/right motions may underlie this stark difference. Motion directly approaching the head captures attention automatically (Lin, Murray & Boynton 2009), warrants immediate action, and may thus be more amenable to processing on very brief time scales. Put another way, humans might not integrate perfectly beyond 200 ms simply because there is rarely pressure to do so; any required action will have already been initiated. On the other hand, although less perfect integration for 3D motion was evident in all subjects, it certainly remains possible that 3D integration might approach 2D integration with more extensive training or instruction.

Relatedly, our 3D motion stimuli contained both disparity-based and velocity-based cues to motion through depth, which have been shown to op-

erate in different regimes with respect to speed and eccentricity (Czuba et al. 2010). It is possible that they also exhibit a different reliance on temporal integration. Future work will be required to understand the differential contribution of these cues to the integration of motion through depth, the impact of monocular cues (e.g., changes in size and looming), and the neural mechanisms subserving this process. Our work here raises the intriguing possibility that 3D motion perception may differentially depend on different sources of information as a function of time and the integration demands of the task at hand. It now seems imperative to understand why signals that are likely to have more direct behavioral and ecological importance are decided upon by a distinct integration scheme that is mathematically less ideal.

Chapter 3

Dissociated functional significance of decision-related activity across the primate dorsal stream

Here I report results from an experiment performed in rhesus macaque. We performed electrophysiological recordings and reversible pharmacological inactivations to ascertain the role of the lateral intraparietal (LIP) cortex in decision making. This work has been submitted for publication and is under review, Katz LN, Yates JL, Pillow JW, Huk AC.

Because the format of our submission is brief, I have included further data analyses and discussion in the following Chapter (Chapter 4). Some figure references in the text below will refer to figures in Chapter 4, where a detailed description may be found.

3.1 Abstract

During decision-making, neurons in multiple brain regions exhibit responses that are correlated with decisions (Britten et al. 1996, Shadlen & Newsome 2001, Gu, DeAngelis & Angelaki 2007, Ding & Gold 2013, Liu, Gu, DeAngelis & Angelaki 2013, Hanks et al. 2015). However, whether or not var-

ious forms of decision-related activity are causally related to decision-making remains uncertain (Nienborg & Cumming 2010, Cohen & Kohn 2011, Pitkow, Liu, Angelaki, DeAngelis & Pouget 2015). Here we test the functional significance of decision-related activity by recording and reversibly inactivating the lateral intraparietal (LIP) and middle temporal (MT) areas of rhesus macaques performing a motion direction discrimination task. Neurons in area LIP exhibited firing rate patterns that directly resemble the evidence accumulation process posited to govern decision making (Shadlen & Newsome 2001, Brunton, Botvinick & Brody 2013), with strong correlations between their response fluctuations and the animal's choices. Neurons in area MT, in contrast, exhibited weak correlations between their response fluctuations and animal choices, and had firing rate patterns consistent with their sensory role in motion encoding (Britten et al. 1996). The behavioral impact of electrophysiological inactivation of each area was inversely related to their degree of decision-related activity: while inactivation of neurons in MT profoundly impaired psychophysical performance, inactivation in LIP exerted no measurable impact on decision-making performance, despite having inactivated the very clusters that exhibit strong decision-related activity. Although LIP inactivation did not impair psychophysical behavior, it did influence spatial selection and oculomotor metrics in a free-choice control task. The unaltered performance in the decision-making task was stable over trials and sessions, ruling out several forms of compensation, and was robust to changes in stimulus type and task geometry. Thus, decision-related signals in LIP may not be necessary

for computing perceptual decisions. If they are, then downstream "read out" mechanisms must be more flexible and/or different than traditionally assumed. More broadly, our findings reveal a dissociation between decision correlation and causation, showing that even strong neuron-decision correlations may reflect secondary or epiphenomenal signals, which do not necessarily constitute a computational crux for task performance.

3.2 Methods

3.2.1 Monkey preparation

We performed electrophysiological recordings and reversible inactivations in the middle temporal (MT) and the lateral intraparietal (LIP) cortices of two rhesus macaques (subject N and subject P), aged 10 and 14 years, weighing 7.7 and 10 kg, respectively. Subject N had a single custom-machined titanium chamber that enabled access to both MT and LIP on the right hemisphere, guided by MRI. Subject P had a cilux chamber (Crist Instruments) over the right LIP and another over the left MT. Standard surgical procedures were applied (Meister et al. 2013). All experimental protocols were approved by The University of Texas Institutional Animal Care and Use Committee and in accordance with National Institute of Health standards for care and use of laboratory animals.

The subject sat comfortably while head-posted in a primate chair (Crist Instruments), facing a linearized 55 inch LCD (LG) monitor (resolution = 1920 x 1080p, refresh rate = 60Hz, background luminance = 26.49 cd/m2) at a dis-

tance of 118cm, in a dark room. Eye position was recorded using an Eyelink eye tracker (SR Research), sampled at 1 kHz. A solenoid-operated reward system was used to deliver liquid reward to the monkey. Stimuli were generated by using the Psychophysics Toolbox (Brainard 1997) in MATLAB (The MathWorks), and task events and neural responses were recorded (Plexon) using a Datapixx I/O box (Vpixx) for precise temporal registration. All of these systems were integrated using the PLDAPS system developed in our lab (Eastman & Huk 2012).

3.2.2 General procedure and experimental design

Recording sessions in either MT or LIP began by lowering an electrode to the known location of the area based on previous mapping and recording sessions. Anatomical identification (MR guided in monkey N; previously established in monkey P, Meister et al. 2013) was followed by functional identification (mapping receptive/response fields (RF) of MT and LIP neurons, detailed below). Inactivations of either area began by lowering both a cannula and multichannel electrode to the region of interest, collaterally, at least 1mm apart. The electrode was used to (i) confirm that the cannula is within the target cortex, (ii) to record electrophysiological responses to relevant task events pre-infusion, and (iii) to confirm the electrophysiological silencing of neurons during and after the infusion. Thus, while it is not feasible to precisely measure the inactivated proportion of an area, we do confirm the silencing of a large swath (>1mm radius), on every session (detailed in Inactivation Proto-

col, below).

MT inactivation was predicted to disrupt motion perception within a specific region of contralateral space, consistent with MT retinotopic organization (Newsome & Pare 1988, Chowdhury & DeAngelis 2008). The behavioral consequence of MT inactivation was measured by comparing psychophysical performance in the direction-discrimination task, before and after muscimol infusion, within the same experimental session, with the motion stimulus placed inside the inactivated region of space. LIP inactivation was predicted to disrupt spatial selection to contralateral space more generally (Wardak et al. 2004, Balan & Gottlieb 2009, Wilke et al. 2012, Erlich et al. 2015, Zirnsak et al. 2015), noting that LIP RF are large and that the topographic organization is less precise than in earlier visual areas (Patel, Shulman, Baker, Akbudak, Snyder, Snyder & Corbetta 2010). The behavioral consequence of LIP inactivation was measured by comparing the proportion of contralateral choices in a double-target memory-guided "free-choice" task, before and after muscimol infusion, within the same session. To measure the impact of LIP inactivation in the direction-discrimination task, we compared psychophysical performance between a pair of sessions, baseline and treatment, in which the treatment session was a muscimol, saline, or sham treatment. The paired sessions took place at the same time of day and after a similar number of tasks and trials, either 1 day apart (n = 28) or 2-3 days apart (n = 6), to minimize the impact of within-session fatigue or motivation on behavior. behavioral data for the muscimol treatment sessions were collected 15 - 30

minutes after infusion end, and typically completed within 150 minutes.

3.2.3 Direction discrimination task

The principal task employed in all session types was a motion direction discrimination task. Subjects were required to discriminate the net direction of a motion stimulus and communicate their decision with an eye movement to one of two targets. The sequence of task events is presented in Fig. 1a. The timing of each event was randomly jittered from trial to trial (Fig. 3.1 B). A trial began with the appearance of a fixation point. Once the monkey acquired fixation and held for 400 - 1200ms (uniform distribution), two targets appeared and remained visible until the end of the trial. 200 - 1000ms after target onset, the motion stimulus was presented at an eccentricity of 5 - 7° for 1050ms. The fixation point was extinguished 200 - 1000ms after motion offset, and the subject was required to shift its gaze towards one of the two targets within 600ms (saccade end points within 3° of the target location were accepted).

We used a reverse-correlation motion stimulus inspired by the classic moving dots stimulus (Newsome & Pare 1988) in which motion was in either one direction or the opposite, with varying motion strength. The motion stimulus consisted of 19 non-overlapping Gabor elements arranged in a hexagonal grid (5-7° across, scaled by eccentricity). The individual elements were set to approximate the RF size of a V1 neuron and in total, the grid approximated the RF size of an MT neuron. Motion was presented by varying the phase

of the sine-wave carrier of the Gabors. Each Gabor underwent a sinusoidal contrast modulation with independent random phase to prevent pop-out effects of individual drifting elements. Gabor spatial frequency (0.9 cycles/$^\circ$, sigma = 0.1 x eccentricity) and temporal frequency (7Hz for monkey N, 5Hz for money P, yielding velocities of 7.77 and 5.55° /s, respectively) were selected to match the approximate sensitivity of MT neurons.

Each trial consisted of seven consecutive motion pulses lasting 150ms each (9 video frames), producing a pulse sequence of 1050ms in duration. On any given pulse X_i, a number of Gabors would drift their carrier sine-waves in unison to produce motion (signal Gabors), and the remaining would counter-phase flicker (noise Gabors). Signal Gabors on pulse X_i were assigned at random within the grid and all signal Gabors drifted in the same direction.

Motion strength was defined as the proportion of signal Gabors out of the total, the value of which was drawn from a Gaussian distribution, $X_i \sim N(\mu_k, \sigma)$ and rounded to the nearest integer, where μ_k was set to one of five values: -50%, -12%, 0%, 12%, and 50% (negative sign indicates motion in the opposite direction), and σ was set to 15%. Thus, while each pulse within a sequence could take on any value (or sign) from distribution $N(\mu_k, \sigma)$, the expectation of a sequence would be μ_k. Motion strength was then z scored over all sessions, for each monkey separately.

On the motion strength axis, we use positive values to indicate motion towards the hemifield contralateral to the LIP under study, and negative values to indicate motion towards the hemifield ipsilateral to the LIP understudy.

We use the term "Proportion choices" to refer to the proportion of choices towards the contralateral target. For consistency, we maintain this convention throughout the paper, such that even on MT inactivations sessions, psychometric performance is evaluated in relation to the LIP under study.

The monkey was rewarded for selecting the target consistent with the sign of the pulse sequence sum, independent of the distribution k from which they were drawn. On trials that summed to exactly zero, the monkey was rewarded at random. 10% of trials consisted of a frozen random seed, generating identical pulse sequences. In addition to the direction discrimination task described here, we performed a subset of experiments (n = 2) using the classical moving dots stimulus (Newsome & Pare 1988) (Fig. 3.7).

3.2.4 Free choice task

A free choice task was used to measure spatial bias to one target over another and confirm a behavioral consequence of LIP inactivation (Wilke et al. 2012, Erlich et al. 2015, Zirnsak et al. 2015). The sequence of events within the free-choice task is illustrated in Fig. 3.6 A and B. Trials began with the appearance of a central fixation point. At a random time after acquiring fixation (500 - 900ms), two targets were simultaneously flashed for a brief 200ms. Subjects were required to maintain fixation until the fixation point disappeared (600 to 3,000ms after target flash), and then saccade to either of the remembered locations of the two targets. On every trial, target position was determined independently from one another and at random, drawn from

a 2D Gaussian with a mean of either [-12, 0] (left target) or [12, 0] (right), and a standard deviation of 2 - 4° for x and 3 - 5° for y position. Means and standard deviations were sometimes adjusted online to better position the distributions within the LIP RF (when recorded) or LIP inactivated field (when inactivated).

A trial was successfully completed when the monkey's saccade entered a circular window (unobservable to the monkey) around either target and held for 300-500ms (window radius scaled by 0.35° x eccentricity, minimum: 3). Successfully completed free-choices were rewarded on 70% of trials irrespective of the target chosen for monkey N, and 100% of trials for monkey P. Monkey N also performed memory-guided saccades to single targets (30% of trials, randomly interleaved) that appeared randomly in space (uniform distribution), and were rewarded 100% of the time. The adjustments in subject N's task were performed to prevent a spatial bias and decrease feedback reliability that may otherwise influence the subject. Overall performance and inactivation effects were similar between monkeys despite subtle differences in task parameters.

3.2.5 behavioral analysis

All analyses were performed in Matlab (The Mathworks). Responses in the direction discrimination task were analyzed with a maximum likelihood fit of a two parameter logistic function (Wichmann & Hill 2001) assuming a Bernoulli distribution of binary choices, in which the probability of a contralateral choice is P and ipsilateral choice is 1 - P, where P is given by:

$$P = \frac{1}{1 + e^{-\beta(x-\alpha)}}$$

where x is the motion strength value (z-scored over all sessions for each monkey separately; positive values indicate rightward motion), α is the logistic function shift parameter (reflecting the midpoint of the function, i.e., bias, in units of motion strength), and β is the slope (i.e., sensitivity, in units of log-odds per motion strength). Error estimates on the parameters were estimated from the hessian numerically. A four-parameter model including sub-perfect response rates for the top and bottom asymptotes (Erlich et al. 2015) was also considered, but did not confer any advantage over the two-parameter model nor change analysis results, and so we focus on the simpler 2-parameter fit (see Table 4.2). The first 10 - 30 trials of every session were excluded from analysis because motion strength was maximal to "warm up" the animal. Median session length for all baseline and treatment sessions was 409 trials. Sessions were excluded from analysis if the animal either completed less than 250 trials or performed poorly (lapse rate $> 10\%$). For inactivation sessions, all sessions were included regardless of performance. A single inactivation session in monkey P was aborted due to a leak in the infusion system, and was not included in the analysis.

Animal strategy in the direction discrimination task (Fig. 2f and 2g) was measured by computing psychophysical weights via logistic regression, where the probability of the binary choice Y 0,1 on every trial is given by

$$P(Y|w,X) \;=\; e^{YXw} \;/\; (1+e^{Xw})$$

where X is a matrix of the seven pulse values on each trial, augmented by a column of ones to capture the bias term, and w is a vector of the monkey's weights. w was estimated via maximum likelihood estimation using Matlab's glmfit function.

In the free-choice task, spatial bias was computed as the proportion of choices to the target contralateral to the LIP under study. Saccade onset and offset were detected in every task by identifying the time at which eye velocity exceeded 30 °/sec (onset) and returned below 50 °/sec (offset). We only analyzed saccades on trials where the task was completed successfully (i.e. no broken fixations and no saccades outside of the target windows). Saccades were analyzed for reaction time, amplitude, duration, and error amplitude (i.e. distance of saccadic end point from saccadic target). Saccadic reaction times less than 100ms from the go signal were excluded to ensure that only task relevant saccades are analyzed.

3.2.6 Neuronal recordings

Recordings were performed in areas MT and LIP with either single-channel glass coated tungsten electrodes (Alpha Omega) or multi-electrode arrays (Plexon U or V Probe). Neuronal signals were amplified, bandpass filtered, digitized, and saved (Plexon MAP server). Neural waveforms passing a manually-set threshold were isolated for online mapping of their receptive

fields (both MT and LIP) and directional tuning (MT).

MT RF locations were hand mapped using drifting dot stimuli in a circular aperture. Once the retinotopic location was identified, direction preference and selectivity were measured using drifting dot stimuli at 100% coherence in 12 directions. LIP RF locations were mapped with a memory-guided delayed saccade task (Gnadt & Andersen 1988).

In monkey P, offline spike sorting was performed by hand refinement of a standard clustering algorithm (Plexon Offline Sorter v3). Single unit isolation quality was established using SNR (Kelly, Smith, Samonds, Kohn, Bonds, Movshon & Lee 2007). In monkey N, spike sorting was performed by fitting a mixture of Gaussians model to clipped waveforms in a reduced dimensional space (Tolias, Ecker, Siapas, Hoenselaar, Keliris & Logothetis 2007). In both monkeys, sorting was refined by maximum a posteriori estimation of a model, where the multi-electrode voltage was the linear superposition of Gaussian white noise and the spike waveforms (Pillow, Shlens, Paninski, Sher, Litke, Chichilnisky & Simoncelli 2008, Pillow, Shlens, Chichilnisky & Simoncelli 2013).

3.2.7 Neuronal Analysis

Peri-stimulus time histograms (PSTHs) were computed by aligning spike times to events (motion onset or saccade time), binned at 10ms resolution, and smoothed with a Gaussian kernel with standard deviation of 25ms. Trial motion strengths were binned into three groups (low, medium,

high), where "low" was strengths between 0 and 0.25, "medium" was between 0.25 and 1, and "high" was anything greater than 1. We averaged spike rates separately for the three motion strengths for each choice. The buildup rate analysis (Fig. 3.2, inset) was performed according to Lafuente et al. (de Lafuente et al. 2015)

3.2.8 Choice Probability

Choice probability (CP) is a metric used to measure the predictive relationship between neural responses and choice, independent of stimulus strength. It is defined as the area under the receiver operating characteristic curve (ROC) for a pair of spiking response distributions sorted by choice (Celebrini & Newsome 1994, Britten et al. 1996). We quantified CP using trials that had zero expected motion and were repeated with identical random seeds (i.e. had no stimulus variation, "frozen noise"). Sometimes more than one random seed was repeated in a session, in which case we calculated the spiking response distributions for each seed separately, subtracted the mean, and then combined them, similar to an analysis known as Grand Choice Probability (Britten et al. 1996). Neurons with >25 "frozen" repeats were included (90/94 MT cells, 96/113 LIP cells), and significance testing against the null (i.e. CP=0.5) was performed using a Student t test. To compare to previous literature, in MT, we counted spikes over a window from motion onset to 200ms after motion offset (before the go signal). In LIP, we counted spikes over a 400ms window counting backwards from the 100ms before the saccade.

3.2.9 Infusion Protocol

Infusions were performed by lowering an infusion cannula into grid locations that had previously yielded the largest number of selective cells during the recording phase of the study (Figure 4.1). The cannula (31-32 gauge) was lowered alongside a multi-electrode array, at least 1mm away (Fig. 3.3 B). The two were lowered to target cortical areas where functional identification took place (mapping). Infusion was then performed, and electrophysiological silencing was confirmed on the recording electrodes, typically within 15 minutes of infusion start.

Infusions were performed with a syringe pump (Harvard Apparatus) through a single and direct line to the cannula (constant rate of 0.1-0.4μl/min, 15-30 minutes), in agreement with infusion parameters proposed by Noudoost and Moore (Noudoost & Moore 2011). We delivered 6.66-8μg/μl muscimol (in phosphate buffered saline) at volumes of 5-12 μl (mean 7.4μl), netting a total mass of 40-80μg (mean 56.4μg). This protocol was chosen to match the very high end of ranges used previously in order to maximize the probability of neural inactivation. Infusions were typically made at multiple depths within a single cannula track. On 5 of the 21 main LIP inactivation sessions, more than one cannulae were lowered (table 4.1). Cannluae were left in situ for at least 15 minutes after infusion end. Saline infusions followed the same protocol and included both a cannula and multi-electrode array. Sham infusions included only a multi-electrode array but followed similar timings, including the operation of the syringe pump with no syringe attached.

3.2.10 Spatial and temporal extent of Inactivation

Previous analyses of the spatial extent of muscimol inactivation have estimated the functional silencing to cover a spherical radius of roughly 2-3mm (Martin 1991, Arikan, Blake, Erinjeri, Woolsey, Giraud & Highstein 2002, Liu et al. 2010, Yttri, Wang, Liu & Snyder 2014). The study most comparable to ours, Liu et al. (Liu et al. 2010), co-infused muscimol and Manganese (Mn) into LIP of awake macaques and imaged the spread. They also estimated a cortical silencing of approximately 2-3mm in radius, in line with the linear dependence of volume distribution (mm^3) on infusion volume (μl) (Heiss, Walbridge, Asthagiri & Lonser 2010).

In our experiments, lowering both a multi-electrode array and infusion cannula collaterally (Fig. 3.3 B) enables direct confirmation of neural silencing at known distances from the cannula tip. This places a lower bound on the spatial extent of functional inactivation. Although our standard protocol placed the multi-electrode array 1mm away from the cannula tip, we sometimes lowered a second array, 2 or 3mm away. On these sessions too, we observed silencing on most recording channels. Taken together, we conservatively estimate neural inactivation in LIP to span a radius of at least 2.5mm, silencing large swaths of LIP while primarily targeting its ventral portion (Lewis & Van Essen 2000*b*, Liu et al. 2010).

On a few occasions, residual firing persisted despite near-complete silencing of electrophysiological activity (example shown in Fig. 3.3 B, voltage traces, channels 5 and 6). We tested the selectivity of residual firing with

the appropriate mapping task (motion for MT, memory guided saccades for LIP) and found that these spikes did not respond selectively, indicating that these residual spikes likely emanate from afferent fibers terminating within the inactivated area (Chapman, Zahs & Stryker 1991)

Previous LIP inactivation studies found no evidence to support within-session compensation that manifests behaviorally (Wardak et al. 2004, Balan & Gottlieb 2009, Liu et al. 2010, Yttri et al. 2014, Kubanek et al. 2015), (but see Wilke et al. 2012). In fact, studies that report the temporal effect of LIP inactivation find an increase in the lesion's impact over time, not a decrease (Wardak et al. 2004, Kubanek et al. 2015). Regardless, we measured the time course of psychophysical performance within a session (Fig. 4.5), and also measured for compensation on longer time scales, across sessions, to explore the possibility of increasing behavioral robustness to inactivation that might develop over time (Fig. 4.6).

3.3 Results

We investigated the functional significance of decision-related activity by recording and inactivating neural activity in two well-studied cortical areas, MT and LIP, while rhesus monkeys performed a challenging direction discrimination task. On each trial, the monkey maintained stable visual fixation while discriminating the net direction of motion, and then made a saccade to one of two choice targets to communicate their choice 3.1. For electrophysiological recordings in MT, we placed the motion stimulus in the receptive field of the

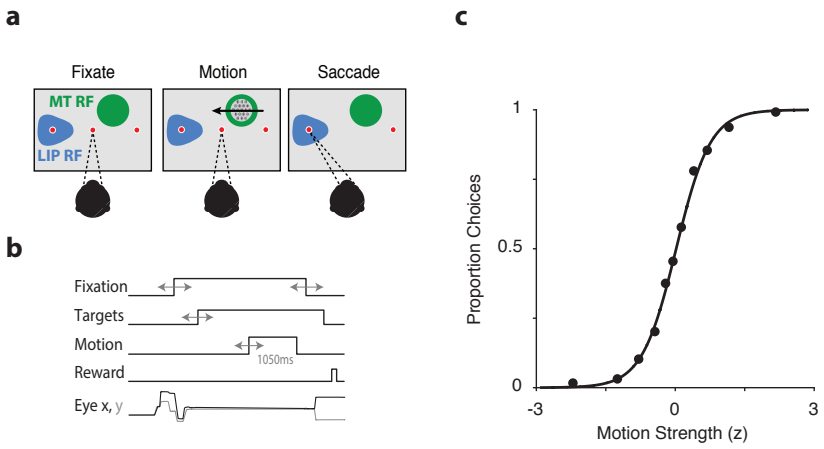

Figure 3.1: **A,** Monkeys were trained to discriminate the direction of visual motion and communicate their decision with a saccadic eye movement to one of two choice targets. For MT recordings, motion was placed in the MT receptive field (RF) (green patch). For LIP recordings, one of the saccade targets was placed in the LIP RF (blue patch). **B,** Sequence of task events. Gray arrows indicate temporal jitter. **C,** Psychophysical performance in the task. The proportion of choices (y-axis) made to the target contralateral to the LIP under study, as a function of motion strength (x-axis), where positive motion strength values represent motion towards the target contralateral to the LIP under study.

neurons and aligned it to the preferred direction of one or more MT neurons on the multi-electrode array. For LIP, we placed one of the two targets in the response field of the neurons, and the other target on the contralateral side of the visual field.

3.3.1 MT and LIP present canonical electrophysiological responses during direction discrimination

We recorded 157 MT neurons and 200 LIP neurons with either single electrodes or multi-electrode linear arrays. MT neurons that were well-targeted by the stimulus (n = 94) had average firing rates that depended on its motion strength and direction (Fig. 3.2, A). As expected in this area, responses increased sharply with motion onset and maintained a robust firing rate throughout motion viewing (Britten et al. 1993). The average responses of well-targeted LIP neurons (n = 113) were also consistent with classical observations (Shadlen & Newsome 2001, Huk & Shadlen 2005), exhibiting ramp-like increases or decreases in firing rate whose slopes were proportional to motion strength, the primary physiological characteristic that has implicated LIP in reflecting the accumulation of evidence over time (Fig. 3.2, B).

We further quantified the decision-related activity of MT and LIP using choice probability (Britten et al. 1996) (CP), a measure of correlation between neural activity and choice behavior, independent of stimulus-driven responses. MT neurons were weakly but reliably correlated with the animal's choice on a trial-by-trial basis (mean CP = 0.54, p = 1e-5; Fig. 3.2, C). LIP neurons were more strongly correlated with choices (mean CP = 0.70, p = 1e-21; Fig. 3.2, D). Thus, the stimulus-dependent responses and choice probability in MT were consistent with its well-established role in representing the motion stimulus, and the response patterns in LIP resembled the temporal accumulation of motion signals. Together, these properties have given rise to a model where

LIP neurons either integrate, or reflect the integration of, motion evidence from area MT in favor of a decision (Mazurek et al. 2003, Gold & Shadlen 2007).

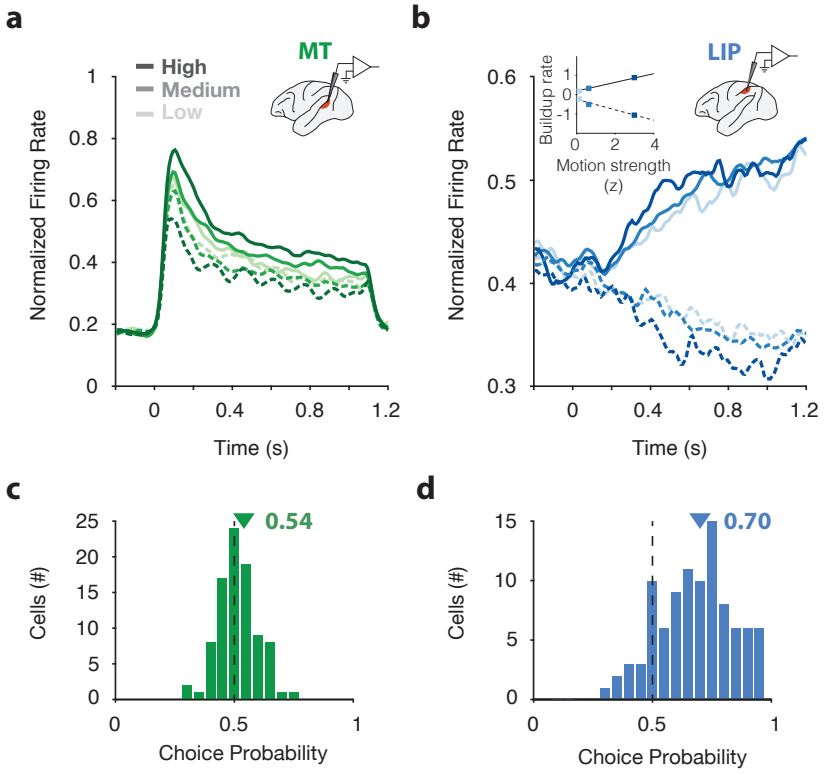

Figure 3.2: **A,** Average response of 94 MT neurons as a function of motion strength (low, medium, high, represented by shade) and direction (in and out of cell's preferred direction, solid and dashed lines, respectively), aligned to motion onset. **B,** Average response of 113 LIP neurons as a function of motion strength (same as in A) and direction (in and out of cell's RF, solid and dashed lines, respectively), aligned to motion onset. Inset graph shows LIP buildup rate as a function of motion strength (z-scored) during putative integration, for choices in and out of cell's RF, solid and dashed linear fits, respectively. **C,** Choice probability for 90 MT neurons computed during the motion epoch. Triangle indicates mean, 0.54. **D,** Choice probability for 96 LIP neurons computed during the motion epoch. Triangle indicates mean, 0.70. Only neurons with >25 repeats of identical stimuli were included in the choice probability analysis.

3.3.2 Inactivation in area MT, but not LIP, influences psychophysical behavior

Having confirmed the neurophysiological properties of areas MT and LIP and their differential degrees of correlations with choices, we tested their respective causal contributions by performing reversible inactivations in each area and evaluating the impacts on psychophysical performance (hypothesized outcomes shown in Fig. 3.3, A). We infused muscimol, a GABA-A agonist which hyperpolarizes cell bodies but not fibers of passage (Hess & Murata 1974) into either MT or LIP, at least 1mm away from a multi-electrode array Fig. 3.3, B). The injection cannula was targeted to locations that had yielded the largest number of canonical MT or LIP units during recording sessions (Fig. 4.1). The multi-electrode array was used to confirm standard physiological properties prior to infusion and post-infusion neural silencing, performed on every inactivation session. Silencing was typically observed across all recording channels of the array (Fig. 3.3, B) and estimated to span a spherical volume of 2.5mm radius (see Methods).

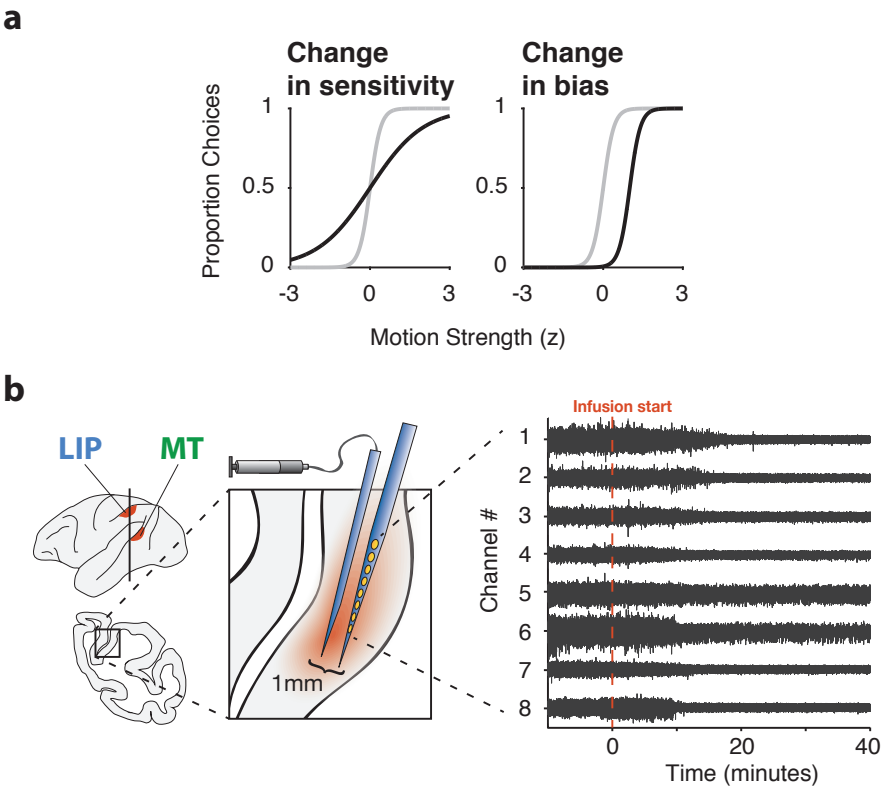

Figure 3.3: **A,** Potential consequences of inactivation that would be captured by changes in logistic model fits to the dependence of choices on motion strength and direction. Left, decreased psychophysical sensitivity would be indicated by a decrease in slope. Right, increased psychophysical bias would be captured by a shifted midpoint. Positive values in the x-axis, z-scored motion strength, refer to motion towards the target contralateral to the LIP under study. Appropriately, the y-axis refers to the proportion of contralateral target choices. This convention is maintained throughout. **B,** Schematic of the inactivation protocol. Left, A multi-electrode array was lowered alongside the cannula to identify target cortex, verify neural selectivity prior to infusion, and confirm neural silencing after. Right, continuous voltage traces from an example inactivation session.

Inactivations in area MT exerted large effects on psychophysical performance. The motion stimulus was placed within a region of visual space retinotopically matched to the inactivated population of MT neurons (Fig. 3.4, A). MT inactivations (n = 6) had a large and consistent impact on direction discrimination sensitivity (68.5% reduction from baseline, $t(5) = -9.7$, $p < 0.002$, paired t test). When the motion stimulus was moved outside the inactivated region and into the non-inactivated hemifield within the same session (n = 3), psychophysical performance was restored to pre-infusion levels, indicating spatial specificity consistent with the retinotopic organization of MT, and confirming that the effects were not due to general changes in arousal or vigilance. These severe and specific impairments in direction discrimination performance were consistent with prior causal perturbations (Newsome & Pare 1988, Chowdhury & DeAngelis 2008).

In contrast, inactivations in area LIP (n = 21) did not exert compelling or substantial effects on psychophysical performance (Fig. 3.4, B). In these experiments, we placed one choice target in the inactivated region of visual space, in line with previous electrophysiological investigations of LIP that place a choice target (as opposed to the visual motion stimulus) in the RF of the neurons to elicit the area's canonical decision-related responses. Although we performed large inactivations in locations where LIP electrophysiology had mirrored the accumulation of evidence and demonstrated strong decision-related activity, we did not detect significant changes in either the animal's sensitivity or bias, as indicated by statistically-indistinguishable dif-

ferences in the slope (3.7% reduction from baseline, $t(20) = -1.4$, $p = 0.16$, paired t test) or midpoint (-0.4% shift, $t(20) = -0.08$, $p = 0.93$, paired t test) of the psychometric functions. Saline and sham control experiments showed similar patterns to the main baseline vs. muscimol treatment comparison, considering either the effect size on average, or on individual session pairs. Thus, while the impact of MT inactivation on sensitivity was substantial, an effect of LIP inactivation was not clearly identifiable using our techniques and task (Fig. 3.4, C).

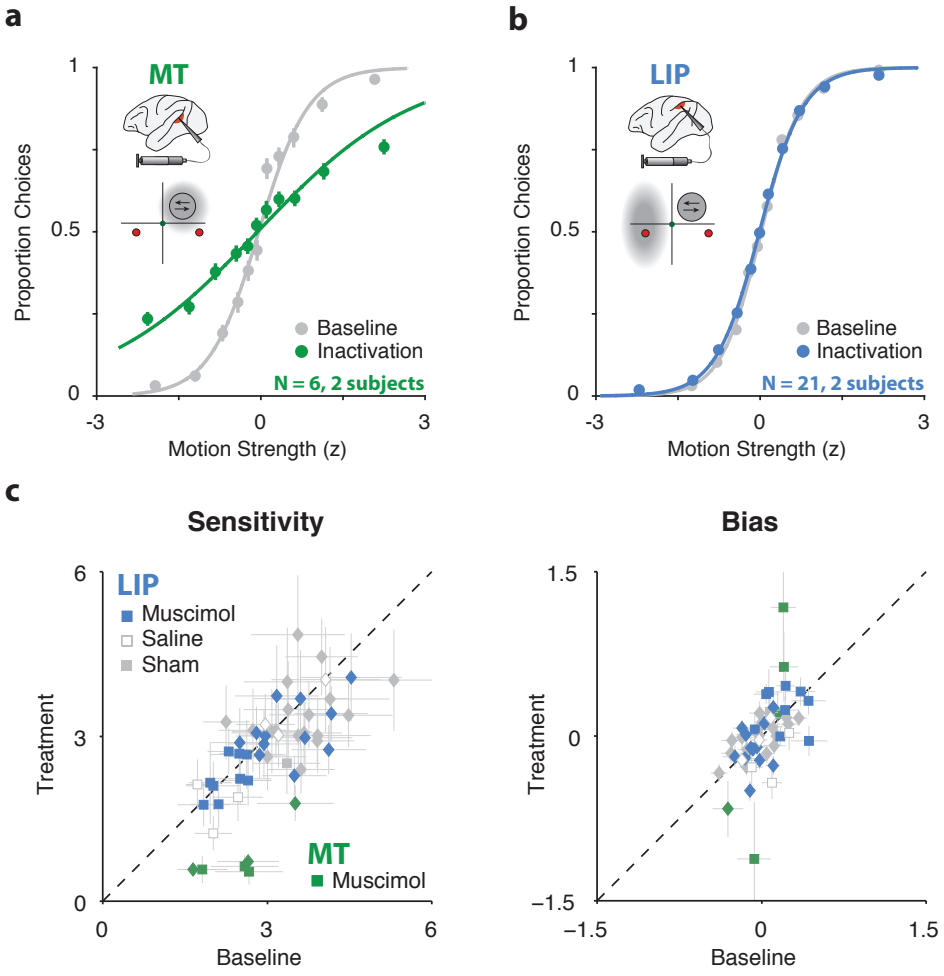

Figure 3.4: Psychophysical data for averaged pairs of baseline and muscimol treatment sessions in MT (**A**), and LIP (**B**). Insets illustrate the brain region inactivated (top) and the corresponding experimental geometry (bottom), along with the estimated inactivated field (gray cloud). Error bars on points show ±1 SEM across all sessions. **C,** The distribution of psychometric function parameters, slope (left) and shift (right), reflecting sensitivity and bias, respectively, for baseline (x-axis) and treatment (y-axis) session pairs for MT inactivations (green symbols) and LIP inactivations (blue symbols), as well as LIP saline and sham experiments (gray open and filled symbols, respectively), for monkey N (diamonds) and monkey P (squares). Error bars show 95% confidence intervals for individual sessions.

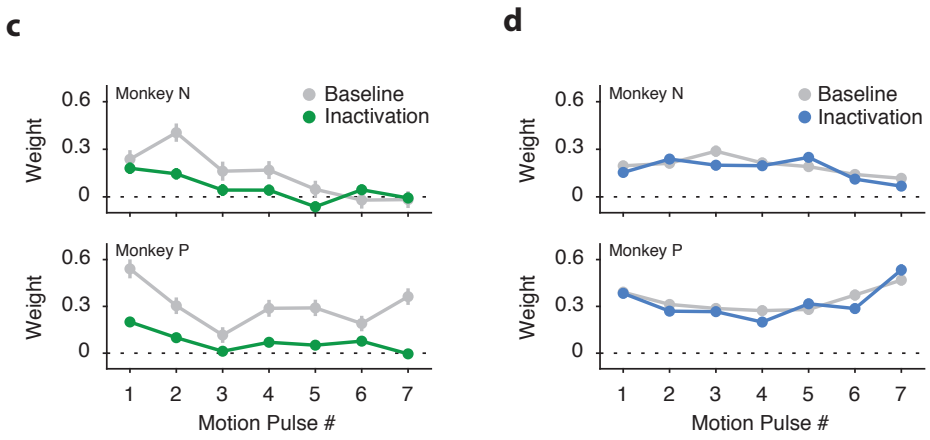

Figure 3.5: Psychophysical weighting, estimated via reverse correlation. Y-axis indicates how much the subject weighed each of the motion stimulus pulses (logistic regression) for all baseline and inactivation session pairs in MT (A) and in LIP (B), for monkey N (top) and monkey P (bottom).

We also assessed whether inactivation affected the timing or strategy of evidence integration (Kiani et al. 2008, Raposo et al. 2014, Erlich et al. 2015). For example, if LIP supports the temporal integration of motion evidence, inactivation could alter the strategy to reflect "leakier" integration that might still support the same overall performance. Contrary to this possibility, psychophysical weighting of the motion stimulus (estimated via reverse correlation) was unaffected by inactivation (Fig. 3.5). Although the two monkeys exhibited slightly different baseline weighting strategies, inactivation did not lead to a greater reliance on late information, nor did it clearly exert other idiosyncratic effects on the psychophysical weighting. Inactivations in area MT reduced the weighting of motion approximately evenly over time.

3.3.3 Inactivation in LIP disrupts behavior in a control task

Although inactivation in LIP had no measurable effect on direction discrimination, it did exert measurable effects on a "free-choice" control task, which was performed on every inactivation session (Fig. 3.6). Inactivation of LIP biased choices away from the contralateral hemifield (8.88% reduction from baseline on average, $t(33) = 3.4$, $p = 0.001$, paired t test), (Fig. 3.7), consistent with previous reports in monkeys (Wardak et al. 2004, Balan & Gottlieb 2009, Wilke et al. 2012), rodents (Erlich et al. 2015), and parietal lesions in humans (Kerkhoff 2001). Thus, our standard electrophysiological confirmation of LIP inactivation was complemented by a behavioral consequence in this free-choice control task. In addition to exerting a spatial bias, LIP inactivation caused an increase in endpoint error of saccades made to the hemifield contralateral to the inactivation (0.36° on average, $t(33) = 4.4$, $p < 0.0001$, Fig. 3.7).

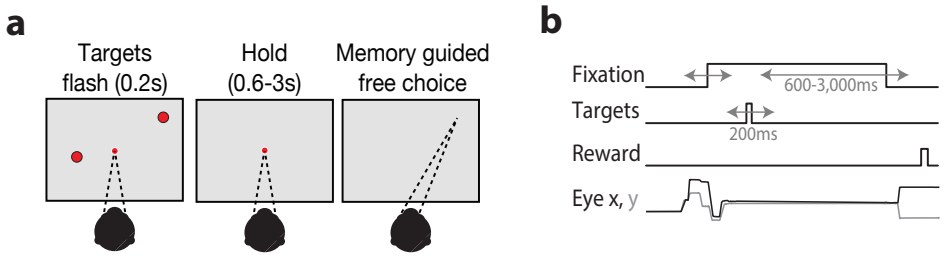

Figure 3.6: Design of the free-choice control task. **A,** The "free-choice" task. Following a 200ms long presentation of two targets at random locations in space, monkeys were required to hold fixation for another 600-3,000ms, and then to move their eyes to the remembered location of either target. **B,** Task timing. Events in the task were presented in sequence and were jittered in time (gray arrows).

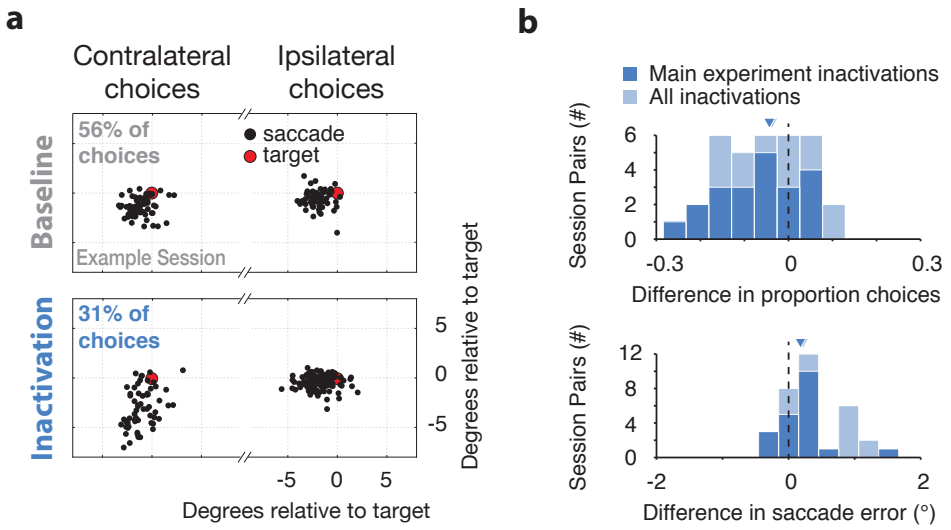

Figure 3.7: Performance in the free-choice task following LIP inactivation. **A,** The effect of LIP inactivation on choice bias and saccade accuracy in the free-choice task, example session. Four panels show data from an example baseline/inactivation pair: saccade landing points (black dots) have been aligned to target position (red dot) for contralateral (left) and ipsilateral target choices (right), during baseline (top) and inactivation (bottom). Percent contralateral choices within a session are noted as text in the top left. **B,** The effect of LIP inactivation on choice bias and saccade accuracy in the free-choice task, over all sessions. Histograms show baseline/inactivation differences in proportion contralateral choices (top) and saccade error (bottom), where positive numbers indicate an increase in metric following inactivation. Dark bars indicate sessions that took place on the same days as the main direction discrimination experiment ("Main experiment inactivations", n=21); dark triangle indicates the median difference. Light bars include additional sessions that took place on other days ("All inactivations", n=34); light triangle indicates median difference (may be hard to discern on plot due to similarity in value).

No systematic change was detected in other free-choice oculomotor metrics (reaction time, peak velocity, or duration), and no change in any oculomotor metric was detected during the direction discrimination task. Despite observing a muscimol-induced effect in the free-choice task, effect magnitude in the free-choice task was not predictive of effect magnitude in the direction discrimination task (Fig. 4.4 A, B), nor was there a dose-response relationship between muscimol mass and behavioral performance (Fig. 4.4 C-E), suggesting that our large muscimol administrations were likely operating within a "ceiling" regime.

3.3.4 Compensation over time or between hemispheres is unlikely

Because muscimol inactivations require comparisons across relatively long time scales, it remains logically possible that LIP normally plays a critical role in decision-making, but that other areas are processing information in parallel (de Lafuente et al. 2015) and are able to quickly compensate when it is artificially inactivated. Although other techniques with faster time scales will allow for more direct tests of this possibility, we did not observe changes indicative of compensation either within a session (Fig. 4.5) or over sessions (Fig. 4.6).

To test for reliance or compensation involving the LIP in the non-inactivated hemisphere, we performed experiments with both choice targets placed within the contralateral hemifield, and again did not observe clear changes in behavioral performance (Fig. 3.7, A). We also found no disrup-

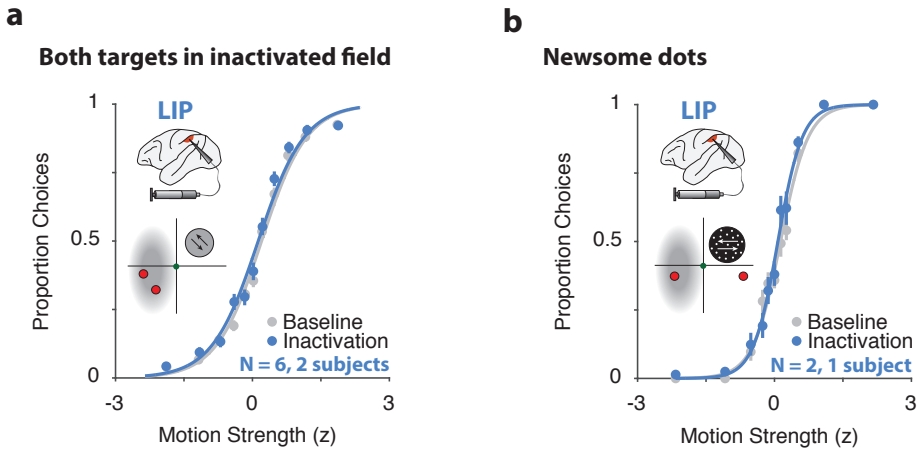

Figure 3.8: **A,** Psychophysical data for pairs of baseline and muscimol treatment in LIP, when both choice targets were placed within the inactivated field. Inset presents stimulus geometry and estimated inactivated field. **B,**, Same format as A, for data collected when the motion stimulus was a random dot kinetogram ("Newsome dots", at motion strengths of 0, 3.2, 6.4, 12.8 25.6 and 51.2% coherence, z scored).

tion of choice behavior using a moving-dot stimulus identical to that used in the classical studies of LIP function during decision making (Newsome & Pare 1988, Shadlen & Newsome 2001) (Fig. 3.8, B)

3.4 Discussion

Our results reveal a dissociation between decision-related activity in LIP and the causal role of such signals in decision-making. Instead, decision-related signals in LIP may be a result of feedback signal flow (Crowe et al. 2013), or perhaps an emergent phenomenon driven by extensive training (Sarma et al. 2015). Although one prior study observed subtle effects of LIP microstimulation in a reaction time direction discrimination task (Hanks et al. 2006), such electrical perturbations can produce orthodromic (and antidromic) activation of connected areas, and their observed effects are reconcilable with multiple alternatives to evidence accumulation (Hanks et al. 2015).

Alternatively, it remains possible that LIP does contribute to decision-making, but does so in a nonessential manner in conjunction with associated brain regions. Indeed, a growing body of work has observed decision-related activity in other brain areas (Ding & Gold 2013, Gu et al. 2007, Nienborg & Cumming 2009, Liu et al. 2013, Hanks et al. 2015), consistent with the prospect of LIP playing a minor and/or nonessential role in decision-making. In fact, our results mirror findings made in rodent posterior parietal cortex, where despite electrophysiological correlates of evidence accumulation, inactivation did not yield clear evidence of a critical role (Erlich et al. 2015). Taken together, decision-related activity is likely represented broadly across the brain, and may be "read out" by a flexible process to support behavior (Pitkow et al. 2015, Raposo et al. 2014, Siegel et al. 2015). Our results call for a broader consideration of both decision-making circuitry and the mechanisms

for reading out decision-related activity— regardless of whether decisions are instantiated, or merely reflected, in a particular brain area.

Chapter 4

Extended analysis of Chapter 3: Dissociated functional significance of decision-related activity across the primate dorsal stream

In Chapter 3 I reported results of an experiment testing whether decision-related activity plays a causal role in perceptual decision-making (under review, Katz LN, Yates JL, Pillow JW, Huk AC). In the experiment we found that reversible inactivation of macaque LIP, an area well known for its decision-related activity, has no impact on decision-making performance despite having exerted effects in a control task. This result stands to overturn a long held view and must therefore be scrutinized for its validity. Here I present further analyses, address specific concerns, and discuss the relation of this result to previous work. Parts of this chapter, with some modification, have been submitted as supplementary material to the results in Chapter 3.

4.1 Validation of the inactivation protocol

4.1.1 Functional targeting of MT and LIP

The goal in any causal manipulation is to target the most canonical feature of a system, and manipulate it. We therefore sought to inactivate

cells that present the defining feature of the brain region under study: spatial selectivity and motion direction tuning in area MT; spatial selectivity and decision-related activity in area LIP. We accomplished this functional targeting in three steps. First, the inactivation phase of the experiment took place only after the chamber of each monkey had been extensively mapped electrophysiologically such that the functional borders of the target area were known. Second, our muscimol (and saline) infusions were performed in grid location that had previously yielded the largest number of canonical MT or LIP cells. Third, the infusion cannula was yoked to a multi-electrode array (1mm away), enabling us to obtain MT or LIP consistent with their canonical role at a distance of at 1mm from the cannula tip, prior to every infusion. Following these steps resulted in a colocalization of recording sites (i.e. sites from which electrophysiological data were recorded, Fig. 3.2) and infusion sites, which took place weeks-to-months after the electrophysiology phase of the experiment. Location of recording and muscimol infusion sites in LIP are presented in Fig. 4.1.

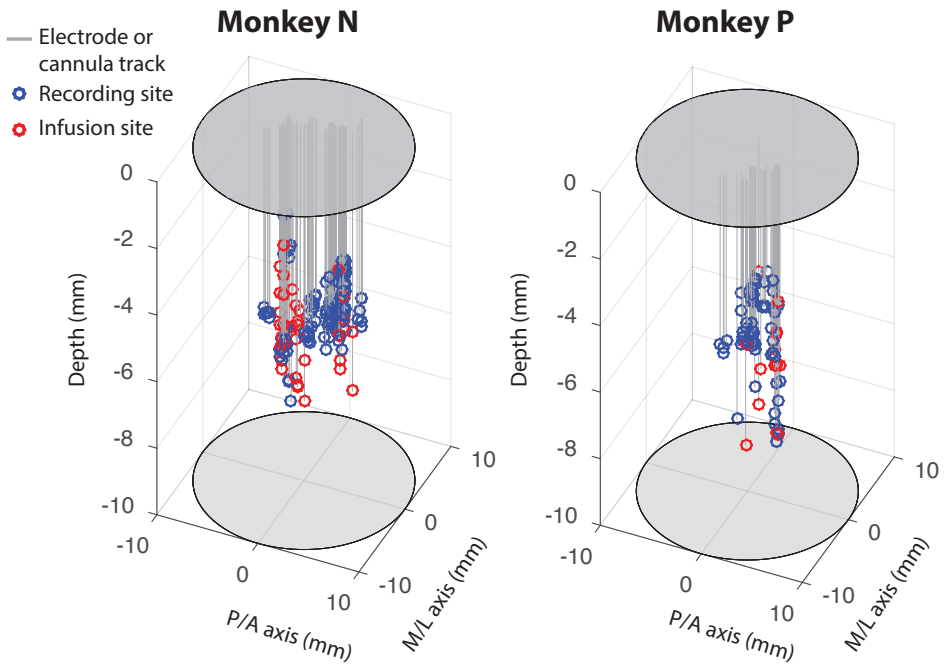

Figure 4.1: Location of recording sites and muscimol infusion sites for LIP. Recording (blue circles; took place early in the experimental phase) and infusion sites (red; took place weeks-to-months after the electrophysiology phase) for the two monkeys along the medial-lateral (M/L) and posterior-anterior (P/A) axes, within the chamber (demarcated by the ovals). Electrode and cannula tracks are represented by the gray lines (with a small jitter on the x-y plane for visualization).

4.1.2 Confirmation of electrophysiological silencing

Electrophysiological silencing was confirmed on every inactivation session. Figure 4.2 shows an example experiment where electrophysiological activity in area MT was recorded by a multi-electrode array for the full 150 minute duration of the experiment. The experiment included a baseline motion discrimination session, the infusion of muscimol, functional confirmation of inactivation, and a muscimol treatment motion discrimination session. The baseline session took place over the first 55 minutes. Shortly after, muscimol was infused at a slow rate for approximately 20 minutes. Electrophysiological silencing was observed quite rapidly in this session, within approximately 7 minutes from infusion start. We quantified silencing onset for each channel by computing the mean squared voltage in 500 bins ranging from 20 minutes before infusion until 40 minutes after. Mean squared voltages were normalized and fit by a 2-parameter logistic function. The value of the midpoint parameter was taken to reflect silencing onset. Over the 8 channels in this example experiment, mean silencing time over the eight recording channels was 6.8 minutes (Fig. 4.2 B). Our method is a good first approximation but it is by no means complete. For example, channel 3 in figure 4.2 A was not well fit by the logistic model because pre-infusion activity was not sufficiently different than post-infusion activity. This is not uncommon when recording electrophysiological activity with a multi-electrode array– some channels may exhibit less activity than others such that electrophysiological silencing is not always obvious on each and every channel of the multi-electrode array. Nev-

ertheless, silencing over the remaining 7 channels appeared to take place in sequence (Fig. 4.2 B), confirming that neural tissue has been silenced 1mm away from the cannula tip, and for a vertical stretch of at least 1.05mm (vertical spacing between each array channels is 150μ). Channels placed at a lower position in the multi-electrode array were silenced first (channel 8 is the lowest), confirming that our muscimol cannula was well positioned near the tip of the multi-electrode array. This approach was chosen in light of previous reports noting a preferential upwards diffusion of muscimol (Liu et al. 2010, Yttri et al. 2014). These measurements serve as further support to our conclusions regarding the spatial extent of inactivation, reported in the Methods of Chapter 3.

Approximately 10 minutes after infusion start, after having observed electrophysiological silencing in the continuous voltage trace, we tested whether MT neurons respond to motion. The test was performed by presenting a motion stimulus in the RF location of the MT units recorded from prior to infusion. Despite strong motion in the RF of the neurons, no electrophysiological responses were observed, confirming that MT neurons had been silenced (see voltage traces in Figure 4.2 A, above the "confirm" block). Approximately 15 minutes after infusion end we began collecting psychophysical data for the "muscimol treatment" session. Figure 4.2 C and D compare MT responses for 4 motion discrimination trials, collected at minute 29 (during baseline) and minute 101 (during treatment), demonstrating the difference in MT responsively to motion.

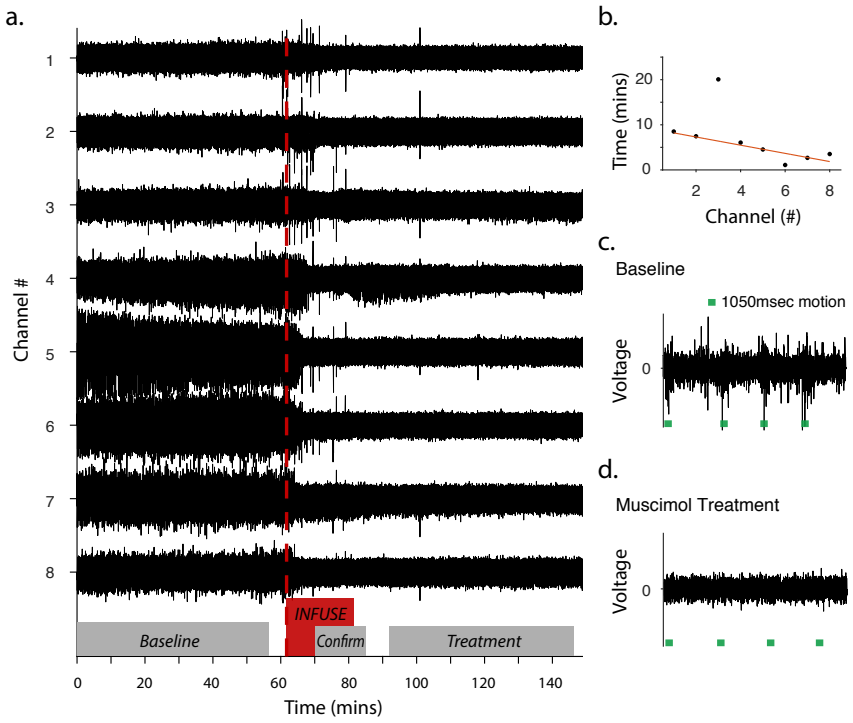

Figure 4.2: **A,** Electrophysiological recording in area MT over a full experiment, including a baseline motion discrimination session, muscimol infusion, functional confirmation of inactivation, and a muscimol treatment session. The duration of each epoch is represented as blocks above the x-axis. Continuous voltage traces over the course of the experiment are shown for an 8 channel multi-electrode array (channels separated vertically by 150μ). **B,** Silencing onset time relative to infusion start in each of the 8 channels. **C,** Example of MT response to 4 motion discrimination trials during the baseline session, collected at minute 29. The 1050msec motion stimulus is marked by green lines. **D,** Example of MT responses during the muscimol treatment session, collected at minute 101. Same format as C.

4.1.3 Spatial mapping between cortex and visual space

Mapping between cortical topography to visual space is possible for a well defined and homogenous area such as MT, where the retinotopic organization is well understood (Maunsell & van Essen 1987). In fact, the retinotopic organization in MT is so well defined, that inactivation of a circumscribed patch in MT cortex results in a spatially circumscribed deficit in visual space (Chowdhury & DeAngelis 2008). Given that our inactivation protocol includes a functional identification of the target area prior to infusion, we obtain an estimate of the neurons' RF– MT or LIP– prior to every infusion. We then assume that once inactivated, any stimulus positioned in that location would be within the inactivated field. This assumption is supported by previous experiments (Chowdhury & DeAngelis 2008) as well as our own: in 3 of the 6 MT inactivation sessions we followed the standard pair of sessions (baseline and muscimol treatment) with a 3rd dataset, placing the motion stimulus outside of the inactivated MT field. In contrast to the severe behavioral deficit after muscimol treatment (Fig. 3.4, A), performance was restored to baseline levels when the motion stimulus was moved outside of the inactivated field (Fig. 4.3), consistent with a focal inactivation in area MT.

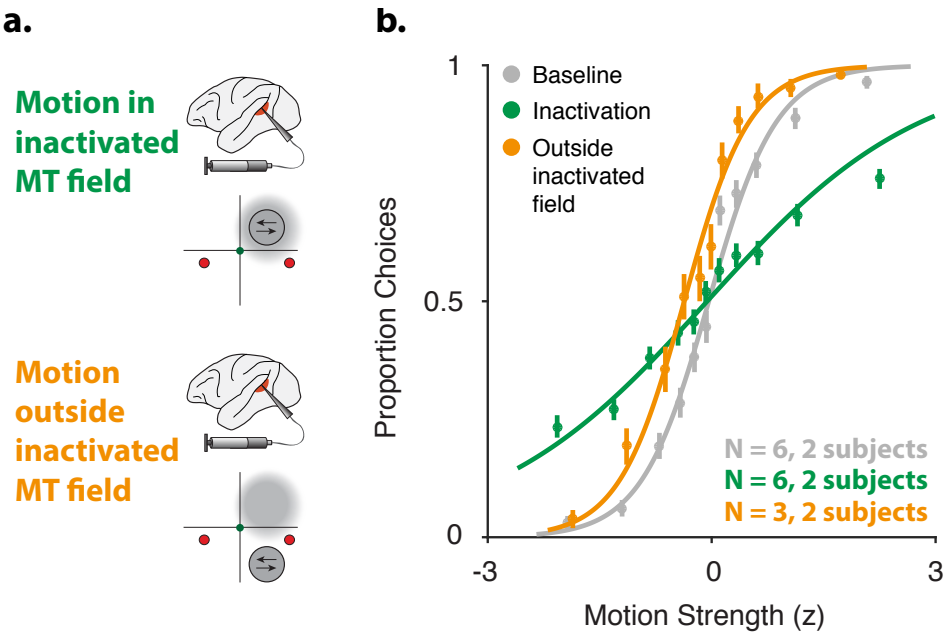

Figure 4.3: Direction discrimination performance is restored when motion is placed outside of the inactivated MT field. **A,** Illustration of the inactivation in MT and the corresponding experimental geometry, along with the estimated inactivated field (gray cloud). **B,** Psychophysical data for averaged pairs of baseline, muscimol treatment, and muscimol treatment when the motion stimulus is placed outside of the inactivated MT field. Error bars on points show ± 1 SEM across all sessions.

Unlike area MT, the retinotopic organization in LIP is far less precise (Hamed et al. 2001, Patel et al. 2010). Nevertheless, the organization is consistent with strong contralateral representation, with approximately 85% of LIP cell RFs directed to the contralateral hemifield (averaged over: Blatt, Andersen & Stoner 1990, Barash, Bracewell, Fogassi, Gnadt & Andersen 1991*b*, Hamed et al. 2001, Dunn & Colby 2010, Patel et al. 2010) (but see Platt & Glimcher 1998). We see a similar proportion of contralateral in our own electrophysiological data (80%). Thus, while inactivation in LIP is not likely to be mapped as precisely as MT inactivation to visual space, it is likely to cause a general deficit in contralateral space, as was the case in previous studies of LIP inactivation (Li et al. 1999, Wardak et al. 2002, Wardak et al. 2004, Balan & Gottlieb 2009, Liu et al. 2010, Suzuki & Gottlieb 2012, Wilke et al. 2012, Yttri et al. 2014, Kubanek et al. 2015). Still, we always placed one the choice targets of the direction discrimination task in the location of the RF of the LIP cells recorded just prior to infusion, to maximize our ability to detect a deficit. In addition, muscimol dosages used in LIP inactivations were close to double those used in MT, and on the highest end of ranges used in the aforementioned LIP inactivation studies.

A recent study by Liu et al. (Liu et al. 2010) drew a functional distinction between the dorsal and ventral portions of LIP: while the dorsal portion (LIPd) was found related to oculomotor planing, the ventral portion (LIPv) was related to both oculomotor planning and attentional allocation. It unknown whether attentional processing in LIP is related to decision-related

activity, but there are anecdotal reports that more decision-related responses are observed in more ventral portions of LIP. We emphasize that the critical component of our protocol was targeting the precise locations at which we measured canonical decision-related activity in LIP, and not targeting a specific subdivision. However, a close look at our recording and infusion depths (Fig. 4.1) reveals that the mean infusion depths for the two monkeys were 7.12 $\pm$ 1.15 (monkey N) and 7.03 $\pm$ 1.39 (monkey P), consistent with targeting LIPv. Given the estimated spread of muscimol in cortex (described in the Methods section of Chapter 3), we estimate that our inactivation volumes targeted substantial territory in LIPv (Lewis & Van Essen 2000*b*).

4.1.4 A "floor" effect is unlikely

Our main experimental result is that we did not observe a deficit in decision-making behavior after inactivating LIP. One concern is that we did not use a sufficient amount of muscimol (i.e. a "floor effect"). We do not believe this is the case for three main reasons. First, our muscimol dosages were on the high end of dosages used in previous studies, where effects had been observed for dosages smaller than ours (Li et al. 1999, Wardak et al. 2002, Wardak et al. 2004, Balan & Gottlieb 2009, Liu et al. 2010, Suzuki & Gottlieb 2012, Wilke et al. 2012, Yttri et al. 2014, Kubanek et al. 2015). Second, while no deficit was observed in the primary decision-making task, we observed two independent deficits in the free-choice control task: a selection bias and an oculomotor deficit 3.7. Third, we manipulated the mass and spatial volume of

muscimol infusion explicitly and found no relationship between muscimol mass and effect magnitude in either the primary direction discrimination task, or the free-choice task 4.4. Thus, it is more likely that our infusions are operating within the "ceiling" regime of the dose-response function than the "floor".

Our attempt to maximize the spatial extent of inactivation in LIP took place by three methods. First, the infusion protocol included multiple infusion sites within a single cannula track (the precise depths within each cannula track, cannula location and infusion details are detailed in table 4.1). Second, having the multi-electrode array placed in parallel to the cannula, enabled us to closely monitor the neural inactivation due to infusion, and adjust the cannula location accordingly. For example, if dorsal channels of the multi-electrode array were silenced first, we would move the infusion cannula 1-2mm ventrally and observe the silencing of ventral channels too. Manipulation of the infusion cannula with this technique allowed for greater vertical inactivation along the lateral wall of the intraparietal sulcus. Third, in 5 out of the 21 muscimol inactivation sessions we simultaneously lowered two infusion cannulae staggered 3-4mm apart, to cover a larger volume of LIP, but these high-volume and high-mass sessions did not exert systematic effects (orange dots in 4.4).

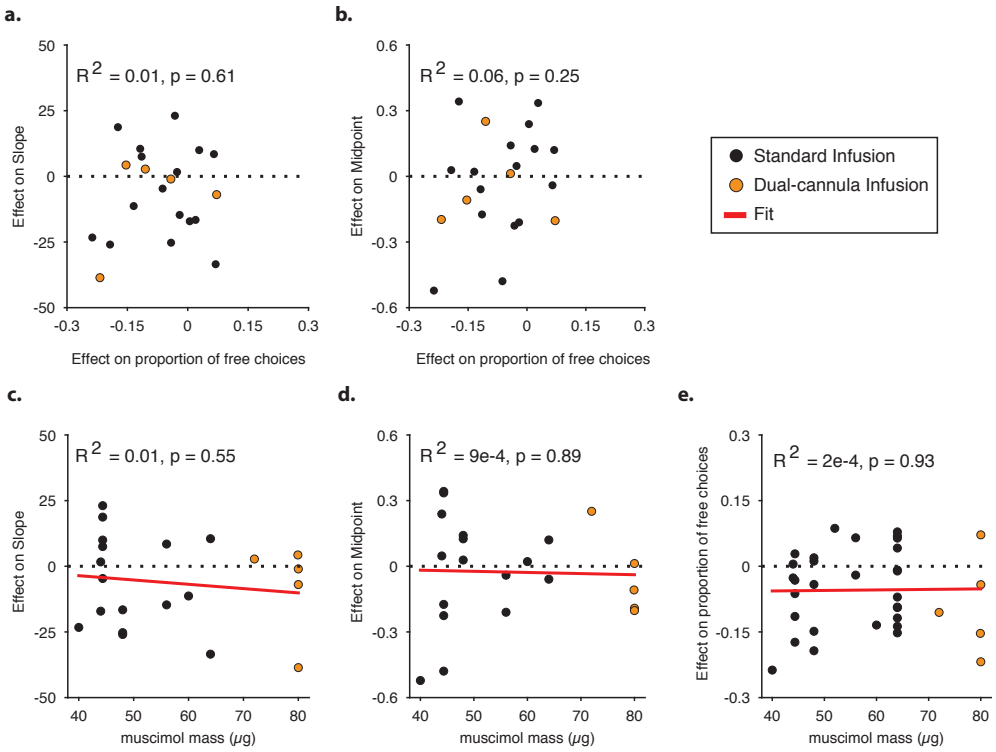

Figure 4.4: No relationship between effect magnitude in control task, effect magnitude in direction discrimination task, and muscimol mass. **A, B,** The relationship between the effect of inactivation in the free-choice task (i.e. shift in proportion of contralateral choices from baseline to muscimol treatment) and the effect of inactivation in the direction discrimination task on psychometric function slope (i.e. %change in psychometric slope, panel A) and bias (i.e. shift in normalized motion strength units, panel B). Orange dots signify sessions in which two infusion cannulae were lowered simultaneously to maximize spatial extent of inactivation. R^2 and associated p values of a Pearson correlation are indicated on the plots. **C, D, E,** Dose-response functions between muscimol mass and the effect in the direction discrimination task on slope (C, same units as panel A), bias (D, same units as panel B), and the effect in the free-choice task (E, same units as A, B). For panel E we used all free-choice sessions (n = 34) and not just the sessions that took place on the same days as the direction discrimination task. R^2 , associated p values and regression lines are indicated on the plots, linear regression.

Task	Area	Monkey	Date	Treatment	Cannula Tracks (#)	Positioning Grid (x, y)	Infusion sites within Track (#)	Average depth (mm)	Total volume (µl)	Total mass (µg)
Standard	**MT**	**P**	20130801	Muscimol	1	(2, -1)	2	8	5	33.3
task			20130826	Muscimol	1	(2, 0)	2	10	9.7	64.3
geometry			20130830	Muscimol	1	(2, 0)	2	11.2	8.5	56.6
		N	20150414	Muscimol	1	(5, -4)	3	10.7	4	32
			20150522	Muscimol	1	(5, -4)	2	10.5	5	40
			20150805	Muscimol	1	(4, -4)	2	6.9	5	40
	LIP	**P**	20130628	Saline	1	(2, -1)	1	7	6.7	-
			20130716	Muscimol	1	(3, 0)	1	6.5	6.7	44.4
			20130723	Muscimol	1	(3, 0)	1	7	6.7	44.4
			20130729	Muscimol	1	(2, -1)	1	7	6.7	44.4
			20130808	Muscimol	1	(3, 0)	1	6	6.7	44.4
			20130814	Muscimol	1	(3, 0)	1	7	6.7	44.4
			20130816	Saline	1	(3, 0)	1	6	6.7	-
			20130821	Muscimol	2	(3, 0); (0, 3)	2; 2	7; 7	12	79.9
			20130823	Saline	1	(3, 0)	1	7	6.7	-
			20140318	Sham	-	-	-	-	-	-
			20140319	Muscimol	1	(3, 0)	1	7	5	40
			20140325	Muscimol	1	(3, 0)	1	7	6	48
			20140328	Muscimol	2	(3, 0); (1, -3)	2; 2	7.5; 7.5	10	80
		N	20150416	Muscimol	1	(2, 4)	2	6.3	6	48
			20150422	Saline	1	(2, 4)	1	7.6	5	-
			20150429	Muscimol	1	(-2, 3)	2	6.6	7.5	60
			20150505	Muscimol	1	(-2, 3)	2	6.5	5.5	44
			20150508	Muscimol	1	(-1, 3)	2	8.6	5.5	44
			20150512	Muscimol	2	(-2, 3); (3, 4)	2; 2	7.9; 7.9	9	72
			20150515	Muscimol	1	(-2, 3)	3	7.6	7	56
			20150626	Sham	-	-	-	-	-	-
			20150630	Muscimol	1	(-2, 3)	2	8	7	56
			20150703	Muscimol	1	(-3, 2)	3	7.1	8	64
			20150707	Muscimol	2	(-3, 2); (2, 4)	3; 3	7.9; 7.9	10	80
			20150710	Muscimol	2	(-3, 2); (2, 3)	2; 2	6.2; 6	10	80
			20150717	Saline	1	(-3, 2)	2	5.3	6	-
			20150721	Muscimol	1	(-3, 2)	2	6.1	8	64
			20150724	Saline	1	(-3, 2)	2	6	5	-
			20150728	Sham	-	-	-	-	-	-
			20150731	Muscimol	1	(-3, 2)	3	6	6	48
Both targets	**LIP**	**P**	20140402	Muscimol	1	(3, 0)	2	7.5	6	48
in			20140407	Sham	-	-	-	-	-	-
			20140409	Muscimol	1	(3, 0)	4	7	8	64
			20140509	Muscimol	1	(3, 0)	3	9	8	64
			20140516	Muscimol	1	(3, 0)	3	9	8	64
		N	20150821	Sham	-	-	-	-	-	-
			20150826	Sham	-	-	-	-	-	-
			20150828	Muscimol	1	(-3, 2)	3	7	6	48
			20150831	Sham	-	-	-	-	-	-
			20150902	Muscimol	1	(-3, 2)	4	6.2	6.5	52
Random Dot	**LIP**	**P**	20140425	Muscimol	1	(3, 0)	3	7.2	8	64
Kinetogram			20140429	Muscimol	1	(3, 0)	3	7.6	8	64

Table 4.1: Table presents all infusion sessions run over the course of the study, for all infusion types (muscimol, saline, sham) in either MT or LIP. Infusions are sorted by date within each task, for each monkey separately. The average depth (column 9) refers to the average depth across all infusion sites within a cannula track.

4.2 Behavioral compensation is unlikely

The study of brain lesions has been invaluable to neuroscience. A lesion can disrupt neural function by either disrupting processing locally, or by obstructing the flow of neural signal, causing large scale disruptions in brain activity. The cerebral imbalance can take multiple forms but is thought to reach a stable homeostatic state over time, often with complete recovery of function (Newsome & Pare 1988, Lomber 1999, Turrigiano 1999, Honey & Sporns 2008). The most common form of recovery takes place over long periods of time in response to a permanent lesion. In contrast, compensation for an acute loss of function, on short time scales, is far less common as it cannot take place through anatomical restructure. The acute perturbation introduced by the infusion of muscimol is short-lived, on the order of hours, but compensation might still take place through other mechanisms. For example, inter-hemispheric competition might alter the response of the hemisphere contralateral to the temporary lesion, or, a neighboring brain region within the same hemisphere may compensate for loss of function (Wilke et al. 2012, Otchy, Wolff, Rhee, Pehlevan, Kawai, Kempf, Gobes & Ölveczky 2015). Regardless to the exact form of compensation in terms of neural dynamics, our concern relates to behavior: could some form of compensation mask an otherwise observable deficit in psychophysical performance following LIP inactivation?

4.2.1 No evidence for compensation within a sessions

We do not think that behavioral compensation is taking place within a session for multiple reasons. First, there is no evidence to favor behavioral compensation in previous studies of LIP inactivation, regardless to whether the task used was simple (Li et al. 1999, Yttri et al. 2014, Kubanek et al. 2015) or complex (Wardak et al. 2004, Balan & Gottlieb 2009, Liu et al. 2010). Second, even when neural compensation was clearly observed following LIP inactivation via fMRI (Wilke et al. 2012), the behavioral deficit persisted. Third, in studies that report the time course of the behavioral deficit, the deficit tended to increase over time, not decrease (Wardak et al. 2004, Kubanek et al. 2015).

Nevertheless, we tested for behavioral compensation by measuring the time course of psychophysical performance within sessions. For MT inactivations (n = 6), a large reduction in performance accuracy was observed in all muscimol treatment sessions compared to baseline (Fig. 4.5, A). The proportion of contralateral choices, in contrast, was not clearly impacted. These findings are consistent with our results from the psychometric fits (main text), where slope is reduced following MT inactivation but bias is not. For LIP inactivations (n = 21), no systematic trends were observed in either accuracy or the proportion of contralateral choices (Fig. 4.5, B). There is a slight increase in variability as time elapses for both MT and LIP data, but this is likely a consequence of less sessions constituting the average (each curve extends to the median trial length of the constituent sessions). On a subset of LIP inactivation sessions, we collected additional psychophysical data during

the time that muscimol was being infused (in addition to the standard baseline and muscimol treatment sessions; 13 of the 21 session pairs; orange curve in Fig. 4.5, B). The goal of collecting "during infusion" data was to test the possibility that inactivation in LIP does, in fact, impact psychophysical performance, but perhaps only immediately after inactivation and within a short time window after which behavior is restored. Contrary to this possibility, the "during infusion" sessions did not reveal clear patterns in either accuracy or bias, ruling out within-session compensation as a potential concern.

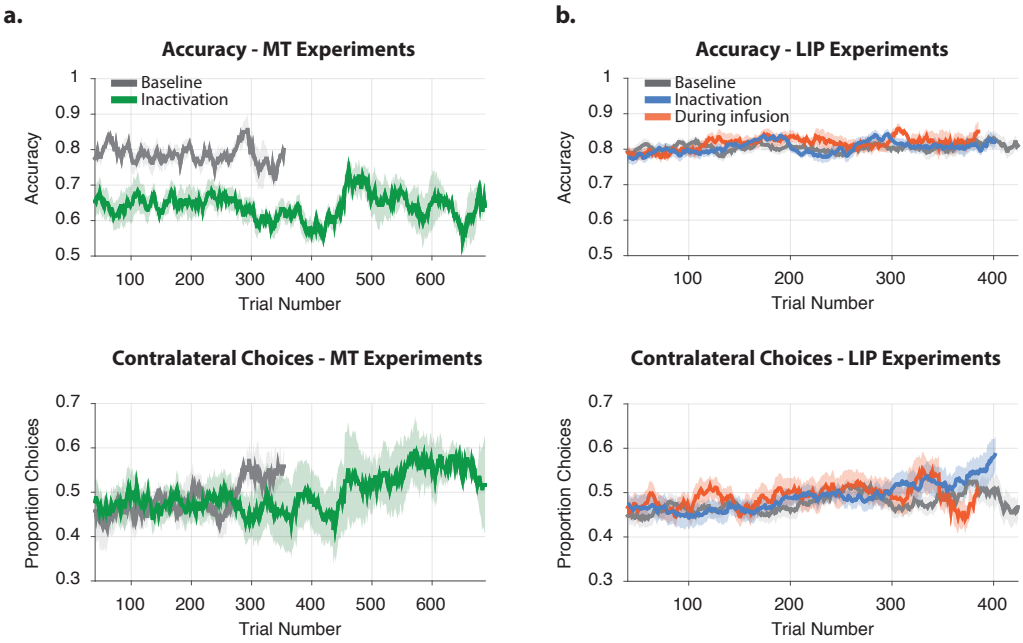

Figure 4.5: Monkey accuracy and bias in the direction discrimination task were computed over time by taking a running mean of correct and contralateral choices, respectively (sliding window of 40 trials). **A,** Inactivation in area MT (n = 6, green curve) had a clear and consistent impact on behavioral accuracy compared to baseline (n = 6, gray), but did not have systematic effects on bias (bottom). Panels show data from trial 40 (sliding window size) to the median trial length of each group of experiments, sometimes resulting in increased variability at later trials. Error bars are ± 1 SEM over experiments. **B,** Inactivations in area LIP (n = 21, blue curve) had no systematic trends in either accuracy (top) or bias (bottom) compared to baseline (n = 21, gray). Data collected during infusion time, "during infusion" did not exhibit departures from the mean trend either. Panel format same as in A.

4.2.2 No evidence for compensation across sessions

Having ruled out within-session compensation, we sought to test whether repeated muscimol infusions exerted subtle effects on animal behavior over a longer time course. Perhaps repeated inactivations increase behavioral robustness to inactivation? Recovery of function has been observed following permanent lesions (Lomber 1999, Turrigiano 1999), but not for repeated reversible inactivations (to our knowledge). Nevertheless, we tested this possibility by evaluating measures of psychophysical performance (midpoint and slope parameters of the psychometric function) over sessions (Fig. 4.6).

No significant change in slope was detected over sessions for either monkey P ($p = 0.22$) or N ($p = 0.63$) (Fig. 4.6, A). When considering the difference in slope between baseline and treatment pairs (ΔSlope), there was a small decrease in ΔSlope over sessions in monkey P (regression line slope = -0.07, $p = 0.023$), indicating that inactivations may have gradually become more effective in reducing monkey sensitivity. However, a similar effect was seen in the interleaved controls (saline and sham, gray markers), indicating that this effect likely reflects nonspecific trends in performance across back-to-back pairs of experiments. Monkey N had no significant change ($p = 0.92$). No significant change was observed in the session to session midpoint values for either monkey P (linear regression, $p = 0.44$) or monkey N ($p = 0.24$). When considering the difference in midpoint value for each dataset pair over time (ΔMidpoint), no significant change was detected either ($p = 0.98$ and $p = 0.4$ for monkey P and N, respectively).

Thus, no systematic changes were observed across the 9 muscimol treatment sessions in monkey P, or 12 muscimol treatment sessions in monkey N. The lack of systematic effect is further evident by a qualitative inspection of the individual session psychometric functions (Fig. 4.7). Figure 4.7 includes data for all baseline and muscimol treatment pairs, baseline and saline/sham pairs, both in areas MT and LIP, in both monkeys, in all tasks: the primary direction discrimination task ("standard geometry"), both targets placed in the inactivated hemifield, and the "Newsome dots".

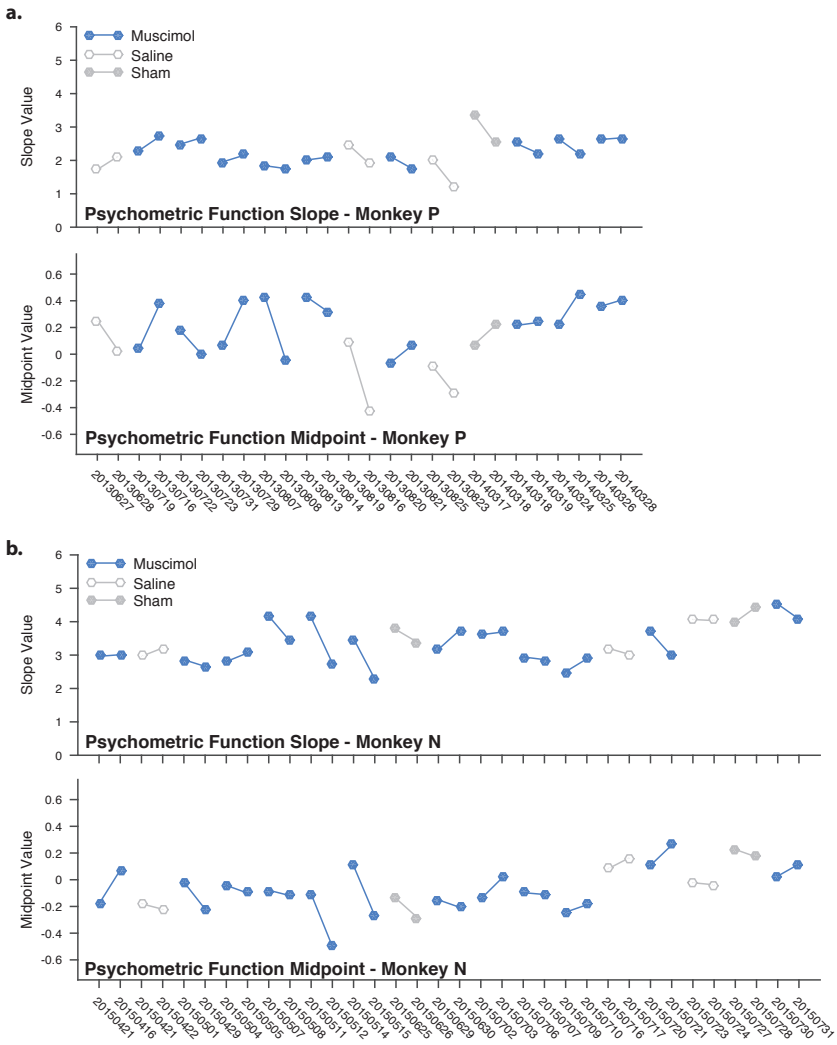

Figure 4.6: Panels show data from monkey P (left) and monkey N (right), for all baseline and treatment pairs: muscimol (blue), saline (unfilled gray) and sham (filled gray). Each pair consists of two sessions that took place in close succession at a similar time of day after a similar number of preceding tasks and trials, and is represented by two markers connected by a line. **A,** Psychometric function slope over sessions. **B,** Psychometric function midpoint over sessions. X-axis dates are in yyyymmdd format.

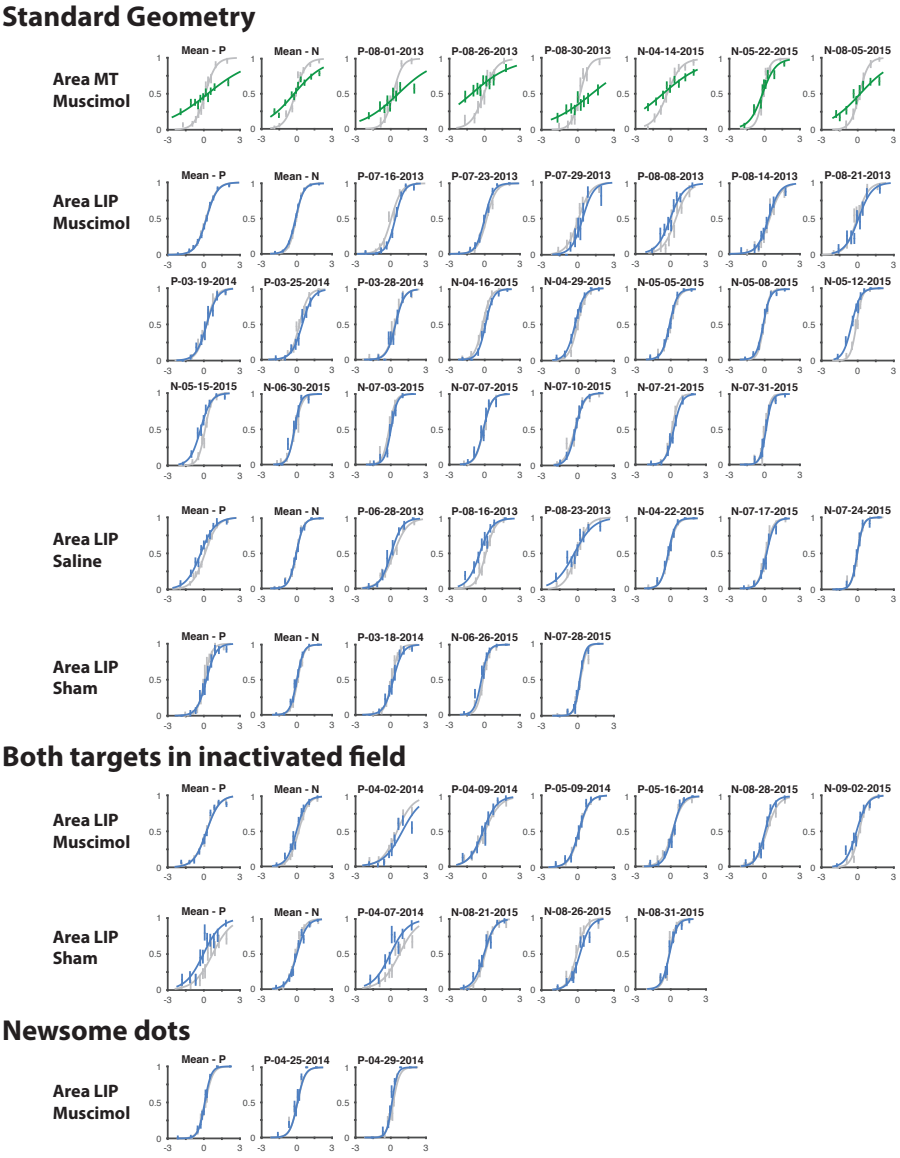

Figure 4.7: All pairs of baseline and treatment sessions for all treatment types: muscimol, saline, and sham, for all variants of the direction discrimination task (bold titles), for both LIP and MT inactivation. In all panels, abscissa represents motion strength towards the direction contralateral to the LIP under study, ordinate represents the proportion of contralateral choices. The gray curve is baseline, the colored curve is treatment. The first panels in each section present mean psychophysical performance for each monkey over sessions. Subsequent panels present individual session pairs.

4.3 Results of the main experiment are robust to various analyses

We considered whether our results might be affected by different forms of analyses and modeling. In Chapter 3, results from the main experiment (i.e. direction discrimination performance for baseline vs. muscimol treatment) were quantified by a 2-parameter logistic function. The two parameters, midpoint and slope (reflecting subject bias and sensitivity), were statistically compared between the two conditions by a parametric test, Student's t, and no differences were detected. Here we consider whether a non-parametric test yields different results. When comparing the datasets with the Wilcoxon signed-rank sum test (WSRST), slight variations in p-values were observed, but the main result remained unchanged (Table 4.2).

We further considered whether a different parameterization of the logistic function would alter the results. We hypothesized that if LIP plays a role in accumulating evidence in favor of a decision, then its inactivation should result in reduced subject sensitivity (i.e. reduction in logistic function slope). However, it is possible that inactivation influences different mechanisms subserved by LIP, resulting in idiosyncratic changes in behavior. Even though the 4-parameter model did not confer any statistical advantage over the 2-parameter model (similar test likelihoods on withheld data), we fit the 4-parameter model in an attempt to capture potential changes such as lapse rates (Erlich et al. 2015). We fit the function by a maximum likelihood procedure assuming a Bernoulli distribution of binary choices, in which the probability

of a contralateral choice is P and ipsilateral choice is $1 - P$, where P is given by:

$$P = \gamma + (1 - \gamma - \delta)\frac{1}{1 + e^{-\beta(x-\alpha)}}$$

where x is the motion strength value (z-scored over all sessions for each monkey separately; positive values indicate contralateral motion), α is the logistic function shift parameter (reflecting the midpoint of the function, i.e., bias, in units of motion strength), β is the slope (i.e., sensitivity, in units of log-odds per motion strength), γ is the minimum P value (i.e. lapse rate for negative motion strength values), and $1 - \delta$ is the maximum P value (i.e. lapse rate for positive motion strength values). Error estimates on the parameters were estimated from the hessian numerically. Despite the increased flexibility in fitting, no compelling differences were observed in either of the four model parameters for either the parametric or non-parametric tests (Table 4.2).

			Muscimol Infusion				Saline & Sham Infusion			
Statistical test	**model**	**monkey**	**midpoint**	**slope**	**minLapse**	**maxLapse**	**midpoint**	**slope**	**minLapse**	**maxLapse**
Student's t	pmf2	N	0.542	0.1734			0.986	0.2444		
		P	0.6731	0.7982			0.2353	0.2166		
		Both	0.9306	0.1659			0.3693	0.1092		
	pmf4	N	0.4028	0.0243	0.7585	0.2352	0.8213	0.2827	0.6065	0.6228
		P	0.6747	0.459	0.3554	0.8337	0.1377	0.3261	0.5675	0.3111
		Both	0.8163	0.0552	0.3904	0.9091	0.2169	0.1595	0.7461	0.2734
WSRST	pmf2	N	0.791	0.3394			0.9308	0.2305		
		P	0.5703	0.9102			na	na		
		Both	0.9032	0.3219			0.4432	0.1036		
	pmf4	N	0.6221	0.021	0.5186	0.2334	0.9032	0.2305	0.3754	0.4761
		P	0.4961	0.4258	0.8203	0.8203	na	na	0.875	0.625
		Both	0.8213	0.0325	0.414	0.566	0.3533	0.1353	0.2758	0.3674

			Muscimol vs. Saline & Sham Infusion			
Statistical test	**model**	**monkey**	**midpoint**	**slope**	**minLapse**	**maxLapse**
Student's t	pmf2	N	0.149	0.2367		
		P	0.0208	0.2461		
		Both	0.2606	0.0704		
	pmf4	N	0.8213	0.2827	0.6065	0.6228
		P	0.1377	0.3261	0.5675	0.3111
		Both	0.2169	0.1595	0.7461	0.2734
WRST	pmf2	N	0.184	0.1496		
		P	0.0503	0.3301		
		Both	0.3898	0.0324		
	pmf4	N	0.184	0.4887	0.184	0.5125
		P	0.0503	0.6042	0.8252	0.8252
		Both	0.3543	0.0895	0.4942	0.2009

na - not enough data

Table 4.2: The table reports p-values for two types of statistical analyses: the non-parametric Wilcoxon signed-rank sum test (WSRST) and parametric Student's t. The tests were performed on model parameters: either a two-parameter psychometric function (pmf2) or four-parameter (pmf4). na: not enough data

4.4 Relation to previous work

Despite extensive correlational study, very few studies have performed causal perturbations in decision-related brain areas to date. Within the context of a random dot direction discrimination task, there are only three causal manipulation studies (to my knowledge) and all used microstimulation: FEF (Gold & Shadlen 2003), Striatum (Ding & Gold 2012*b*), and LIP (Hanks et al. 2006). The most relevant study to our work is the one conducted by Hanks et al. who microstimulated LIP during the motion viewing epoch of a reaction time discrimination task. Microstimulation produced small but reliable reductions in monkey response times to the target within the stimulated LIP RF and increased response time to the target outside of the RF. Microstimulation also shifted monkey responses towards the target in the microstimulated LIP RF, but this shift was of small magnitude and was observed in only one of two monkeys. Together, Hanks et al. took these result to indicate that LIP plays a causal role in evidence accumulation. However, there are multiple problems with this interpretation.

Chief of these is the fact that while microstimulation is tremendously instrumental in elucidating the function of different brain areas (Cohen & Newsome 2004), its primary means of neural recruitment is axonal and not somatic (Histed, Bonin & Reid 2009). Thus, effects observed in microstimulation studies could be attributed to antidromic stimulation. Given the abundance of anatomical connections between LIP and adjacent areas (Lewis & Van Essen 2000*a*), it is not entirely clear whether the behavioral effect is

driven by LIP, or by antidromically connected areas.

A more nuanced problem is that the facilitation in reaction times could be explained in terms other than evidence accumulation. Two studies support this idea. First, Cutrell and Marrocco (Cutrell & Marrocco 2002) used a comparable protocol to microstimulate LIP during a simple visually guided saccade task, where the location of the target could either be cued ahead of presentation or not. Cutrell and Marrocco found that microstimulation shortened response times by a similar magnitude to that observed by Hanks et al., and attributed the effect to a shift in spatial attention. Indeed, there was no sensory evidence to accumulate in their task. Second, Dai et al. (Dai, Brooks & Sheinberg 2014) stimulated LIP either by microstimulation or optogenetic techniques during a task where one target was to be selected out of two. They found that stimulation both facilitated saccade reaction times and biased choices towards the target in the RF of the stimulated neuron. In a similar vein to Cutrell and Marracco, Dai et al. attribute their effect to a shift in spatial attention or "salience" (Bisley 2003). Thus, while the study conducted by Hanks et al. is informative in revealing that LIP is connected to a circuit that has a causal influence in the task, it cannot attribute the effect to LIP itself. Further, it cannot definitively ascribe the effect to a manipulation of evidence accumulation over other cognitive functions, such as a shift in spatial attention that is unrelated to the accumulation of sensory evidence.

Regardless to the nature of LIP function during the direction discrimination task, it is not straightforward why Hanks et al. had observed an effect

for microstimulating LIP while we observed no effect for inactivating LIP. This apparent conflict may be resolved by two arguments. First, it is important to recall that while we employed a fixed duration task, Hanks et al. used a response time task in which the "evidence accumulation" epoch includes a number of nuisance signals, such as response preparation or reward expectation. Microstimulation could have affected these (or other unknown functions) to elicit the reported effects on RT and choice. Second, it is possible that while LIP is not necessary for performance in the direction discrimination task, it is sufficient to affect it, such that adding spikes to LIP neurons results in a behavioral response. This sufficiency argument may be mediated by either orthodromic or antidromic projections to or from LIP to neighboring structures involved in the task.

Other than the experiment performed by Hanks et al. and the experiment reported in this thesis, no other causal manipulations have been performed in LIP during a direction discrimination task. This is why discerning the function of LIP during evidence accumulation has become such a challenging endeavor. In an attempt to gain deeper insight into the function of LIP I have reviewed a large number of experiments that causally perturbed the activity of LIP, in any task 4.3. (Note that I have only added the main result of each study in sake of simplicity and comparison. The "main result" reported within the table is by no means a full description of the study within). The first section of the table, "simple saccades", is fairly straightforward: stimulation of LIP elicits saccades whereas inactivation of LIP disrupts some metric

of the oculomotor command. This is consistent with the role of LIP in oculomotor planning and execution (Andersen & Buneo 2002). The second section, "attention/selection", consists of studies that either include an attentional cue to a target or present the target amongst distractors.

Domain	Task	Causal perturbation	Main result	Reference
Simple saccades	**Free viewing**	**Electrical stimulation**	Evoked contralateral saccadic eye movements. Led to the name "parietal eye field"	Ferrier, 1876
	Fixation	**µStim**	Evoked saccadic eye movements to neuron RF	Constantin, Wang, Martinez-Trujillo, & Crawford, 2007; Shibutani, Sakata, & Hyvärinen, 1984; Thier & Andersen, 1998
	Immidiately before saccade to target	**µStim**	Evoked saccadic eye movements consistent with a predictive mapping	Mushiake, Fujii, & Tanji, 1999
	Memory guided saccade	**Muscimol**	Decreased accuracy of memory guided saccades	Li, Pietro Mazzoni, & Andersen, 1999
		Muscimol	Increased SRT of memory guided saccades	Liu, Yttri, & Snyder, 2010
Attention / selection	**Cued selection task**	**µStim** (sub-threshold)	Decreased SRT for selection of target in RF when uncued, but not when cued	Cutrell & Marrocco, 2002
	Select one target out of two (either free choice, target onset asynchrony, or instructed)	**µStim / optogenetic stimulation** (sub-threshold)	Decreased SRT for selection of target in RF; Increased probability of saccade to target in RF	Dai, Brooks, & Sheinberg, 2014
		Muscimol	Decreased probabilty of saccade to target in RF	Balan & Gottlieb, 2009; Kubanek, Li, & Snyder, 2015; Wardak et al., 2002; 2004; Wilke, Kagan, & Andersen, 2012; Zirnsak et al. 2015
	Visual search amongst multiple distractors	**µStim** (sub-threshold)	Increased probability of saccade to RF only if a target is present in RF	Mirpour, Ong, & Bisley, 2010
		Muscimol	Increased visual search time, independent of response modality. Effect sclaed with task complexity	Balan & Gottlieb, 2009; Liu et al., 2010; Wardak, Olivier, & Duhamel, 2002; 2004
Decision-making	**Double target, RT direction discrimination task**	**µStim** (sub-threshold)	Decreased SRT for selection of target in RF, small increase in choices to target in RF	Hanks, Ditterich, & Shadlen, 2006
	Double target, VD direction discrimination task	**Muscimol**	No oculomotor effect, no psychophysical effects	Chapters 3 and 4 of thesis

Table 4.3: A summary of causal perturbations in monkey LIP. Summary is divided into three main domains: simple saccades, attention/selection, and decision-making. The main result of either stimulation or inactivation is detailed in brief. Sub-threshold indicates microstimulation at current below threshold to elicit a saccade. SRT- saccade reaction time, RT- reaction time, VD- variable duration.

Synthesizing results from these studies is difficult due to experimental differences but superficially, microstimulation at sub-saccadic thresholds appears to facilitate selection towards the target that is positioned within the RF the cluster of LIP neurons microstimulated. This is manifested by both a reduction in saccade reaction time, and an increase in selection bias towards that target. Studies of inactivation reveal the other side of the coin, where saccade reaction times to the contralesional target are increased, and the bias is shifted away it (similar to our result in the "free-choice" task, Chapter 3). The third section of the table, "decision-making", includes the observations made by Hanks et al. (discussed above). The striking similarity between these observations to findings made in the attention/selection studies compel me to (parsimoniously) ascribe the results made by Hanks et al. to a facilitation of saccadic selection, and not of evidence accumulation. Especially, given that the inactivation of LIP reported in this thesis, has unmeasurable impact on psychophysical behavior.

4.5 Exploratory analyses

In addition to results reported so far we performed a number of exploratory analyses in an attempt to uncover a potential role for LIP in the motion discrimination task. In this section I report analyses that tested whether inactivation affects monkey reliance on previous trial outcome (i.e. sequential effects), and whether inactivation exerts effect on evidence accumulation when the stimulus duration is varied from trial to trial.

4.5.1 Contribution of trial history to behavioral variability is unaffected by inactivation in LIP

Decisions made in sequence may present sequential effects where the outcome of a previous trial influences the trial that follows. For example, if monkeys adopt a win-stay-lose-switch strategy then they choose the same target given a reward on the previous trial, and switch to the other target if unrewarded. We hypothesized that LIP might be involved in this process and that disrupting LIP activity might change monkey reliance on previous trial outcome. To test this idea we computed psychophysical weights via logistic regression on three history terms and a general bias, using the same method described in Chapter 3 (behavioral analysis section). We found that both monkey N and monkey P had weights significantly different than zero, indicating that trial history had contributed to their choice variability. However, the weights were not different between baseline and muscimol treatment sessions, indicating that inactivation in LIP had no impact on the contribution of trial history to behavioral variability (Fig. 4.8).

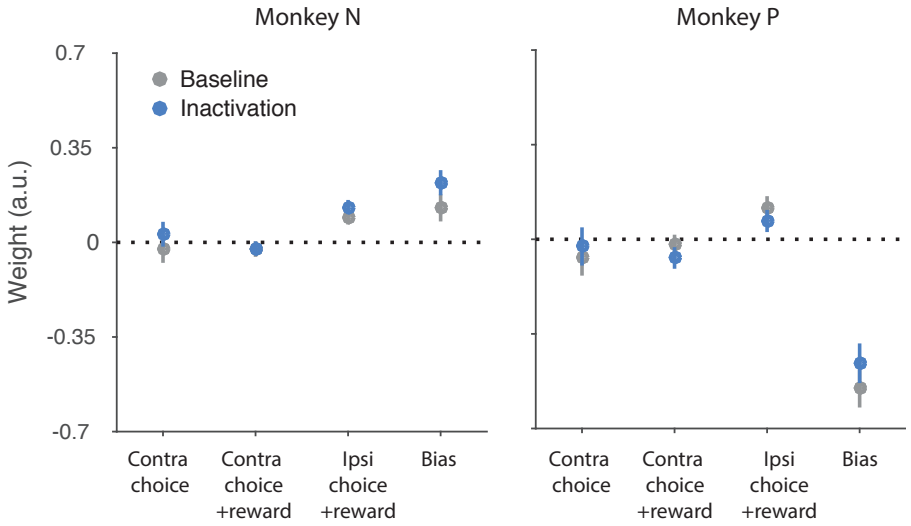

Figure 4.8: Psychophysical weights on trial history and bias terms, for baseline and muscimol treatment, over all trials (6201 and 3709 baseline trials for monkey N and P, respectively; 6733 and 3647 muscimol treatment trials for monkey N and monkey P, respectively). Weights represent the contribution of each term to a contralateral choice on trial n. The first three terms refer to the outcome on trial n-1: Contra choice, a contralateral choice on trial n-1; Contra choice +reward, a contralateral choice that was rewarded on trial n-1; Ipsi choice +reward, an ipsilateral choice that was rewarded on trial n-1. The bias term is a general bias for trial n.

4.5.2 Integration on faster time scales is unaffected by inactivation in LIP

Our standard stimulus lasted for 1050msec on every trial. Even though similar stimulus duration reliably produce decision-related activity in LIP (Shadlen & Newsome 2001), we contemplated whether shorter and unknown stimulus durations would rely more heavily on LIP such that disruption of LIP activity would reveal a behavioral deficit. We designed a variable duration (VD) version of the motion discrimination task by presenting either 1, 2, 3 or 7 motion pulses on every trial, resulting in either 150, 300, 450 or 1050msec of motion. Stimulus duration on every trial was drawn randomly from a truncated exponential distribution that approximated a flat hazard rate. A similar VD design was used in the past in which decision-related activity was observed in LIP (Kiani et al. 2008). However, Kiani et al. rewarded the animal for choosing the target consistent with the stimulus expectation, not the empirical stimulus shown. For example, a given stimulus presentation may be drawn from a distribution with an expectation slightly larger than 0 (e.g. rightward moving stimulus), but fluctuations in spatiotemporal patterns of the stimulus result in empirical motion to the left (see motion energy analysis in Kiani et al. for more details), and the monkey would be mis-rewarded even though it discriminated the direction of motion correctly. In our VD task, we measure monkey performance in the same way as Kiani et al. (i.e. conditioned on the expectation of the stimulus) but rewarded the animal for correctly discriminating the net motion shown, independent of the expectation.

The proportion of correct responses are presented as a function of motion duration (Fig. 4.9 A), for six baseline and three muscimol treatment sessions in one monkey. Performance increased with prolonged stimulus duration for all but the weakest motion stimulus strength, consistent with integration of motion evidence over multiple hundreds of milliseconds. Despite slight variations, there were no significant differences between performance in the baseline and muscimol treatment conditions. We further quantified the relationship between monkey performance and stimulus duration by computing the sensitivity (inverse of perceptual threshold) for each duration condition (Fig. 4.9 B). Sensitivity increased linearly on logarithmic coordinates for both the baseline and muscimol treatment conditions, with slope values of 0.69 (68.2% confidence intervals = [0.63 0.76]) for baseline, and 0.6 (C.I. = [0.54 0.66]) for muscimol treatment, indicating no significant difference between the two conditions. The precise value of the slope is slightly higher than that for perfect integration (0.5), likely resulting from inclusion of the first data point in the linear model, which may be more closely tied to early sensory integration than evidence accumulation (see Chapter 2 for details). Importantly though, we do not have sufficient data points to make claims about the form of integration, only about the comparison between baseline and treatment.

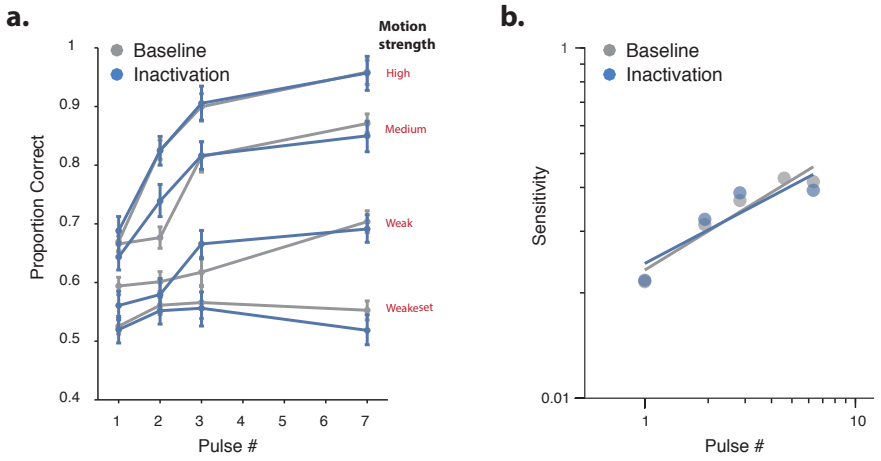

Figure 4.9: Performance over variable stimulus durations is unaffected by LIP inactivation. One monkey performed 6 baseline sessions with variable stimulus durations, and 3 muscimol treatment sessions, netting 10644 and 5135 trials, respectively. **A,** Proportion correct responses as a function of stimulus duration (i.e. number of motion pulses), for four ranges of motion strength (indicated in red text on the plot), for baseline sessions and muscimol treatment sessions. **B,** Psychophysical sensitivity (i.e. inverse perceptual threshold) over duration (i.e. number of motion pulses) computed for baseline sessions and muscimol treatment sessions.

Chapter 5

Decision-related perturbations of decision-irrelevant eye-movements

This work, with some modifications, has been published in the *Proceedings of the National Academy of Sciences* on February 16, 2016. Joo SJ, Katz LN, Huk AC: Decision-related perturbations of decision-irrelevant eye movements. Proceedings of the National Academy of Sciences,113(7),1925-1930. Supplementary material to this work can be found in the online version of the manuscript.

5.1 Abstract

It is well established that ongoing cognitive functions affect the trajectories of limb movements mediated by corticospinal circuits, suggesting an interaction between cognition and motor action. Although there are also many demonstrations that decision formation is reflected in the ongoing neural activity in oculomotor brain circuits, it is not known whether the decision-related activity in those oculomotor structures interacts with eye movements that are decision-irrelevant. Here we tested for an interaction between decisions and instructed saccades unrelated to the perceptual decision. Observers per-

formed a direction-discrimination decision-making task, but made decision-irrelevant saccades before registering their motion decision with a button press. Probing the oculomotor circuits with these decision-irrelevant saccades during decision-making revealed that saccade reaction times and peak velocities were influenced in proportion to motion strength, and depended on the directional congruence between decisions about visual motion and decision-irrelevant saccades. These interactions disappeared when observers passively viewed the motion stimulus but still made the same instructed saccades, and when manual reaction times were measured instead of saccade reaction times confirming that these interactions result from decision formation as opposed to visual stimulation, and are specific to the oculomotor system. Our results demonstrate that oculomotor function can be affected by decision formation even when decisions are communicated without eye movements, and that this interaction has a directionally specific component. These results not only imply a continuous and interactive mixture of motor and decision signals in oculomotor structures, but also suggest non-motor recruitment of oculomotor machinery in decision-making.

5.2 Introduction

Perception, cognition, and action are often modeled as discrete, serial stages of processing (Donders 1969, Luce 1986). In the context of a simple perceptual decision-making task, it is conventional to assume that motor output is generated only after a decision regarding the sensory information is

complete. However, a growing body of literature suggests a more interactive model, in which actions are continuously affected by ongoing cognitive processing (Song & Nakayama 2009). In a variety of reaching tasks, limb trajectories have been shown to be modulated by attention (Song & Nakayama 2008*b*), language processing (Spivey et al. 2005), and numeric representation (Song & Nakayama 2008*a*). And during a well-studied motion direction-discrimination task (Newsome et al. 1989), the reflex gain in limb muscles during decision-making was modulated by the accumulated evidence of motion direction (Selen et al. 2012).

It is not known, however, whether cognitive signals similarly affect oculomotor functions. There are many reasons why such interactions might not be present, or may not have been detected. In principle, limb movements are relatively slow and more continuous, and so online correction may be more appropriate than for fast and ballistic saccadic eye movements. In practice, it might have been difficult to assess how decision formation affects oculomotor output, because in previous perceptual decision-making studies, the oculomotor output is typically consistent with the sensory stimuli and the corresponding decisions (e.g., making a rightward saccade after viewing rightward motion).

Given the ample electrophysiological evidence in nonhuman primates showing decision-making related neural responses in oculomotor brain areas such as the lateral intraparietal area (Bennur & Gold 2011, Shadlen & Newsome 2001, de Lafuente et al. 2015), the superior colliculus (Horwitz

& Newsome 1999) and the frontal eye fields (Ding & Gold 2012*a*, Gold & Shadlen 2000, Gold & Shadlen 2003), and human neuroimaging evidence suggesting decision-related neural activity in counterpart brain areas such as posterior parietal cortex (Hebart, Donner & Haynes 2012, Liu & Pleskac 2011, Kayser, Buchsbaum, Erickson & D'Esposito 2010), we hypothesized that such decision-related activity in oculomotor structures might affect eye movements themselves. To test this, we devised a dual-task paradigm in which instructed saccadic eye movements had to be made, but were independent of a concurrent perceptual decision-making task. Our dual-task paradigm is different from previous paradigms that assessed how saccadic eye-movements affect concurrent processes in which observers perform a task during saccades (Irwin & Brockmole 2004, Shioiri & Cavanagh 1989, Burr, Morrone & Ross 1994). We reversed the logical order, measuring saccade metrics during an ongoing decision-making task (Fig. 5.1). Observers were required to judge the net direction of a random-dot motion stimulus, and later, to press a button indicating the net direction of motion. But in between the motion stimulus and the decision response, we presented a saccade target in particular locations following the offset of the motion stimulus. Observers had to make a saccade to this decision-irrelevant target. After the saccadic eye movement was made, the decision was reported. We emphasized speeded responses for the saccade to the target location, whereas accuracy was emphasized for the motion direction judgment.

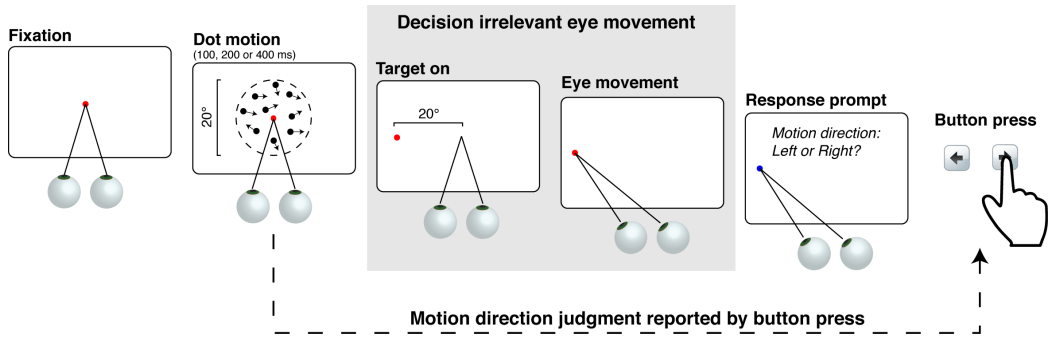

Figure 5.1: Procedure. On a given trial, random dot motion stimuli were displayed after observers fixated stably for 1 s. At motion offset, a saccadic target appeared to either the left or right side of the visual field. Observers made a saccadic eye movement to the target as quickly as possible. After the saccade, they were instructed to report the motion direction with a button press. The contrast polarity of dots and the background in the figure is reversed for illustrative purpose only. The dashed lines depicting the aperture was not shown in the experiments. An example trial from Experiment 1 is shown here

5.3 Materials and Methods

5.3.1 Participants

A total of seven observers, including authors with normal or corrected-to-normal vision, participated in the experiment voluntarily. Distinct subsets of 5 observers from this pool participated in each experiment. All experimental sessions were conducted with the written consent of each observer and in accordance with the University of Texas at Austin Institutional Review Board.

5.3.2 Apparatus, stimuli, and procedure

Eye position was recorded monocularly with an Eyelink1000 (SR Research, Ltd.) in "remote mode" with a sampling rate of 500 Hz. Stimuli were created using MATLAB (The Mathworks, Inc.) in conjunction with the Psychophysics Toolbox Brainard:1997we on a Mac Pro. They were displayed on a Samsung liquid crystal display (LCD) TV (1920 x 1080 resolution, 60 Hz refresh rate, subtending 80 horizontally). The viewing distance was 60 cm.

We used random dot motion stimuli (300 dots) that were displayed in a circular aperture (20 in diameter) centered around the fixation mark. Dots were white (78.43 cd/m^2), subtended 0.17, and moved at the speed of 5/s on a black background (0.23 cd/m^2). Each dot was assigned a random lifetime from a uniform distribution between 0 and 150 ms (9 video frames). When a dot's lifetime expired, it was randomly placed within the aperture and assigned the maximum lifetime (150 ms). The central 3 around fixation was blank. Motion coherence was defined as the percentage of dots moving together in the same

direction among dots moving in random directions. We used five coherence levels: 3, 6,12, 24, and 48%. We also manipulated the viewing duration of motion stimuli (100, 200, or 400 ms).

Each trial started with a fixation mark (red,15.08 cd/m^2) at the center of the display. After establishing stable fixation for 1 s, random dot motion stimuli were displayed for variable duration. At the offset of the motion stimulus, the fixation mark disappeared and a saccadic target (red,15.08 cd/m^2) appeared at a location that was displaced by 20° horizontally (either left or right) from the center of display. Observers made a saccadic eye movement to the saccade target as quickly as possible. After re-establishing stable fixation after the saccade landing for 500 ms, the color of the saccadic target changed from red to blue (5.44 cd/m^2) prompting observers to report the net direction of the random dot stimulus. Observers used computer keyboard arrow keys to report the motion direction with a finger button-press. The experiment did not proceed until observers report the motion direction. The inter-trial interval (ITI) was 1 s, and after this interval the fixation mark appeared at the center of the display. Auditory feedback was presented for the motion discrimination task (correct vs. incorrect). A 3° wide square window was used to determine whether stable fixation was established. When observers broke fixation (i.e., their eye position moved outside of this square window), the trial was aborted and discarded.

In Experiment 1, the motion direction (left or right) was the same as the axis of saccadic eye movements (left or right). Because the motion

direction and the saccadic eye movements shared the same axis, there were two more conditions in this experiment: congruent (the saccadic direction and motion direction were the same) and incongruent (the saccadic direction was the opposite of the motion direction). Observers used left and right arrow keys to report their decision about motion direction. In Experiment 2, all aspects of the experiment remained the same as in Experiment 1 except that there was no motion direction discrimination component: observers were not prompted to report the motion direction after making the instructed saccade. In Experiment 3, the motion direction (up or down) was perpendicular to the axis of saccadic eye movements (left or right). Observers used up and down arrow keys to report the motion direction. In Experiment 4, all aspects of the experiment remained the same as in Experiment 3 except that manual reaction times were measured instead of saccade reaction times. Observers reported the target location using left or right arrow keys as quickly as possible after target onset using their right hand, and they used designated buttons to report the motion direction, up ("a") or down ("z") using their left hand. The fixation mark was always displayed to force observers to maintain fixation. We later excluded trials where observers made eye movement to the target ($< 1\%$).

Each experimental session consisted of 31 experimental blocks. Within each block,15 trials (3 durations x 5 coherences) were randomized in order (Experiments 1, 2, and 3) and 10 trials (2 durations x 5 coherences) were randomized (Experiment 4). The motion direction and saccadic direction were randomized across trials. The first block served as a practice block and was not

included in the data analysis. Each observer participated in 3-4 experimental sessions for Experiment 1 and 3, and 2 experimental sessions for Experiment 2 and 4.

5.3.3 Data Analysis

We detected saccades offline by applying velocity threshold. We slid a 10 ms moving window and defined saccade onset as the first time point of the window during which velocity exceeded 20°/s. Saccade reaction times were defined as the elapsed time from saccade target presentation to the detected onset of the saccade. Only saccade reaction times between 150 ms and 500 ms ($< 1\%$ trials in Experiment 1, 2, and 3) were included in data analysis. We included all the data regardless of whether the reported motion direction was correct or not for analyses. Only including correct trials did not change the pattern of the results. For statistical evaluation, we used repeated measures ANOVA. The assumptions for ANOVA were met, unless otherwise stated.

Motion discrimination performance was evaluated by defining a psychometric function. We used maximum likelihood procedure to estimate the best-fitting Weibull function to the data. Then, we used a parametric bootstrapping procedure to calculate the confidence intervals (CIs) of the estimated psychophysical thresholds.

5.4 Results

5.4.1 Interactions between decision-making and decision-irrelevant saccades

In Experiment 1, we tested for direction-specific interactions between motion strength and saccade generation in the context of a motion-direction discrimination task (Shadlen & Newsome 2001, Selen et al. 2012, de Lafuente et al. 2015, Bennur & Gold 2011, Horwitz & Newsome 1999, Ding & Gold 2012*a*, Gold & Shadlen 2000, Gold & Shadlen 2003). Observers performed decision and saccade tasks in which the axes of visual motion and saccade direction were aligned. On a given trial, after fixation was established, a random-dot motion stimulus of variable coherence (3, 6,12, 24, or 48%) and variable duration (100, 200, or 400 ms) was displayed around fixation. After the offset of the motion stimulus, a saccade target was displayed on either the left or right side of the display, displaced 20° horizontally from the fixation point. Observers were instructed to make a saccadic eye movement to the target as quickly as possible. After the saccade, they reported their motion direction judgment by pressing designated keyboard buttons with fingers on their right hand. This arrangement is schematized in Fig. 5.1. Motion direction could be either toward the left or right, and the saccade target could appear in either the left or right visual field. In this geometric arrangement, motion direction and saccade direction could either be congruent (i.e., rightward visual motion and a rightward instructed saccade) or incongruent (i.e., rightward visual motion and a leftward instructed saccade). Note that although the axes

of visual motion and saccade direction were aligned, making a saccadic eye movement was irrelevant to motion-direction discrimination.

Motion direction-discrimination accuracy varied systematically with motion coherence. This conventional dependency confirms that observers were engaged in the decision task (Fig. 5.2). The psychometric functions were nearly identical between the congruent and incongruent conditions, indicating that congruency between saccade and motion direction did not affect psychophysical performance, even though the saccade took place in between motion viewing and the subsequent decision response. This independence supports the notion that observers treated the saccade task as irrelevant to performance of the direction discrimination task; the intervening saccades did not affect choices in a direction-selective manner. This allowed us to test whether motion strength and/or direction affected the reaction time or other oculomotor metrics of the decision-irrelevant saccade.

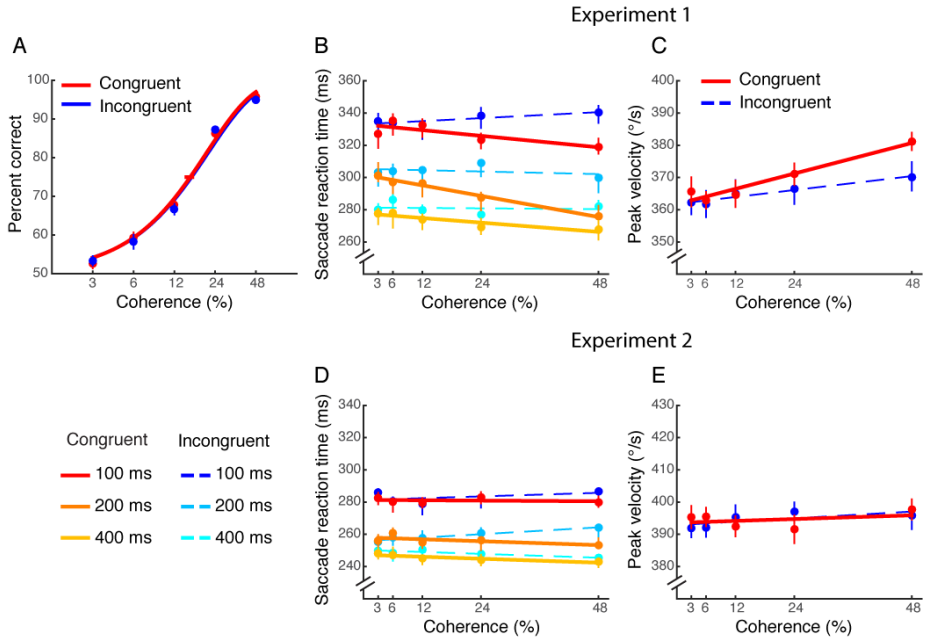

Figure 5.2: Psychometric functions and saccade metrics in Experiment 1 and 2. **A,** The psychometric functions for congruent vs. incongruent conditions, depicted by red and blue lines, respectively. The error bars on the data points reflect SEM across observers, and the error bars on the 75% performance threshold indicate bootstrapped 68% confidence intervals (CIs). **B, C,** Saccade reaction times (left panel) and Saccade peak velocities (right panel) as a function of motion coherence in Experiment 1. **B,** Color scaled data represent viewing duration in the congruent and the incongruent condition (red vs. blue: 100 ms, orange vs. light blue: 200 ms, and yellow vs. cyan: 400 ms). **C,** Red and blue indicate saccade peak velocities in the congruent and incongruent conditions, respectively. Solid and dashed lines are the best-fitting lines for the congruent and incongruent conditions, respectively. Error bars are bootstrapped 95% CIs. **D, E,** Saccade reaction times (D) and Saccade peak velocities (E) as a function of motion coherence in Experiment 2.

Indeed, saccade reaction times were affected by the directional congruency of the preceding visual motion. Reaction times were faster in the congruent condition than in the incongruent condition (Fig. 5.2B; main effect of congruency on saccade reaction times, $F(1,4) = 10.11$, $P = 0.03$). Interestingly, the effect of motion coherence on saccade reaction times was different between congruent and incongruent conditions (interaction between congruency and coherence, $F(4,16) = 6.28$, $P = 0.003$). In the congruent condition, reaction times decreased as coherence increased ($F(4,16) = 7.24$, $P = 0.002$) whereas in the incongruent condition this was not the case ($F(4,16) = 0.05$, $P = 0.99$). Thus, decision-irrelevant saccade reaction times were modulated by motion coherence, suggesting an interaction between decision-making and the initiation of saccades, and this interaction occurred only when motion was directionally congruent with the saccade. Motion viewing duration also affected saccade reaction times ($F(2,8) = 114.53$, $P < 0.0001$), but the range of viewing durations we used did not strongly affect psychophysical performance in the motion direction discrimination task. Thus, it is likely that the effect of viewing duration on saccade reaction times is a distinct consequence of simple response readiness (Ross & Ross 1980, Kingstone & Klein 1993) and not of decision formation, in which longer viewing durations increased subject readiness, resulting in shorter reaction times.

Saccade peak velocities were also influenced differentially by the congruency of the visual motion. Fig. 5.2C depicts peak velocities for the congruent and incongruent conditions as a function of motion coherence (after

collapsing across motion viewing duration). Congruent trials led to saccades with higher velocities than incongruent trials ($F(1, 4) = 7.24$, $P = 0.05$). Motion coherence also had an effect, with higher coherences leading to faster velocities ($F(4,16) = 8.04$, $P = 0.001$). Similar to saccade reaction times, motion coherence affected the saccade peak velocity in the congruent condition ($F(4,16) = 8.78$, $P = 0.001$) but not in the incongruent condition ($F(4,16) = 1.92$, $P = 0.16$); although the interaction between congruency and coherence was not statistically significant ($F(4,16) = 1.88$, $P = 0.16$).

We tested whether this linear dependency between motion coherence and saccade peak velocity was simply predictable by the saccadic "main sequence" (Bahill, Clark & Stark 1975). For example, higher motion coherence might have resulted in larger saccade amplitude and thus higher saccade peak velocity. However, we found that saccade amplitude did not vary with coherence. This suggests that our reported modulation of saccade peak velocity cannot be explained as a simple consequence of the main sequence.

Overall, our results suggest that saccade reaction times and saccade peak velocity were modulated by motion strength, and that saccade generation can interact with decision-related signals in direction-specific parts of the oculomotor circuitry.

5.4.2 Saccades are affected by decision-making but not motion viewing

In Experiment 2, we conducted a single-task experiment in which observers only performed the saccade task. This allowed us to test whether the oculomotor consequences we observed in Experiment 1 were simply due to viewing visual motion, as opposed to the formation of decisions per se. In this experiment, the stimuli and procedure were identical to the preceding experiment in which the motion direction and the axis of saccadic eye movements were aligned, but now observers were instructed to ignore the motion stimulus that preceded the saccadic target appearance, and simply perform the instructed saccades.

Although the visual stimuli in Experiment 2 were identical to those in Experiment 1, motion coherence no longer modulated saccade reaction times, in either the directionally congruent or incongruent conditions (Fig. 5.2D; congruent condition, $F(4,16) = 1.06$, $P = 0.40$; incongruent condition, $F(4,16) = 0.89$, $P = 0.49$, respectively). Congruency itself had only subtle effects on saccade reaction times that were not statistically significant ($F(1,4) = 5.80$, $P = 0.07$). Only motion viewing duration significantly affected reaction time ($F(2,8) = 54.67$, $P < 0.0001$), supporting our interpretation that the effects of motion viewing duration seen in the first experiment are more likely to indicate general response readiness as compared to motion evidence (as there was no decision component in this experiment). Saccade peak velocity was not affected by congruency either (Fig.5.2D; $F(1,4) = 0.02$, $P = 0.89$). Fi-

nally, there was no longer a clear relationship between saccade peak velocity and coherence (congruent condition, $F(4,16) = 3.74$, $P = 0.07$; incongruent condition, $F(4,16) = 2.94$, $P = 0.05$) (Fig.5.2E).

To compare the results from this passive-viewing experiment (Experiment 2) to the results of the active decision-making experiment (Experiment 1), we collapsed the data over duration for each condition and plotted the difference between the congruent and the incongruent conditions as a function of motion coherence (Fig. 5.3). The difference in saccade reaction time between these conditions increased systematically with coherence for the decision-making task, but remained close to zero for the passive viewing task. At the very highest motion coherence, there was a slight increase when passively viewing the motion stimulus (mean $\pm$ SEM; 7.19 $\pm$ 2 ms), but this increase is smaller that that of the active decision-making experiment (21.59 $\pm$ 7 ms). We suspect that this small effect might be because some of our observers failed to completely ignore the motion stimuli, given that 4 of 5 observers conducted the active decision-making experiment before conducting the passive-viewing control experiment. Taken together, these results suggest that the relationship between decision difficulty and saccade metrics — linear decreases in saccade reaction times, and linear increases in saccade peak velocity, as a function of coherence — cannot be explained by sensory signals alone.

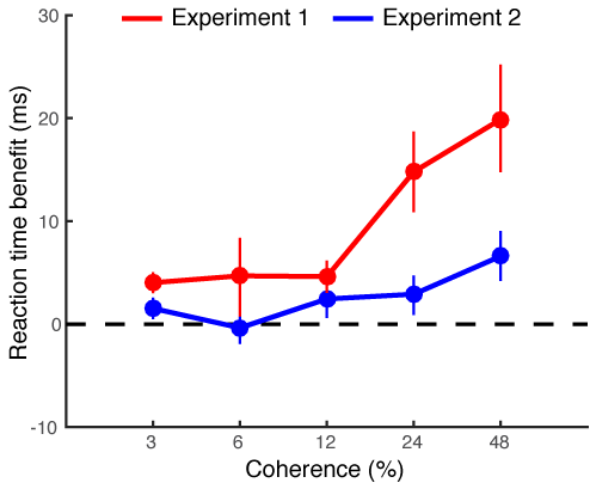

Figure 5.3: Comparison of saccade reaction time benefits between Exps. 1 and 2. Saccade reaction time benefit was calculated by subtracting saccade reaction times for the congruent condition from saccade reaction times for the incongruent condition. Red and blue lines represent saccade reaction time benefit in Exps. 1 and 2, respectively. Error bars are bootstrapped 95% CIs.

5.4.3 Decision-making but not spatial attention modulates decision-irrelevant saccades

Although the preceding experiments lend support for the notion of decision making modulating the oculomotor system, we sought to isolate purely decisional factors from other processes that likely co-occur with decision-making. It is possible that the observed modulation in saccade metrics is a function of attentional allocation in concert with the direction of motion. For example, strong rightward motion could serve as an attentional cue to the right, resulting in a facilitation of rightward saccade reaction time and velocity (Bosbach, Prinz & Kerzel 2004).

In Experiment 3, we tested whether the modulation of saccade metrics in prior experiments could be due to stimulus-driven spatial attention, specifically, a shift of attention to a target location congruent with the direction of discriminated motion. In this experiment, the axis of visual motion for direction discrimination was now perpendicular to the axis of potential saccade target locations (i.e., up versus down visual motion, and left or right saccade targets). In this geometric configuration, a direction-specific shift in spatial attention would be either above or below the motion aperture, both spatially unrelated to the left/right saccade. If an attentional shift accounts for the results of our Experiment 1, then we would not expect to observe a modulation of saccade metrics here.

As in Experiment 1, direction-discrimination accuracy varied systematically with motion coherence. Because there was no explicit mapping between

motion direction (up/down) and the saccade target location (left/right), the saccadic eye movements should not be affected by the motion direction, but could still be affected by the nondirectional magnitude of the motion coherence. Consistent with this, motion direction did not exert a reliable effect on saccade reaction times ($F(1,4) = 2.27$, $P = 0.21$). Thus, we collapsed the data over motion direction for further analyses.

Saccade reaction times to the decision-irrelevant saccade target were systematically affected by motion coherence (Fig. 5.4A). Saccade reaction times were slower while making a decision based on weaker motion evidence, and quickened progressively with increased motion coherence ($F(4,16) = 7.12$, $P = 0.002$). A roughly linear inverse dependency between motion coherence and saccade reaction times was evident. The reaction time modulation by motion coherence was largest for the longer viewing durations (for 200 ms, slope = -0.61, r = 0.97, $P = 0.001$; for 400 ms, slope = -0.63, r = 0.99, $P = 0.0001$), and was weak if present at all in the shortest duration (for 100 ms, slope = -0.10, r = 0.73, $P = 0.14$), confirmed by an interaction between motion viewing duration and coherence ($F(8, 32) = 3.78$, $P = 0.003$).

Motion viewing duration also affected saccade reaction times (Fig. 5.4A; $F(2, 8) = 61.32$, $P < 0.0001$), likely because general response readiness increased as motion viewing duration increased (Ross & Ross 1980, Kingstone & Klein 1993). Saccade peak velocity was also linearly dependent on motion coherence. Peak velocity increased progressively as the coherence increased (Fig. 5.4B; $F(4,16) = 9.85$, $P = 0.0003$). Motion viewing duration also af-

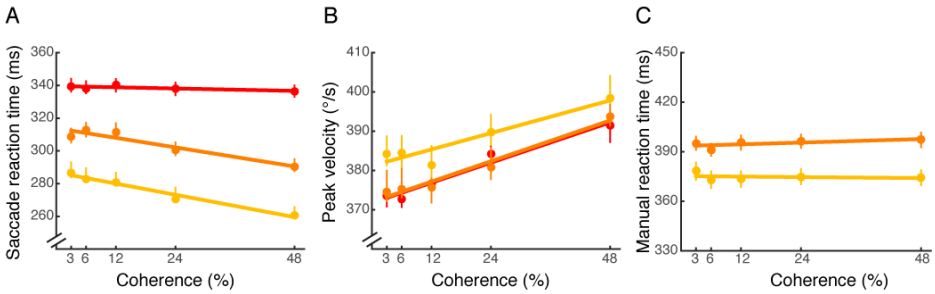

Figure 5.4: Saccade metrics in Experiment 3 and 4. **A,** Saccade reaction times in Experiment 3 are plotted as a function of motion coherence for each viewing duration (red: 100 ms, orange: 200 ms, and yellow: 400 ms), averaged across motion direction (up and down). **B,** Saccade peak velocities in Experiment 3 are plotted as a function of motion coherence for each viewing duration (red: 100 ms, orange: 200 ms, and yellow: 400 ms), averaged across motion direction (up and down). **C,** Manual reaction times in Experiment 4 are plotted as a function of motion coherence for each viewing duration (orange: 200 ms and yellow: 400 ms), averaged across motion direction (up and down). Best-fitting lines are shown. Error bars are bootstrapped 95% CIs.

fected saccade peak velocity ($F(2, 8) = 9.89$, $P < 0.01$). Consistent with the results in Experiment 1, there was no linear relationship between saccade amplitude and motion coherence ($F(4,16) = 2.431$, $P = 0.09$) whereas motion viewing duration affected saccade amplitude ($F(2, 8) = 11.645$, $P < 0.005$).

To summarize Experiment 3, saccade reaction times and peak velocities were modulated by motion coherence even in the absence of a geometrical mapping between saccade and motion direction. This argues against an attentional shift in congruence with motion direction, and instead, supports the idea that the difficulty of the decision governs interactions between decisions and saccades.

5.4.4 Dual-task interference due to decision-making is oculomotor-specific

It is also logically possible that the results of Experiment 1 depend on task difficulty, but not a specific interaction between decision-making signals and oculomotor circuits, as a result of general dual-task interference (25). To test whether our results are more precisely specific to decisions interacting with oculomotor functions, we conducted Experiment 4, in which we changed the mappings between decisions and motor responses, under otherwise identical experimental settings to Experiment 3.

If our results were due to general dual-task interference, the modality of the response to the decision-irrelevant target (i.e. an eye-movement or a button press) should not matter, because general dual-task interference by definition, affects all effectors equally. Thus, the procedure of Experiment 4 was identical to Experiment 3 but instead of a saccade to a decision-irrelevant target, subjects were instructed to report the location of the decision-irrelevant target with a speeded button press. To maximize statistical power, we used only the two longer motion durations (200 and 400ms) for which the modulation of saccade reaction times was most pronounced.

Inconsistent with the predictions of general dual-task interference, we found no modulation of manual reaction times as a function of motion coherence (Fig. 5.4C; $F(4,16) = 1.14$, $P = 0.37$). Motion viewing duration affected manual reaction times ($F(1, 4) = 18.164$, $P = 0.01$), consistent with our previous experiments that suggested duration separately affected general

task readiness. Performance on the motion direction discrimination task was nearly identical to the one in Experiment 3, confirming that the different results in the manual reaction time task were not due to different psychophysical performance levels between experiments. To summarize Experiment 4, manual reaction times were not affected by motion coherence when the location of the decision-irrelevant target was reported with a button press, arguing against general dual-task interference, and in addition, add further support to the notion that our main finding is specific to the oculomotor system.

Overall, our results demonstrate that performing a challenging perceptual decision task results in significant modulations of oculomotor performance. The observed changes in saccade reaction times and peak velocities point to interactions within the oculomotor circuit, in which activity related to accumulating evidence during a perceptual decision-making and activity related to generation of decision-irrelevant saccades are not kept completely separate.

5.5 Discussion

We tested whether visually-guided instructed saccades to a single target were influenced by the formation of perceptual decisions known to elicit decision-related activity in the oculomotor brain structures of primates. We found that saccadic eye movements to a decision-irrelevant target were systematically modulated by the motion strength that informed perceptual decisions about visual motion direction. This pattern of results suggests that

decision-making processes interact with saccadic eye movements: specifically, saccade reaction times and peak velocities were slower given difficult motion judgments (i.e., decisions driven by weaker sensory evidence). We also found that the spatial congruency between motion direction and saccade direction mattered: motion strength did not affect saccadic eye movements when the decision-irrelevant saccades were opposite the direction of the motion decision.

The results reported here are most consistent with an explanation based an active decision-making process. Passively viewing the motion stimulus did not result in the same effects on saccades (Experiment 2). We also observed changes in saccade reaction times and velocities when motion and saccade directions were uncoupled (Experiment 3), ruling out a directional form of spatial attention as a possible explanation of our results. And when manual reaction times were measured instead of saccade reaction times (Experiment 4), reaction times were no longer modulated as a function of motion coherence, even though all other aspects of experiment remained the same as in Experiment 3. This constellation of results suggests an oculomotor-specific dual-task interference effect, and support the prospect of oculomotor circuitry being involved in decision-making, even when decisions are not communicated with eye movements.

An interesting remaining question is whether attending to the stimuli without making decisions can result in the coherence dependent effect in our paradigm. Attention and decision processes are tightly related, and it is difficult to distinguish an effect due to one process from the other. For ex-

ample, even when observers perform an attention-demanding task on moving stimuli, it is difficult to know whether they covertly make decisions on motion direction. In the same vein, we speculate that making covert decisions on motion direction may have caused a very small effect in the highest coherence condition in Experiment 2 where there was no decision component.

Our results show that only when there is a conflict between saccade and motion direction (the incongruent condition in Experiment 1), saccade metrics were not modulated by motion strength. This might be due to the fact that saccades in the incongruent condition involve an unnatural stimulus-response mapping. In fact, during visual inspection of raw eye position traces, we found that in a small portion of trials in the incongruent condition (which were removed from the main analyses), observers initiated saccades towards the location congruent with motion direction (opposite to the target location) and then corrected their gaze towards to the target location. Interestingly, the number of these error trials increased as the motion coherence increased (3, 6, 7,15, and 19 trials across observers for 3, 6,12, 24, 48% coherence, respectively). These results suggest that the higher motion coherence, the more interference between motion evidence and saccades in the incongruent condition, and thus less of a speed-up as a function of motion strength.

It is known that saccade peak velocities can be influenced not only by the intrinsic value of the saccadic target (Bahill et al. 1975, Bosbach et al. 2004) but also by the subjective preference or value to the saccadic target (Pashler, Carrier & Hoffman 1993). It is possible, therefore, that the saccadic target in

our experiments might have been associated with a value based on the task difficulty. For example, the saccadic target in difficult (low coherence) conditions (where observers made more incorrect responses) might have been associated with low values, resulting in slower saccade reaction times. However, in Experiment 1, there was not only an effect of motion coherence but also a dependency on congruency. In congruent versus incongruent trials, the motion judgment was equally hard (for matched coherences), but the coherence effect was only pronounced in the directionally-congruent condition. This argues against interpretations of our results based on the value of targets and/or simple effects of task difficulty.

Although the majority of behavioral studies addressing cognitive influences on motor output have focused on tasks using arm reaches as the motor response, there has been some evidence suggesting an interaction between decision-making and oculomotor output. Microstimulation in FEF during perceptual decision-making tasks evokes saccadic eye movements that deviate in proportion with motion evidence (e.g., coherence) along the motion direction, suggesting that accumulated evidence is represented in this oculomotor planning structure, or in structures connected to it (Gold & Shadlen 2000, Gold & Shadlen 2003). Our findings are consistent with this type of decision and premotor multiplexing, and demonstrate that such interactions are tacitly present even without artificial perturbation of brain circuits. Furthermore, saccadic trajectories exhibit systematic deviations in their endpoints when saccadic eye movements are used to report decisions in a motion direction discrimination

task (Xu-Wilson, Zee & Shadmehr 2009). Our results are not only consistent with such observations of oculomotor output being affected by decisions, but also reveal that eye movements can be affected even when the decision-making task does not involve an oculomotor response. This suggests that oculomotor circuits may be recruited during decision-making even when they are not tightly tied to premotor or motor function.

A growing body of literature has revealed multiplexing of parallel signals in oculomotor areas. Recent single-cell recordings have documented that neural responses in oculomotor brain areas show heterogeneous selectivity for different sources such as visual events, decision formation and saccade execution, often within the same neurons and the same single-trial spike trains. These include LIP (Bennur & Gold 2011, Meister et al. 2013, Rishel et al. 2013, Park et al. 2014), FEF (Mante, Sussillo, Shenoy & Newsome 2013), and SC (Horwitz & Newsome 1999). Our findings suggest that the multiple signals in oculomotor areas interact with each other at least between decision-forming signals and oculomotor execution. Ultimately, it appears that the read-out of oculomotor structures cannot completely distinguish activity driven by decision formation from activity related to the planning of even decision-irrelevant eye movements (Raposo et al. 2014).

Chapter 6

Discussion

In this thesis, I have described my attempts to gain an understanding of decision formation in the primate brain. To accomplish this I utilized psychophysical methods, multi-channel electrophysiological recordings, and causal manipulations. While I believe the work presented here serves to advance the field, it may have opened more questions than supplied answers. In this final section, I briefly discuss some pertinent points and note the key questions that arise from this work.

"I would rather have questions that can't be answered than answers that can't be questioned"

— Richard Feynman

In the first experimental chapter of the thesis (Chapter 2) I reported the use of simple psychophysical procedures to characterize how motion information is temporally integrated to guide decisions. The main finding of the experiment was that motion through depth ("3D motion") is integrated very differently than standard frontoparallel motion ("2D"). It is well established that sensitivity to stereoscopic stimuli is reduced compared to dichoptic stimuli (Regan & Tyler 1971, Tyler & Foley 1974, Harris, McKee &

Watamaniuk 1998, Brooks & Stone 2006, Cottereau, McKee & Norcia 2014), but it is unclear why the signal– regardless of its magnitude– would be integrated differentially. Neural recordings of 3D sensitive cells would shed light on this process but unlike the extensive study of binocular disparity (Parker 2007), electrophysiology study of 3D motion is still in its infancy. To date, only two studies have identified neural responses tuned to 3D motion, both in area MT of either fixating (Sanada & DeAngelis 2014) or anesthetized monkeys (Czuba, Huk, Cormack & Kohn 2014). Extending the electrophysiological study to behaving macaques would be an important step towards elucidating the downstream integration of 3D motion signals. For example, comparing MT sensitivity to 2D vs. 3D motion, over time, could identify whether the difference in psychophysical sensitivity observed in Chapter 2 is a result of differential neural integrators, or rather, a result of a single integrator that relies on very different sensory representations.

The integration puzzle was tackled more directly in the 2nd experiment of the thesis (Chapters 3 and 4), by testing a long standing hypothesis: that the locus of neural integration during decision formation takes place in the LIP. The first identification of decision-related activity in LIP (Shadlen & Newsome 1996) was the first to identify decision-related signals *anywhere* within the brain. Following this pioneering finding, decision-related activity was identified in a dizzying number of brain regions (presented in Fig. 1.3, Chapter 1). While the original finding may be considered extraordinary and those to follow incremental, I would argue the reverse. The most intriguing

feature of decision-related activity in the brain is not its residence in area LIP per se, but rather, its pervasive nature across swaths of cortical and subcortical territory. The distributed means by which decision signals are processed compels me to consider whether asking *"what do neurons in LIP do?"* is the right question to be asking at all.

"Who are you?"
–"No one of consequence"
–"I must know"
–"Get used to disappointment"

— Inigo Montoya and the Man in Black, The Princess Bride

Although the area-centric approach has been extremely effective in characterizing sensory and motor systems, it may fall short for brain regions associated with higher forms of cognitive function. Perhaps a more appropriate question is *"why should a particular function be distributed across multiple sites within the brain?"*. Answering this question could provide a more mechanistic understanding of the architecture with which to unpack the function of individual network nodes. The results reported in Chapters 3 and 4 may shed some light on the mechanism of evidence accumulation. How does inactivation of a region that is clearly correlated with decision formation *not* disrupt decision-making? There are two lines of thought to consider in answering this question, that are not mutually exclusive. The first takes a somewhat

LIP-centric approach by supposing that LIP *is* necessary for some aspects of making decisions, but that the decision-making task we employed was insufficient in revealing its critical function. The second considers the result from a broader perspective: if LIP is not necessary, why would it reflect the decision-related computation at all?

First, is the motion direction discrimination task not sufficiently complex to rely on LIP? The task we employed requires the monkey to peripherally view a motion stimulus for a given duration, discriminate the direction of motion, and communicate its decision by moving its eyes to one of two choice targets. Although this task relies on cognitive processing, it is not particularly complex. In fact, considering the vast behavioral repertoire of primates, the task is rather impoverished. It is almost unsurprising, then, that the sensitivity of single MT neurons can be as sensitive as the entire organism in discriminating the direction of motion in a similar task (Shadlen et al. 1996). It is important to remember that the decision-making process is far more complex than the task used to probe it. Decision-making incorporates a number of "meta-decision" components such as decision value, decision cost, bias, motivation, confidence, and any other variable pertinent to making good choices (Cisek & Kalaska 2010, Shadlen & Kiani 2013).

The task we employed did not manipulate any of these factors explicitly, so it is possible that inactivation in LIP had exerted disruptions we were not privy to. For example, in a visual categorization task where the monkey could either choose between two choice targets or "opt-out" by choosing a

third, inactivation of neurons in the pulvinar did not disrupt decision-making performance. Instead, it increased the number of opt-out choices made by the monkey (Komura, Nikkuni, Hirashima, Uetake & Miyamoto 2013). This indicates that while the pulvinar is not necessary for evidence accumulation in service of categorization, it is necessary for keeping the monkey "on-task". The authors interpret the deficit as a disruption in confidence. Interestingly, LIP function has also been linked to confidence (Kiani & Shadlen 2009, Fetsch, Kiani, Newsome & Shadlen 2014). Thus, while our results show that LIP is not necessary for the accumulation of sensory evidence in favor of an oculomotor decision, they cannot exclude the possibility that inactivation exerts effects on meta-decision aspects such as confidence, or subjective value (Platt & Glimcher 1997, Louie & Glimcher 2010). Tasks of higher dimensionality might be better poised to untangle the complexity of areas the likes of LIP (Rigotti, Barak, Warden, Wang, Daw, Miller & Fusi 2013, Fusi, Miller & Rigotti 2016), and these should be complemented by analysis methods designed to untangle the multiplexing nature of the area such as regression based models (Rorie, Gao, McClelland & Newsome 2010, Park et al. 2014, Siegel et al. 2015) or state space analyses (Mante et al. 2013, Cunningham & Yu 2014, Kaufman, Churchland, Ryu & Shenoy 2014).

The function of LIP may be better understood by considering the functional inputs to LIP. In the standard integration model (Mazurek et al. 2003) it was assumed that LIP receives feed-forward input from area MT. However, there is more evidence in support of the reverse: LIP-to-MT feedback con-

nections (Saalmann et al. 2007, Herrington & Assad 2010, Siegel et al. 2015). The MT-to-LIP feed-forward hypothesis has been recently tested by Yates et al. (Yates JL, Park IM, Katz LN, Pillow JW & Huk AC, in preparation) who performed simultaneous recordings in areas MT and LIP during a direction discrimination task. They found no evidence for functional feed-forward coupling between the areas, and instead, detected LIP-to-MT feedback coupling. From where, then, is LIP receiving input? Gottlieb and colleagues have noted that while parietal neurons encode multiple forms of spatial and non-spatial information, inactivation of LIP only disrupts functions that are spatial, leaving the non-spatial functions intact (Balan & Gottlieb 2009). They take this finding to indicate that the non spatial information in LIP is likely feedback from frontal regions of the brain that are more heavily engaged in executive functioning and motivational aspects of the task (Gottlieb & Snyder 2010). Support for this idea can be found in a recent simultaneous recording of LIP and the prefrontal cortex (PFC) (Crowe et al. 2013), where task related information was found to flow from PFC to LIP and not the other way round. Thus, processing in LIP may be more related to rule-dependent information coming from the PFC than incoming sensory evidence. If this is the case, then it is not surprising that inactivation in LIP does not affect evidence accumulation. Instead, inactivation may disrupt other features of behavior such as the ability to follow task rules and/or associate a particular cue with the appropriate motor response (Toth & Assad 2002, Sarma et al. 2015), but these have yet to be tested directly.

Results from the 3rd experiment of this thesis (Chapter 5) may provide a clue in understanding the pervasive nature of decision-related activity in the brain. The experiment revealed that when a decision is formed but not yet communicated, decision-irrelevant oculomotor commands are influenced by the decision process. It showed that oculomotor regions are recruited during decision formation, despite the fact that the decision is not communicated by an eye movement. The finding is complimented by a recent electrophysiological study, showing that neurons in LIP present decision-related activity even when the decision is communicated with a reach (de Lafuente et al. 2015). Further, Lafuente et al. found that neurons in the parietal reach region (PRR) of cortex exhibited the mirror response– exhibiting decision-related activity even when the decision was communicated by a saccade (albeit not as strongly as when the response is made with a reach). The psychophysical findings made in Chapter 5, together with the electrophysiological responses observed by Lafuente et al., invite me to speculate that the decision-related activity observed in LIP, FEF, SC, PRR, caudate, and even in EMG responses of the bicep (Fig 1.3) are part of a general and distributed process with little dependence on the effector by which the decision is ultimately communicated (but see Andersen & Cui 2009). Such a distributed network, over large neural territories, is seen for other cognitive functions such as attentional control (Noudoost, Chang, Steinmetz & Moore 2010), and may be a fundamental neural principle to support complex and flexible behavior.

Within this framework it is not readily obvious whether any one node

is more important than another. Perhaps neurons in LIP *do* have a causal role in evidence accumulation, but their contribution is rendered inconsequential given the amalgam of brain regions operating together. It might be possible that to reveal the causal contribution of LIP neurons, perturbation of an additional brain region might be necessary. It is unknown what such a manipulation would yield in the primate, but a similar manipulation in rats may hint at the outcome. Brody and colleagues (Erlich et al. 2015) trained rats to perform an evidence accumulation task and inactivated either the posterior parietal cortex (PPC) or the frontal orienting field (FOF). The PPC and FOF are thought to be analogous to LIP and FEF, respectively, but the degree of homology is not yet clear. Nevertheless, the group found that inactivation of PPC — similar to results reported in Chapters 3 and 4 — did not impact evidence accumulation in the decision-making task (but see Raposo et al. 2014). However, when coupling PPC inactivation with a bilateral inactivation in FOF, a spatially selective deficit in behavior was, in fact, observed. Thus, perturbation of PPC only disrupts behavior if other areas of the brain are removed from the equation too.

Could this be the case in primates? Is it possible that inactivation of LIP during decision-making, in addition to other the FEFs, will reveal a behavioral consequence otherwise unseen? The leap from rodents to primates is substantial given the differences in cortical organization and limited similarity in behavior (Uylings, Groenewegen & Kolb 2003, Cooke, Goldring, Recanzone & Krubitzer 2014, Belmonte, Callaway, Caddick, Churchland, Feng, Homanics,

Lee, Leopold, Miller, Mitchell, Mitalipov, Moutri, Movshon, Okano, Reynolds, Ringach, Sejnowski, Silva, Strick, Wu & Zhang 2015), but the notion is enticing. Despite the questionable homology between rodent and primate, the Brody lab has taken great strides in developing new models for evidence accumulation that capture decision-making behavior (Brunton et al. 2013) and can be fit to neural data (Hanks et al. 2015). Together with causal manipulations, the group has taken a systematic approach to dissecting the functional contribution of each area that exhibits decision-related activity (Brody & Hanks 2016). While results from the rodent cannot guarantee replication in primate, the rodent model affords far more flexibility for electrophysiological recordings and perturbations in multiple sites simultaneously. These efforts may prove extremely valuable in guiding future primate research.

The results presented in this thesis help to elucidate the functional significance of decision-related activity, and to constrain future models of processing in the primate brain. Further explication of the principles governing evidence accumulation, within or over multiple brain sites, will become increasingly feasible in the near future. This will likely rely on the development of novel tasks, sophisticated statistical analyses, increased use of multi-site electrophysiological recording, and utilization of causal multi-site manipulations. Now that optogenetic techniques are becoming increasingly used in primate neurophysiology (Diester, Kaufman, Mogri, Pashaie, Goo, Yizhar, Ramakrishnan, Deisseroth & Shenoy 2011, Gerits & Vanduffel 2013, Dai et al. 2014), circuits may be manipulated on fine temporal and spatial scales, along with

precise targeting of specific cell classes. Together, this confluence of methods stands to unravel the mechanism subserving the accumulation of evidence in the primate brain and lead to a deeper understanding of the circuit, that in time, could inform therapies in humans.

Bibliography

Andersen, R. A., Asanuma, C. & Cowan, W. M. (1985), 'Callosal and prefrontal associational projecting cell populations in area 7A of the macaque monkey: a study using retrogradely transported fluorescent dyes.', *The Journal of comparative neurology* **232**(4), 443–455.

Andersen, R. A., Asanuma, C., Essick, G. & Siegel, R. M. (1990), 'Corticocortical connections of anatomically and physiologically defined subdivisions within the inferior parietal lobule', **296**(1), 65–113.

Andersen, R. A. & Buneo, C. (2002), 'Intentional maps in posterior parietal cortex', **25**(1), 189–220.

Andersen, R. A. & Cui, H. (2009), 'Intention, Action Planning, and Decision Making in Parietal-Frontal Circuits', *Neuron* **63**(5), 568–583.

Andersen, R. A., Snyder, L. H., Bradley, D. C. & Xing, J. (1997), 'Multimodal representation of space in the posterior parietal cortex and its use in planning movements.', *Annual review of neuroscience* **20**(1), 303–330.

Arikan, R., Blake, N. M. J., Erinjeri, J. P., Woolsey, T. A., Giraud, L. & Highstein, S. M. (2002), 'A method to measure the effective spread of focally injected muscimol into the central nervous system with electrophysiology and light microscopy.', *Journal of Neuroscience Methods* **118**(1), 51–57.

Bahill, A. T., Clark, M. R. & Stark, L. (1975), 'The main sequence, a tool for studying human eye movements', *Mathematical Biosciences* **24**(3), 191–204.

Bair, W. & Movshon, J. A. (2004), 'Adaptive temporal integration of motion in direction-selective neurons in macaque visual cortex.', *The Journal of neuroscience : the official journal of the Society for Neuroscience* **24**(33), 7305–7323.

Balan, P. F. & Gottlieb, J. (2009), 'Functional Significance of Nonspatial Information in Monkey Lateral Intraparietal Area', *Journal of Neuroscience* **29**(25), 8166–8176.

Barash, S., Bracewell, R. M., Fogassi, L., Gnadt, J. & Andersen, R. A. (1991*a*), 'Saccade-related activity in the lateral intraparietal area. I. Temporal properties; comparison with area 7a.', *Journal of Neurophysiology* **66**(3), 1095–1108.

Barash, S., Bracewell, R. M., Fogassi, L., Gnadt, J. & Andersen, R. A. (1991*b*), 'Saccade-related activity in the lateral intraparietal area. II. Spatial properties.', *Journal of Neurophysiology* **66**(3), 1109–1124.

Barlow, H. B. (1958), 'Temporal and spatial summation in human vision at different background intensities', *The Journal of physiology* **141**(2), 337.

Barlow, H. & Tripathy, S. P. (1997), 'Correspondence noise and signal pooling in the detection of coherent visual motion.', *The Journal of Neuroscience*

17(20), 7954–7966.

Beck, J. M., Ma, W. J., Kiani, R., Hanks, T., Churchland, A. K., Roitman, J., Shadlen, M. N., Latham, P. E. & Pouget, A. (2008), 'Probabilistic Population Codes for Bayesian Decision Making', *Neuron* **60**(6), 1142–1152.

Belmonte, J. C. I., Callaway, E. M., Caddick, S. J., Churchland, P., Feng, G., Homanics, G. E., Lee, K.-F., Leopold, D. A., Miller, C. T., Mitchell, J. F., Mitalipov, S., Moutri, A. R., Movshon, J. A., Okano, H., Reynolds, J. H., Ringach, D., Sejnowski, T. J., Silva, A. C., Strick, P. L., Wu, J. & Zhang, F. (2015), 'Brains, Genes, and Primates', *Neuron* **86**(3), 617–631.

Bennur, S. & Gold, J. (2011), 'Distinct Representations of a Perceptual Decision and the Associated Oculomotor Plan in the Monkey Lateral Intraparietal Area', *Journal of Neuroscience* **31**(3), 913–921.

Bisley, J. W. (2003), 'Neuronal Activity in the Lateral Intraparietal Area and Spatial Attention', *Science* **299**(5603), 81–86.

Bisley, J. W. & Goldberg, M. E. (2010), 'Attention, Intention, and Priority in the Parietal Lobe', **33**(1), 1–21.

Blatt, G. J., Andersen, R. A. & Stoner, G. R. (1990), 'Visual receptive field organization and cortico-cortical connections of the lateral intraparietal area (area LIP) in the macaque.', *The Journal of comparative neurology* **299**(4), 421–445.

Bloch, A. M. (1885), 'Experiences sur la vision', *CR Seances Soc. Biol. Paris* **37**, 493–495.

Bollimunta, A., Totten, D. & Ditterich, J. (2012), 'Neural Dynamics of Choice: Single-Trial Analysis of Decision-Related Activity in Parietal Cortex', *Journal of Neuroscience* **32**(37), 12684–12701.

Born, R. T. & Bradley, D. C. (2005), 'Structure and function of visual area MT.', *Annual review of neuroscience* **28**(1), 157–189.

Bosbach, S., Prinz, W. & Kerzel, D. (2004), 'A Simon effect with stationary moving stimuli.', *Journal of Experimental Psychology: Human Perception and Performance* **30**(1), 39.

Brainard, D. H. (1997), 'The Psychophysics Toolbox.', *Spatial vision* **10**(4), 433–436.

Britten, K., Newsome, W., Shadlen, M. N., Celebrini, S. & Movshon, J. (1996), 'A relationship between behavioral choice and the visual responses of neurons in macaque MT', *Visual neuroscience* **13**, 87–100.

Britten, K., Shadlen, M. N., Newsome, W. & Movshon, J. (1992), 'The analysis of visual motion: a comparison of neuronal and psychophysical performance', *The Journal of Neuroscience* **12**(12), 4745–4765.

Britten, K., Shadlen, M. N., Newsome, W. & Movshon, J. (1993), 'Responses of neurons in macaque MT to stochastic motion signals.', *Visual neuroscience* **10**(6), 1157–1169.

Brody, C. D. & Hanks, T. D. (2016), 'ScienceDirect Neural underpinnings of the evidence accumulator', *Current Opinion in Neurobiology* pp. 1–9.

Brooks, K. R. & Stone, L. S. (2006), 'Stereomotion suppression and the perception of speed: accuracy and precision as a function of 3D trajectory.', *Journal of Vision* **6**(11), 1214–1223.

Brunton, B. W., Botvinick, M. M. & Brody, C. D. (2013), 'Rats and Humans Can Optimally Accumulate Evidence for Decision-Making', **340**(6128), 95–98.

Burr, D. C. (1981), 'Temporal Summation of Moving Images by the Human Visual System', *Proceedings of the Royal Society B: Biological Sciences* **211**(1184), 321–339.

Burr, D. C., Morrone, M. C. & Ross, J. (1994), 'Selective suppression of the magnocellular visual pathway during saccadic eye movements.', *Nature* **371**(6497), 511–513.

Burr, D. C. & Santoro, L. (2001), 'Temporal integration of optic flow, measured by contrast and coherence thresholds.', *Vision Research* **41**(15), 1891–1899.

Celebrini, S. & Newsome, W. (1994), 'Neuronal and psychophysical sensitivity to motion signals in extrastriate area MST of the macaque monkey.', *The Journal of Neuroscience* **14**(7), 4109–4124.

Chapman, B., Zahs, K. R. & Stryker, M. P. (1991), 'Relation of cortical cell orientation selectivity to alignment of receptive fields of the geniculocortical afferents that arborize within a single orientation column in ferret visual cortex.', *The Journal of Neuroscience* **11**(5), 1347–1358.

Chen, Y., Geisler, W. S. & Seidemann, E. (2008), 'Optimal Temporal Decoding of Neural Population Responses in a Reaction-Time Visual Detection Task', *Journal of Neurophysiology* **99**(3), 1366–1379.

Chowdhury, S. A. & DeAngelis, G. C. (2008), 'Fine Discrimination Training Alters the Causal Contribution of Macaque Area MT to Depth Perception', *Neuron* **60**(2), 367–377.

Churchland, A. K., Kiani, R., Chaudhuri, R., Wang, X.-J., Pouget, A. & Shadlen, M. N. (2011), 'Variance as a Signature of Neural Computations during Decision Making', *Neuron* **69**(4), 818–831.

Churchland, A. K., Kiani, R. & Shadlen, M. N. (2008), 'Decision-making with multiple alternatives', *Nature Neuroscience* **11**(6), 693–702.

Cisek, P. & Kalaska, J. F. (2010), 'Neural Mechanisms for Interacting with a World Full of Action Choices', **33**(1), 269–298.

Cohen, M. R. & Kohn, A. (2011), 'Measuring and interpreting neuronal correlations', *Nature Neuroscience* **14**(7), 811–819.

Cohen, M. R. & Newsome, W. T. (2004), 'What electrical microstimulation has revealed about the neural basis of cognition.', *Current Opinion in Neurobiology* **14**(2), 169–177.

Colby, C. & Goldberg, M. (1999), 'Space and attention in parietal cortex.', *Annual review of neuroscience* **22**(1), 319–349.

Cooke, D. F., Goldring, A., Recanzone, G. H. & Krubitzer, L. (2014), 'The evolution of parietal areas associated with visuomanual behavior: from grasping to tool use', *The New Visual Neurosciences* pp. 1049–1063.

Cottereau, B. R., McKee, S. P. & Norcia, A. M. (2014), 'Dynamics and cortical distribution of neural responses to 2D and 3D motion in human', *Journal of Neurophysiology* **111**(3), 533–543.

Crowe, D. A., Goodwin, S. J., Blackman, R. K., Sakellaridi, S., Sponheim, S. R., MacDonald, A. W. & Chafee, M. V. (2013), 'Prefrontal neurons transmit signals to parietal neurons that reflect executive control of cognition.', *Nature Neuroscience* **16**(10), 1484–1491.

Cumming, B. G. & Nienborg, H. (2016), 'ScienceDirect Feedforward and feedback sources of choice probability in neural population responses', *Current Opinion in Neurobiology* **37**, 126–132.

Cunningham, J. P. & Yu, B. M. (2014), 'Dimensionality reduction for large-scale neural recordings.', *Nature Neuroscience* **17**(11), 1500–1509.

Cutrell, E. B. & Marrocco, R. T. (2002), 'Electrical microstimulation of primate posterior parietal cortex initiates orienting and alerting components of covert attention', *Experimental Brain Research* **144**(1), 103–113.

Czuba, T. B., Huk, A. C., Cormack, L. K. & Kohn, A. (2014), 'Area MT Encodes Three-Dimensional Motion', *The Journal of Neuroscience* **34**(47), 15522–15533.

Czuba, T. B., Rokers, B., Huk, A. C. & Cormack, L. K. (2010), 'Speed and Eccentricity Tuning Reveal a Central Role for the Velocity-Based Cue to 3D Visual Motion', *Journal of Neurophysiology* **104**(5), 2886–2899.

Dai, J., Brooks, D. I. & Sheinberg, D. L. (2014), 'Optogenetic and electrical microstimulation systematically bias visuospatial choice in primates.', *Current biology : CB* **24**(1), 63–69.

de Lafuente, V., Jazayeri, M. & Shadlen, M. N. (2015), 'Representation of Accumulating Evidence for a Decision in Two Parietal Areas', *The Journal of Neuroscience* **35**(10), 4306–4318.

Desimone, R. & Ungerleider, L. G. (1986), 'Multiple visual areas in the caudal superior temporal sulcus of the macaque', *The Journal of comparative neurology* **248**(2), 164–189.

Diester, I., Kaufman, M. T., Mogri, M., Pashaie, R., Goo, W., Yizhar, O., Ramakrishnan, C., Deisseroth, K. & Shenoy, K. V. (2011), 'An optogenetic toolbox designed for primates', *Nature Neuroscience* **14**(3), 387–397.

Ding, L. & Gold, J. (2010), 'Caudate Encodes Multiple Computations for Perceptual Decisions', *Journal of Neuroscience* **30**(47), 15747–15759.

Ding, L. & Gold, J. (2012*a*), 'Neural Correlates of Perceptual Decision Making before, during, and after Decision Commitment in Monkey Frontal Eye Field', *Cerebral Cortex* **22**(5), 1052–1067.

Ding, L. & Gold, J. I. (2012*b*), 'Separate, Causal Roles of the Caudate in Saccadic Choice and Executionin a Perceptual Decision Task', *Neuron* **75**(5), 865–874.

Ding, L. & Gold, J. I. (2013), 'Perspective', *Neuron* **79**(4), 640–649.

Ditterich, J. (2006*a*), 'Evidence for time-variant decision making.', *The European journal of neuroscience* **24**(12), 3628–3641.

Ditterich, J. (2006*b*), 'Stochastic models of decisions about motion direction: behavior and physiology.', *Neural Networks* **19**(8), 981–1012.

Ditterich, J., Mazurek, M. E. & Shadlen, M. N. (2003), 'Microstimulation of visual cortex affects the speed of perceptual decisions', *Nature Neuroscience* **6**(8), 891–898.

Donders, F. C. (1969), 'On the speed of mental processes', *Acta psychologica* **30**, 412–431.

Dunn, C. A. & Colby, C. L. (2010), 'Representation of the ipsilateral visual field by neurons in the macaque lateral intraparietal cortex depends on the forebrain commissures.', *Journal of Neurophysiology* **104**(5), 2624–2633.

Eastman, K. M. & Huk, A. C. (2012), 'PLDAPS: A Hardware Architecture and Software Toolbox for Neurophysiology Requiring Complex Visual Stimuli and Online Behavioral Control.', *Frontiers in neuroinformatics* **6**, 1.

Eccles, J. C. (1957), 'The physiology of nerve cells'.

Erlich, J. C., Brunton, B. W., Duan, C. A., Hanks, T. D. & Brody, C. D. (2015), 'Distinct effects of prefrontal and parietal cortex inactivations on an accumulation of evidence task in the rat.', *eLife* **4**, 8166.

Fanini, A. & Assad, J. A. (2009), 'Direction selectivity of neurons in the macaque lateral intraparietal area.', *Journal of Neurophysiology* **101**(1), 289–305.

Fechner, G. T. (1860), 'Elemente der Psychophysik (2 Vols). Breitkopf and Hartel. Vol. 1 trans, by HE Adler (1966)', *Elements of psychophysics* .

Felleman, D. J. & Van Essen, D. (1991), 'Distributed hierarchical processing in the primate cerebral cortex.', *Cerebral Cortex* **1**(1), 1–47.

Ferraina, S., Paré, M. & Wurtz, R. H. (2002), 'Comparison of cortico-cortical and cortico-collicular signals for the generation of saccadic eye movements.', *Journal of Neurophysiology* **87**(2), 845–858.

Ferrier, D. (1876), *The functions of the brain*, GP Putnam's Sons.

Festa, E. K. & Welch, L. (1997), 'Recruitment mechanisms in speed and fine-direction discrimination tasks.', *Vision Research* **37**(22), 3129–3143.

Fetsch, C. R., Kiani, R., Newsome, W. T. & Shadlen, M. N. (2014), 'Effects of Cortical Microstimulation on Confidence in a Perceptual Decision', *Neuron* **83**(4), 797–804.

Freedman, D. J. & Assad, J. A. (2006), 'Experience-dependent representation of visual categories in parietal cortex', *Nature* **443**(7107), 85–88.

Fründ, I., Haenel, N. V. & Wichmann, F. A. (2011), 'Inference for psychometric functions in the presence of nonstationary behavior', *Journal of Vision* **11**(6), 16–16.

Fusi, S., Miller, E. K. & Rigotti, M. (2016), 'ScienceDirect Why neurons mix: high dimensionality for higher cognition', *Current Opinion in Neurobiology* **37**, 66–74.

Gerits, A. & Vanduffel, W. (2013), 'Optogenetics in primates: a shining future?', *Trends in Genetics* **29**(7), 403–411.

Gnadt, J. & Andersen, R. A. (1988), 'Memory related motor planning activity in posterior parietal cortex of macaque', *Experimental Brain Research* **70**(1), 216–220.

Gold, J. I. & Shadlen, M. N. (2000), 'Representation of a perceptual decision in developing oculomotor commands', *Nature* **404**(6776), 390–394.

Gold, J. I. & Shadlen, M. N. (2002), 'Banburismus and the Brain', *Neuron* **36**(2), 299–308.

Gold, J. I. & Shadlen, M. N. (2003), 'The influence of behavioral context on the representation of a perceptual decision in developing oculomotor commands.', *The Journal of neuroscience : the official journal of the Society for Neuroscience* **23**(2), 632–651.

Gold, J. I. & Shadlen, M. N. (2007), 'The neural basis of decision making.', *Annual review of neuroscience* **30**, 535–574.

Gold, J. & Shadlen, M. N. (2001), 'Neural computations that underlie decisions about sensory stimuli', *Trends in Cognitive Sciences* **5**(1), 10–16.

Goldman-Rakic, P. S. (1987), 'Circuitry of primate prefrontal cortex and regulation of behavior by representational memory', *Comprehensive Physiology* .

Gottlieb, J. & Snyder, L. H. (2010), 'Spatial and non-spatial functions of the parietal cortex.', *Current Opinion in Neurobiology* **20**(6), 731–740.

Graham, C. H. & Margaria, R. (1935), 'Area and the intensity-time relation in the peripheral retina', *American Journal of Physiology–Legacy Content* **113**(2), 299–305.

Green, D. M. & Swets, J. A. (1966), 'Signal detection theory and psychophysics'.

Gu, Y., DeAngelis, G. C. & Angelaki, D. E. (2007), 'A functional link between area MSTd and heading perception based on vestibular signals', *Nature Neuroscience* **10**(8), 1038–1047.

Hamed, S. B., Duhamel, J. R., Bremmer, F. & Graf, W. (2001), 'Representation of the visual field in the lateral intraparietal area of macaque monkeys: a quantitative receptive field analysis', *Experimental Brain Research* **140**(2), 127–144.

Hanks, T. D., Ditterich, J. & Shadlen, M. N. (2006), 'Microstimulation of macaque area LIP affects decision-making in a motion discrimination task.', *Nature Neuroscience* **9**(5), 682–689.

Hanks, T. D., Kopec, C. D., Brunton, B. W., Duan, C. A., Erlich, J. C. & Brody, C. D. (2015), 'Distinct relationships of parietal and prefrontal cortices to evidence accumulation.', *Nature* **520**(7546), 220–223.

Hanks, T. D., Mazurek, M. E., Kiani, R., Hopp, E. & Shadlen, M. N. (2011), 'Elapsed Decision Time Affects the Weighting of Prior Probability in a Perceptual Decision Task', *The Journal of Neuroscience* **31**(17), 6339–6352.

Harris, J. M., McKee, S. P. & Watamaniuk, S. N. (1998), 'Visual search for motion-in-depth: Stereomotion does not'pop out'from disparity noise', *Nature Neuroscience* **1**(2), 165–168.

Harvey, C. D., Coen, P. & Tank, D. W. (2012), 'Choice-specific sequences in parietal cortex during a virtual-navigation decision task.', *Nature* **484**(7392), 62–68.

Hebart, M. N., Donner, T. H. & Haynes, J.-D. (2012), 'Human visual and parietal cortex encode visual choices independent of motor plans.', *NeuroImage* **63**(3), 1393–1403.

Heiss, J. D., Walbridge, S., Asthagiri, A. R. & Lonser, R. R. (2010), 'Image-guided convection-enhanced delivery of muscimol to the primate brain.', *Journal of neurosurgery* **112**(4), 790–795.

Herrington, T. M. & Assad, J. A. (2010), 'Temporal Sequence of Attentional Modulation in the Lateral Intraparietal Area and Middle Temporal Area during Rapid Covert Shifts of Attention', *Journal of Neuroscience* **30**(9), 3287–3296.

Hess, R. & Murata, K. (1974), 'Effects of glutamate and GABA on specific response properties of neurones in the visual cortex', *Experimental Brain Research* **21**(3), 285–297.

Hikosaka, O. & Wurtz, R. H. (1983), 'Visual and oculomotor functions of monkey substantia nigra pars reticulata. III. Memory-contingent visual and saccade responses', *Journal of Neurophysiology* **49**(5), 1268–1284.

Histed, M. H., Bonin, V. & Reid, R. C. (2009), 'Direct activation of sparse, distributed populations of cortical neurons by electrical microstimulation.', *Neuron* **63**(4), 508–522.

Honey, C. J. & Sporns, O. (2008), 'Dynamical consequences of lesions in cortical networks.', *Human brain mapping* **29**(7), 802–809.

Horwitz, G. D., Batista, A. P. & Newsome, W. T. (2004), 'Representation of an abstract perceptual decision in macaque superior colliculus.', *Journal of Neurophysiology* **91**(5), 2281–2296.

Horwitz, G. & Newsome, W. (1999), 'Separate signals for target selection and movement specification in the superior colliculus', *Science* **284**(5417), 1158–1161.

Horwitz, G. & Newsome, W. (2001), 'Target selection for saccadic eye movements: prelude activity in the superior colliculus during a direction-discrimination task', *Journal of Neurophysiology* **86**(5), 2543–2558.

Huk, A. C. (2012), 'Multiplexing in the primate motion pathway', *Vision Research* **62**, 173–180.

Huk, A. C., Katz, L. N. & Yates, J. L. (2015), 'Accumulation of Evidence in Decision-Making', *Encyclopedia of Computational Neuroscience* pp. 125–128.

Huk, A. C. & Shadlen, M. N. (2005), 'Neural activity in macaque parietal cortex reflects temporal integration of visual motion signals during perceptual decision making.', **25**(45), 10420–10436.

Irwin, D. E. & Brockmole, J. R. (2004), 'Suppressing where but not what: the effect of saccades on dorsal- and ventral-stream visual processing.', *Psychological Science* **15**(7), 467–473.

Janssen, P. & Shadlen, M. N. (2005), 'A representation of the hazard rate of elapsed time in macaque area LIP', *Nature Neuroscience* **8**(2), 234–241.

Jazayeri, M. & Shadlen, M. N. (2015), 'A Neural Mechanism for Sensing and Reproducing a Time Interval.', *Current biology : CB* **25**(20), 2599–2609.

Kaufman, M. T., Churchland, M. M., Ryu, S. I. & Shenoy, K. V. (2014), 'Cortical activity in the null space: permitting preparation without movement', *Nature Neuroscience* **17**(3), 440–448.

Kayser, A. S., Buchsbaum, B. R., Erickson, D. T. & D'Esposito, M. (2010), 'The functional anatomy of a perceptual decision in the human brain.', *Journal of Neurophysiology* **103**(3), 1179–1194.

Kelly, R. C., Smith, M. A., Samonds, J. M., Kohn, A., Bonds, A. B., Movshon, J. A. & Lee, T. S. (2007), 'Comparison of recordings from microelectrode arrays and single electrodes in the visual cortex.', **27**(2), 261–264.

Kerkhoff, G. (2001), 'Spatial hemineglect in humans.', *Progress in Neurobiology* **63**(1), 1–27.

Kiani, R., Hanks, T. D. & Shadlen, M. N. (2008), 'Bounded Integration in Parietal Cortex Underlies Decisions Even When Viewing Duration Is Dictated by the Environment', *Journal of Neuroscience* **28**(12), 3017–3029.

Kiani, R. & Shadlen, M. N. (2009), 'Representation of Confidence Associated with a Decision by Neurons in the Parietal Cortex', *Science* **324**(5928), 759–764.

Kim, J. & Shadlen, M. N. (1999), 'Neural correlates of a decision in the dorsolateral prefrontal cortex of the macaque', *Nature Neuroscience* **2**, 176–185.

Kingstone, A. & Klein, R. M. (1993), 'What are human express saccades?', *Perception & Psychophysics* **54**(2), 260–273.

Kira, S., Yang, T. & Shadlen, M. N. (2015), 'A neural implementation of Wald's sequential probability ratio test.', *Neuron* **85**(4), 861–873.

Komura, Y., Nikkuni, A., Hirashima, N., Uetake, T. & Miyamoto, A. (2013), 'Responses of pulvinar neurons reflect a subject's confidence in visual categorization', *Nature Neuroscience* **16**(6), 749–755.

Kubanek, J., Li, J. M. & Snyder, L. H. (2015), 'Motor role of parietal cortex in a monkey model of hemispatial neglect.', *Proceedings of the National Academy of Sciences* **112**(16), E2067–72.

Laming, D. R. J. (1968), 'Information theory of choice-reaction times.'.

Latimer, K. W., Yates, J. L., Meister, M. L. R., Huk, A. C. & Pillow, J. W. (2015), 'NEURONAL MODELING. Single-trial spike trains in parietal cortex reveal discrete steps during decision-making.', *Science* **349**(6244), 184–187.

Law, C.-T. & Gold, J. I. (2008), 'Neural correlates of perceptual learning in a sensory-motor, but not a sensory, cortical area.', *Nature Neuroscience* **11**(4), 505–513.

Lennie, P. (1998), 'Single units and visual cortical organization.', *Perception* **27**(8), 889–935.

Leon, M. I. & Shadlen, M. N. (2003), 'Representation of time by neurons in the posterior parietal cortex of the macaque.', *Neuron* **38**(2), 317–327.

Lewis, J. & Van Essen, D. (2000*a*), 'Corticocortical connections of visual, sensorimotor, and multimodal processing areas in the parietal lobe of the macaque monkey', *The Journal of comparative neurology* **428**(1), 112–137.

Lewis, J. & Van Essen, D. (2000*b*), 'Mapping of architectonic subdivisions in the macaque monkey, with emphasis on parieto-occipital cortex', *The Journal of comparative neurology* **428**(1), 79–111.

Li, C.-S. R., Mazzoni, P. & Andersen, R. A. (1999), 'Effect of Reversible Inactivation of Macaque Lateral Intraparietal Area on Visual and Memory Saccades', *Journal of Neurophysiology* .

Lin, J. Y., Murray, S. O. & Boynton, G. M. (2009), 'Capture of attention to threatening stimuli without perceptual awareness.', *Current biology : CB* **19**(13), 1118–1122.

Link, S. W. (1992), 'The wave theory of difference and similarity'.

Liu, S., Gu, Y., DeAngelis, G. C. & Angelaki, D. E. (2013), 'Choice-related activity and correlated noise in subcortical vestibular neurons.', *Nature Neuroscience* **16**(1), 89–97.

Liu, T. & Pleskac, T. J. (2011), 'Neural correlates of evidence accumulation in a perceptual decision task.', *Journal of Neurophysiology* **106**(5), 2383–2398.

Liu, Y., Yttri, E. A. & Snyder, L. H. (2010), 'Intention and attention: different functional roles for LIPd and LIPv.', *Nature Neuroscience* **13**(4), 495–500.

Lomber, S. G. (1999), 'The advantages and limitations of permanent or reversible deactivation techniques in the assessment of neural function', *Journal of Neuroscience Methods* **86**(2), 109–117.

Louie, K. & Glimcher, P. W. (2010), 'Separating value from choice: delay discounting activity in the lateral intraparietal area.', *Journal of Neuroscience* **30**(16), 5498–5507.

Luce, R. D. (1986), *Response times*, Oxford University Press.

Mante, V., Sussillo, D., Shenoy, K. V. & Newsome, W. T. (2013), 'Context-dependent computation by recurrent dynamics in prefrontal cortex.', *Nature* **503**(7474), 78–84.

Martin, J. H. (1991), 'Autoradiographic estimation of the extent of reversible inactivation produced by microinjection of lidocaine and muscimol in the rat.', *Neuroscience Letters* **127**(2), 160–164.

Maunsell, J. H. & Van Essen, D. (1983), 'Functional properties of neurons in middle temporal visual area of the macaque monkey. I. Selectivity for

stimulus direction, speed, and orientation.', *Journal of Neurophysiology* **49**(5), 1127–1147.

Maunsell, J. H. & van Essen, D. C. (1987), 'Topographic organization of the middle temporal visual area in the macaque monkey: representational biases and the relationship to callosal connections and myeloarchitectonic boundaries', *The Journal of comparative neurology* **266**(4), 535–555.

Mazurek, M. E., Roitman, J. D., Ditterich, J. & Shadlen, M. N. (2003), 'A role for neural integrators in perceptual decision making.', *Cerebral Cortex* **13**(11), 1257–1269.

Meister, M. L., Hennig, J. A. & Huk, A. C. (2013), 'Signal multiplexing and single-neuron computations in lateral intraparietal area during decision-making', *The Journal of Neuroscience* **33**(6), 2254–2267.

Melcher, D., Crespi, S., Bruno, A. & Morrone, M. C. (2004), 'The role of attention in central and peripheral motion integration.', *Vision Research* **44**(12), 1367–1374.

Morrone, M. C., Burr, D. C. & Vaina, L. M. (1995), 'Two stages of visual processing for radial and circular motion.', *Nature* **376**(6540), 507–509.

Mountcastle, V. B., Lynch, J., Georgopoulos, A., Sakata, H. & Acuna, C. (1975), 'Posterior parietal association cortex of the monkey: command functions for operations within extrapersonal space', *Journal of Neurophysiology* **38**(4), 871–908.

Neri, P., Morrone, M. C. & Burr, D. C. (1998), 'Seeing biological motion.', *Nature* **395**(6705), 894–896.

Newsome, W. T., Britten, K. H. & Movshon, J. A. (1989), 'Neuronal correlates of a perceptual decision.', *Nature* .

Newsome, W. T. & Pare, E. B. (1988), 'A selective impairment of motion perception following lesions of the middle temporal visual area (MT)', *The Journal of Neuroscience* **8**(6), 2201–2211.

Nienborg, H. & Cumming, B. (2010), 'Correlations between the activity of sensory neurons and behavior: how much do they tell us about a neuron's causality?', *Current Opinion in Neurobiology* **20**(3), 376–381.

Nienborg, H. & Cumming, B. G. (2009), 'Decision-related activity in sensory neurons reflects more than a neuron's causal effect.', *Nature* **459**(7243), 89–92.

Noudoost, B., Chang, M. H., Steinmetz, N. A. & Moore, T. (2010), 'Top-down control of visual attention.', *Current Opinion in Neurobiology* **20**(2), 183–190.

Noudoost, B. & Moore, T. (2011), 'A reliable microinjectrode system for use in behaving monkeys.', *Journal of Neuroscience Methods* **194**(2), 218–223.

Oristaglio, J., Schneider, D. M., Balan, P. F. & Gottlieb, J. (2006), 'Integration of visuospatial and effector information during symbolically cued limb

movements in monkey lateral intraparietal area.', *The Journal of neuroscience : the official journal of the Society for Neuroscience* **26**(32), 8310–8319.

Osborne, L. C., Bialek, W. & Lisberger, S. G. (2004), 'Time course of information about motion direction in visual area MT of macaque monkeys.', **24**(13), 3210–3222.

Otchy, T. M., Wolff, S. B. E., Rhee, J. Y., Pehlevan, C., Kawai, R., Kempf, A., Gobes, S. M. H. & Ölveczky, B. P. (2015), 'Acute off-target effects of neural circuit manipulations.', *Nature* **528**(7582), 358–363.

Palmer, J., Huk, A. C. & Shadlen, M. N. (2005), 'The effect of stimulus strength on the speed and accuracy of a perceptual decision', *Journal of Vision* **5**(5), 1–1.

Pare, M. & Wurtz, R. H. (1997), 'Monkey posterior parietal cortex neurons antidromically activated from superior colliculus', *Journal of Neurophysiology* **78**(6), 3493–3497.

Park, I. M., Meister, M. L. R., Huk, A. C. & Pillow, J. W. (2014), 'Encoding and decoding in parietal cortex during sensorimotor decision-making', *Nature Neuroscience* **17**(10), 1395–1403.

Parker, A. J. (2007), 'Binocular depth perception and the cerebral cortex.', *Nature Reviews Neuroscience* **8**(5), 379–391.

Parker, A. J. & Newsome, W. (1998), 'Sense and the single neuron: probing the physiology of perception.', *Annual review of neuroscience* **21**(1), 227–277.

Pashler, H., Carrier, M. & Hoffman, J. (1993), 'Saccadic eye movements and dual-task interference', *The Quarterly Journal of Experimental Psychology* **46**(1), 51–82.

Patel, G. H., Shulman, G. L., Baker, J. T., Akbudak, E., Snyder, A. Z., Snyder, L. H. & Corbetta, M. (2010), 'Topographic organization of macaque area LIP.', *Proceedings of the National Academy of Sciences* **107**(10), 4728–4733.

Pillow, J. W., Shlens, J., Chichilnisky, E. J. & Simoncelli, E. P. (2013), 'A Model-Based Spike Sorting Algorithm for Removing Correlation Artifacts in Multi-Neuron Recordings', *PLoS ONE* **8**(5), e62123.

Pillow, J. W., Shlens, J., Paninski, L., Sher, A., Litke, A. M., Chichilnisky, E. J. & Simoncelli, E. P. (2008), 'Spatio-temporal correlations and visual signalling in a complete neuronal population', *Nature* **454**(7207), 995–999.

Pitkow, X., Liu, S., Angelaki, D. E., DeAngelis, G. C. & Pouget, A. (2015), 'How Can Single Sensory Neurons Predict Behavior?', *Neuron* **87**(2), 411–423.

Platt, M. L. & Glimcher, P. (1998), 'Response fields of intraparietal neurons quantified with multiple saccadic targets.', *Experimental Brain Research*

121(1), 65–75.

Platt, M. L. & Glimcher, P. (1999), 'Neural correlates of decision variables in parietal cortex.', *Nature* **400**(6741), 233–238.

Platt, M. L. & Glimcher, P. W. (1997), 'Responses of Intraparietal Neurons to Saccadic Targets and Visual Distractors', *Journal of Neurophysiology* **78**(3), 1574–1589.

Premereur, E., Vanduffel, W. & Janssen, P. (2011), 'Functional Heterogeneity of Macaque Lateral Intraparietal Neurons', *Journal of Neuroscience* **31**(34), 12307–12317.

Rao, V., DeAngelis, G. C. & Snyder, L. H. (2012), 'Neural correlates of prior expectations of motion in the lateral intraparietal and middle temporal areas', *The Journal of Neuroscience* .

Raposo, D., Kaufman, M. T. & Churchland, A. K. (2014), 'A category-free neural population supports evolving demands during decision-making.', *Nature Neuroscience* **17**(12), 1784–1792.

Ratcliff, R. (1978), 'A theory of memory retrieval.', *Psychological Review* **85**(2), 59.

Ratcliff, R. & McKoon, G. (2008), 'The Diffusion Decision Model: Theory and Data for Two-Choice Decision Tasks', *Neural computation* **20**(4), 873–922.

Ratcliff, R. & Smith, P. L. (2004), 'A Comparison of Sequential Sampling Models for Two-Choice Reaction Time.', *Psychological Review* **111**(2), 333–367.

Ratcliff, R., Smith, P. L., Brown, S. D. & McKoon, G. (2016), 'Diffusion Decision Model: Current Issues and History.', *Trends in Cognitive Sciences* **20**(4), 260–281.

Regan, D. & Tyler, C. W. (1971), 'Temporal summation and its limit for wavelength changes: an analog of Bloch's law for color vision', *JOSA* **61**(10), 1414.

Rigotti, M., Barak, O., Warden, M. R., Wang, X.-J., Daw, N. D., Miller, E. K. & Fusi, S. (2013), 'The importance of mixed selectivity in complex cognitive tasks.', *Nature* **497**(7451), 585–590.

Rishel, C. A., Huang, G. & Freedman, D. J. (2013), 'Independent Category and Spatial Encoding in Parietal Cortex', *Neuron* **77**(5), 969–979.

Rizzolatti, G., Riggio, L., Dascola, I. & Umiltá, C. (1987), 'Reorienting attention across the horizontal and vertical meridians: evidence in favor of a premotor theory of attention', *Neuropsychologia* **25**(1), 31–40.

Roitman, J. D., Brannon, E. M. & Platt, M. L. (2007), 'Monotonic coding of numerosity in macaque lateral intraparietal area.', *PLoS biology* **5**(8), e208.

Roitman, J. & Shadlen, M. N. (2002), 'Response of neurons in the lateral intraparietal area during a combined visual discrimination reaction time task', *The Journal of Neuroscience* **22**(21), 9475–9489.

Rorie, A. E., Gao, J., McClelland, J. L. & Newsome, W. T. (2010), 'Integration of sensory and reward information during perceptual decision-making in lateral intraparietal cortex (LIP) of the macaque monkey.', *PLoS ONE* **5**(2), e9308.

Ross, L. E. & Ross, S. M. (1980), 'Saccade latency and warning signals: Stimulus onset, offset, and change as warning events', *Perception & Psychophysics* **27**(3), 251–257.

Saalmann, Y. B., Pigarev, I. N. & Vidyasagar, T. R. (2007), 'Neural Mechanisms of Visual Attention: How Top-Down Feedback Highlights Relevant Locations', *Science* **316**(5831), 1612–1615.

Salzman, C. D., Murasugi, C. M., Britten, K. & Newsome, W. (1992), 'Microstimulation in visual area MT: effects on direction discrimination performance.', *The Journal of Neuroscience* **12**(6), 2331–2355.

Sanada, T. M. & DeAngelis, G. C. (2014), 'Neural Representation of Motion-In-Depth in Area MT.', *Journal of Neuroscience* **34**(47), 15508–15521.

Sarma, A., Masse, N. Y., Wang, X.-J. & Freedman, D. J. (2015), 'Task-specific versus generalized mnemonic representations in parietal and prefrontal cortices', *Nature Neuroscience* **19**(1), 143–149.

Scase, M. O., Braddick, O. J. & Raymond, J. E. (1996), 'What is noise for the motion system?', *Vision Research* **36**(16), 2579–2586.

Selen, L. P. J., Shadlen, M. N. & Wolpert, D. M. (2012), 'Deliberation in the Motor System: Reflex Gains Track Evolving Evidence Leading to a Decision', *Journal of Neuroscience* **32**(7), 2276–2286.

Sereno, A. B. & Maunsell, J. H. R. (1998), 'Shape selectivity in primate lateral intraparietal cortex', *Nature* **395**(6701), 500–503.

Shadlen, M. N., Britten, K., Newsome, W. & Movshon, J. (1996), 'A computational analysis of the relationship between neuronal and behavioral responses to visual motion.', *The Journal of Neuroscience* **16**(4), 1486–1510.

Shadlen, M. N. & Gold, J. (2004), 'The neurophysiology of decision-making as a window on cognition', *The cognitive neurosciences* .

Shadlen, M. N. & Kiani, R. (2013), 'Decision Making as a Window on Cognition', *Neuron* **80**(3), 791–806.

Shadlen, M. N. & Newsome, W. (1994), 'Noise, neural codes and cortical organization.', *Current Opinion in Neurobiology* **4**(4), 569–579.

Shadlen, M. N. & Newsome, W. (1996), 'Motion perception: seeing and deciding.', *Proceedings of the National Academy of Sciences of the United States of America* **93**(2), 628–633.

Shadlen, M. N. & Newsome, W. (2001), 'Neural basis of a perceptual decision in the parietal cortex (area LIP) of the rhesus monkey', *Journal of Neurophysiology* **86**(4), 1916–1936.

Shioiri, S. & Cavanagh, P. (1989), 'Saccadic suppression of low-level motion.', *Vision Research* **29**(8), 915–928.

Siegel, M., Buschman, T. J. & Miller, E. K. (2015), 'Cortical information flow during flexible sensorimotor decisions.', *Science* **348**(6241), 1352–1355.

Smith, P. L. & Ratcliff, R. (2004), 'Psychology and neurobiology of simple decisions', *TRENDS in Neurosciences* **27**(3), 161–168.

Song, J.-H. & Nakayama, K. (2008*a*), 'Numeric comparison in a visually-guided manual reaching task.', *COGNITION* **106**(2), 994–1003.

Song, J.-H. & Nakayama, K. (2008*b*), 'Target selection in visual search as revealed by movement trajectories.', *Vision Research* **48**(7), 853–861.

Song, J.-H. & Nakayama, K. (2009), 'Hidden cognitive states revealed in choice reaching tasks', *Trends in Cognitive Sciences* **13**(8), 360–366.

Spivey, M., Grosjean, M. & Knoblich, G. (2005), 'Continuous attraction toward phonological competitors', *Proceedings of the National Academy of Sciences of the United States of America* **102**(29), 10393.

Stone, M. (1960), 'Models for choice-reaction time', *Psychometrika* **25**(3), 251–260.

Sugrue, L. P., Corrado, G. S. & Newsome, W. T. (2005), 'Choosing the greater of two goods: neural currencies for valuation and decision making', *Nature Reviews Neuroscience* **6**(5), 363–375.

Suzuki, M. & Gottlieb, J. (2012), 'Distinct neural mechanisms of distractor suppression in the frontal and parietal lobe', *Nature Neuroscience* **16**(1), 98–104.

Tolias, A. S., Ecker, A. S., Siapas, A. G., Hoenselaar, A., Keliris, G. A. & Logothetis, N. K. (2007), 'Recording Chronically From the Same Neurons in Awake, Behaving Primates', *Journal of Neurophysiology* **98**(6), 3780–3790.

Toth, L. J. & Assad, J. A. (2002), 'Dynamic coding of behaviourally relevant stimuli in parietal cortex.', *Nature* **415**(6868), 165–168.

Turrigiano, G. G. (1999), 'Homeostatic plasticity in neuronal networks: the more things change, the more they stay the same', *TRENDS in Neurosciences* **22**(5), 221–227.

Tyler, C. W. (1971), 'Stereoscopic Depth Movement: Two Eyes Less Sensitive than One', *Science* **174**(4012), 958–961.

Tyler, C. W. & Foley, J. M. (1974), 'Stereomovement suppression for transient disparity changes', *Perception* **3**(3), 287–296.

Uylings, H., Groenewegen, H. J. & Kolb, B. (2003), 'Do rats have a prefrontal cortex?', *Behavioural brain research* .

von Helmholtz, H. (1867), 'Treatise on Physiological Optics Vol. III'.

Wald, A. (1947), Sequential analysis. 1947, Technical report.

Wald, A. & Wolfowitz, J. (1948), 'Optimum character of the sequential probability ratio test', *The Annals of Mathematical Statistics* .

Wardak, C., Olivier, E. & Duhamel, J.-R. (2002), 'Saccadic target selection deficits after lateral intraparietal area inactivation in monkeys', *The Journal of Neuroscience* **22**(22), 9877–9884.

Wardak, C., Olivier, E. & Duhamel, J.-R. (2004), 'A Deficit in Covert Attention after Parietal Cortex Inactivation in the Monkey', *Neuron* **42**(3), 501–508.

Wardak, C., Olivier, E. & Duhamel, J.-R. (2011), 'The relationship between spatial attention and saccades in the frontoparietal network of the monkey', *European Journal of Neuroscience* **33**(11), 1973–1981.

Watamaniuk, S. N. & Sekuler, R. (1992), 'Temporal and spatial integration in dynamic random-dot stimuli', *Vision Research* **32**(12), 2341–2347.

Watson, A. B. (1979), 'Probability summation over time', *Vision Research* **19**(5), 515–522.

Watson, A. B. (1986), 'Temporal sensitivity', *Handbook of perception and human performance* **1**, 6–1.

Wichmann, F. A. & Hill, N. J. (2001), 'The psychometric function: I. Fitting, sampling, and goodness of fit', *Perception & Psychophysics* **63**(8), 1293–1313.

Wilke, M., Kagan, I. & Andersen, R. A. (2012), 'Functional imaging reveals rapid reorganization of cortical activity after parietal inactivation in monkeys.', *Proceedings of the National Academy of Sciences* **109**(21), 8274–8279.

Wong, K.-F. (2007), 'Neural circuit dynamics underlying accumulation of time-varying evidence during perceptual decision making', *Frontiers in Computational Neuroscience* **1**.

Wurtz, R. H., Sommer, M. A., Pare, M. & Ferraina, S. (2001), 'Signal transformations from cerebral cortex to superior colliculus for the generation of saccades.', *Vision Research* **41**(25-26), 3399–3412.

Xu-Wilson, M., Zee, D. S. & Shadmehr, R. (2009), 'The intrinsic value of visual information affects saccade velocities', *Experimental Brain Research* **196**(4), 475–481.

Yang, T. & Shadlen, M. N. (2007), 'Probabilistic reasoning by neurons', *Nature* **447**(7148), 1075–1080.

Yttri, E. A., Wang, C., Liu, Y. & Snyder, L. H. (2014), 'The parietal reach region is limb specific and not involved in eye-hand coordination', *Journal of Neurophysiology* **111**(3), 520–532.

Zandbelt, B., Purcell, B. A., Palmeri, T. J., Logan, G. D. & Schall, J. D. (2014), 'Response times from ensembles of accumulators.', *Proceedings of the National Academy of Sciences* **111**(7), 2848–2853.

Zirnsak, M., Chen, X., Lomber, S. G. & Moore, T. (2015), Effects of reversible inactivation of parietal cortex on the processing of visual salience in the frontal eye field, *in* 'Society for Neuroscience', Chicago.

Zohary, E., Shadlen, M. N. & Newsome, W. T. (1994), 'Correlated neuronal discharge rate and its implications for psychophysical performance', *Nature* **370**(6485), 140–143.

Vita

Leor Nadav Katz was born in Kfar Saba, Israel, in 1983. He grew up in a small town near Tel Aviv, cultivating interests in science from a young age. After three years of mandatory military service Leor took some time off and traveled South America for a year. Upon his return he began his undergraduate studies in Neuroscience, in the University of Bar Ilan, Israel. During that time he worked as a research assistant under the guidance of Abraham Zangen in the Weizmann Institute for Science and Shalvata mental health hospital, where he studied the effects of transcranial magnetic stimulation on patients suffering from depression. In 2010 Leor left his home country and ventured to the United States where he joined the lab of Alex Huk in the University of Texas at Austin, in pursuit of his PhD, focusing on sensorimotor decision-making in the primate brain. Leor is scheduled to start his postdoc position in the lab of Rich Krauzlis at the National Institute of Health, where he aims to carry on researching and continue being himself (despite the better judgement of his peers).

Permanent address: leor.katz@gmail.com

This dissertation was typeset with LaTeX[†] by the author.

[†]LaTeX is a document preparation system developed by Leslie Lamport as a special version of Donald Knuth's TeX Program.